ALMA MATER STUDIORUM
UNIVERSITÀ DI BOLOGNA

DOTTORATO DI RICERCA IN

SCIENZE BIOMEDICHE E NEUROMOTORIE

Ciclo 36

**Settore Concorsuale:** 06/A3 - MICROBIOLOGIA E MICROBIOLOGIA CLINICA

**Settore Scientifico Disciplinare:** MED/07 - MICROBIOLOGIA E MICROBIOLOGIA CLINICA

# FUNCTIONAL ANALYSIS OF INTERACTION BETWEEN PRIMARY HIV-1 NEF ALLELES AND HOST PROTEINS

**Presentata da**: Martina Tamburello

**Coordinatore Dottorato**

Prof.ssa Matilde Yung Follo

**Supervisore**

Dott.ssa Isabella Bon

**Co-supervisore**

Prof.ssa Matilde Yung Follo

Prof.ssa Antonella Marangoni

Esame finale anno 2024

# Abstract

The HIV-1 accessory protein Nef plays a pivotal role in viral pathogenesis due to its multifunctional character. Nef facilitates immune evasion by promoting the down-modulation of cell surface molecules, including major histocompatibility complex class I (MHC-I), CD4 and a member of the serine incorporator family, SERINC5. This allows the virus to persist and replicate within the host organism. Despite this understanding, the role of Nef-mediated downregulation of the cell surface receptors in HIV-1 pathogenesis, along with several underlying mechanisms, remains unclear. Furthermore, Nef alters the cellular environment interacting with several proteins involved in the intracellular traffic. Among these, the human peroxisomal thioesterase 8 (ACOT8) has been shown to be an important cellular partner of Nef and this interaction may be involved in Nef-dependent endocytosis and in the modulation of lipid composition in membrane rafts. However, detailed information regarding this interaction and an in-depth analysis of primary nef alleles are still lacking.

This study investigated the impact of primary individuals-derived *nef* alleles on the modulation of MHC-I, CD4 and SERINC5 and their capability to interact with ACOT8.

26 *nef* alleles derived from ART-naïve HIV-1-positive individuals, corresponding to subtypes B, F1, G, C, and CRF02_AG within the M group, were isolated for functional analysis. Primary Nef constructs were obtained by cloning the alleles into a pIRES-eGFP vector. Receptor modulation of MHC-I and CD4 at an endogenous level was evaluated by transfecting HEK293T and/or Jurkat T cells with the pIRES-eGFP vector, followed by quantification of Nef-mediated receptor downregulation using flow cytometry. Additionally, Nef's capability to modulate SERINC5 surface expression was examined by transfecting HEK293T cells to express *nef* alleles together with SERINC5. Finally, Nef polymorphisms potentially associated with these activities were identified and correlated with their respective functions. The interaction between Nef and ACOT8 was assessed through a co-immunoprecipitation approach in an ACOT8-mScarlet overexpression context.

This study showed that the majority of primary nef alleles led to a significant downregulation of MHC-I, CD4, and SERINC5 from the cell surface, which also correlated with a high conservation of the known functional domains. Moreover, it demonstrated for the first time an interaction between primary nef alleles and ACOT8, revealing that this interaction was highly

variable among viral subtypes and might depend on amino acid residues within the central core domain of Nef.

In summary this study highlighted the conserved function across HIV-1 subtypes in downregulating MHC-I, CD4, and SERINC5, and revealed a surprising variability in primary Nef interaction with ACOT8. Overall, the obtained data contributed to enhancing the understanding of Nef's biological functions and identified new mechanisms potentially involved in HIV pathogenesis.

# Table of content

# 1 Introduction

## 1.1 Human Immunodeficiency Virus

The Human Immunodeficiency Virus (HIV) is the etiologic agent of Acquired Immune Deficiency Syndrome (AIDS) (1). According to the Baltimore classification, HIV belongs to the Retroviridae family, Orthoretrovirinae subfamily, genus Lentivirus (2).

The syndrome was first reported in the literature in 1981, following the identification of a case involving *Pneumocystis carinii*, a particular pathogen well-known for its aggressiveness in individuals with compromised immune systems (3), and the occurrence of a rare blood vessel tumour, Kaposi's sarcoma. Only in 1983 HIV was isolated and identified as the causative agent of AIDS (1).

Since its discovery, intensive research efforts have enabled the study of virus characterization, its pathogenesis, its interaction with the host and the development of approaches for testing, treating, and preventing the spread of the infection.

According to the epidemiological data published in the UNAIDS 2023 annual report, it is revealed that in 2022, 39 million people globally were living with HIV, 1.3 million people became newly infected and approximately 630,000 people died from AIDS-related illnesses. Among these, the highest number of cases of morbidity and mortality related to HIV/AIDS is observed in young adults, particularly women, in sub-Saharan Africa (4).

Despite the ongoing HIV pandemic, the number of new infections has been reduced by 59% since the peak in 1995, and AIDS-related deaths have been reduced by 69% since the peak in 2004 and by 51% since 2010 (Fig. 1 A, B). These important results demonstrate the effectiveness of widespread screening, the success of Pre-Exposure Prophylaxis (PrEP), and the use of antiretroviral therapy (ART) in combating the infection and ensuring a better quality of life for people leaving with HIV (4).

Further scientific efforts and increased access to therapeutic treatments are still necessary to achieve complete viral eradication.


**Figure 1**A) Number of new HIV infections and B) Number of AIDS-related deaths global, 1990–2022, and 2025 target UNAIDS epidemiological estimates, 2023 (https://aidsinfo.unaids.org/).

## 1.2 Origin and Classification

Epidemiological and phylogenetic analyses revealed that the virus's introduction into the human population occurred between 1920 and 1940. Specifically, sequence alignments found with the Simian Immunodeficiency Virus (SIV) demonstrated a spillover from chimpanzees to humans, likely occurring during a hunting expedition in Kinshasa (present-day Democratic Republic of Congo) (5).

Population genetic studies have differentiated HIV into two types, HIV-1 and HIV-2, both associated with AIDS but originating from two distinct progenitors. HIV-1 is the most globally prevalent type, and is phylogenetically linked to SIVcpz, infecting chimpanzees *Pan Troglodytes troglodytes*. HIV-2 is associated with the SIVsmm virus, infecting *Sooty Mangabey monkeys*, and is less virulent, leading to a milder disease course. HIV-2 is primarily endemic in West Africa, South America, and the Caribbean, reviewed in (6) (Fig. 2).

HIV-1, responsible for more than 95% of all infections worldwide, is categorized into four groups: M (major), O (outlier), N (non-M non-O), and P, resulted from independent cross-species transmission of Simian Immunodeficiency Viruses (SIV). Groups N, O, and P are confined to West Africa, while Group M, the most widespread, is responsible for the global pandemic, reviewed in (7).

HIV-1 group M encompasses nine distinct pure subtypes (A–D, F–H, J, and K), sub-subtypes (A1 and A2, F1 and F2). Subtype C accounts for over 50% of global infections, with a significant prevalence in East and Southern Africa, as well as India. Meanwhile, Subtype B has become prevalent in almost all parts of Europe and America, reviewed in (6). Further, around 100 circulating recombinant forms (CRFs), and various unique (unclassified) recombinant forms (URFs) are known within the M group. Thereby, CRFs are generated through the recombination of viral genomes from different subtypes, occurring in individuals dually infected with different HIV-1 subtypes. This process leads to the creation of a mosaic genome with regions derived from each original subtype. Notably, CRF02_AG, a common form combining subtype A and G, is the predominant virus in West Africa.

(HIV and SIV nomenclature. HIV sequence database. Available at https://hiv.lanl.gov/content/sequence/HelpDocs/subtypes-more.html; LANL: HIV circulating

recombinant forms (CRFs). HIV sequence database. Available at http://hiv.lanl.gov/content/sequence/HIV/CRFs/CRFs.html (2018)).

HIV-2, less infectious than HIV-1, remains largely restricted to the western part of Africa, although viral introductions have been reported in Europe, India, and the United States of America. It is composed of at least nine groups (formerly referred to as subtypes; A to I), of which groups A and D are currently circulating (8).

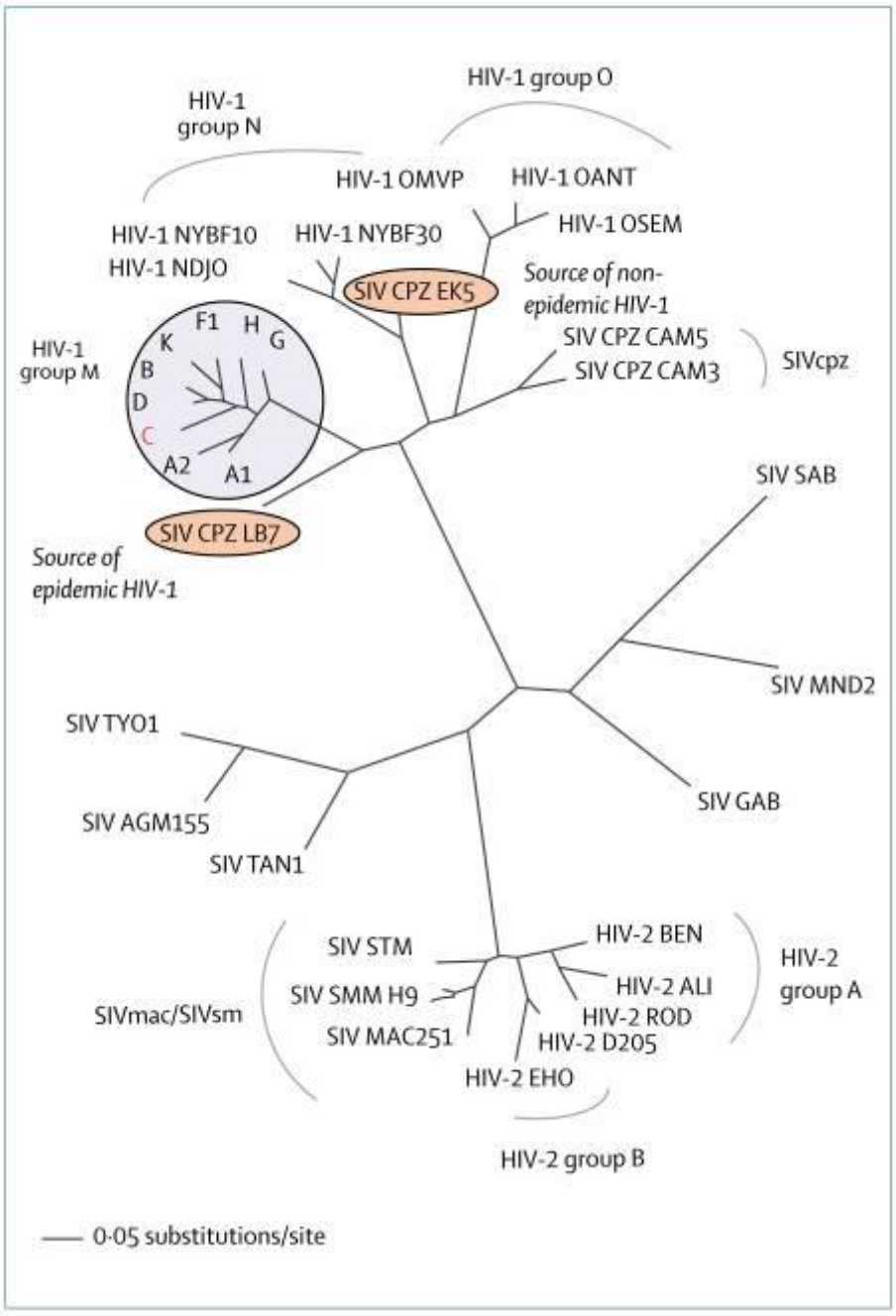


**Figure 2** Phylogenetic relation of lentiviruses in man and non-human primates (9).

## 1.3 Viral particle

Electron microscopy revealed the structural characteristics of HIV, showing membrane-enveloped virions with a spherical to pleomorphic shape and a diameter ranging from approximately 100 to 120 nm (10). Moving from the outermost layer to the inner core of the mature viral particle, the key structural elements include the envelope, the matrix composed of the viral protein p17, and the capsid consisting of assembled capsid protein p24 that encloses the viral genome along with the nucleocapsid protein p7 and the enzymes crucial for integration (reverse transcriptase and integrase) (10) (11) (Fig. 3).

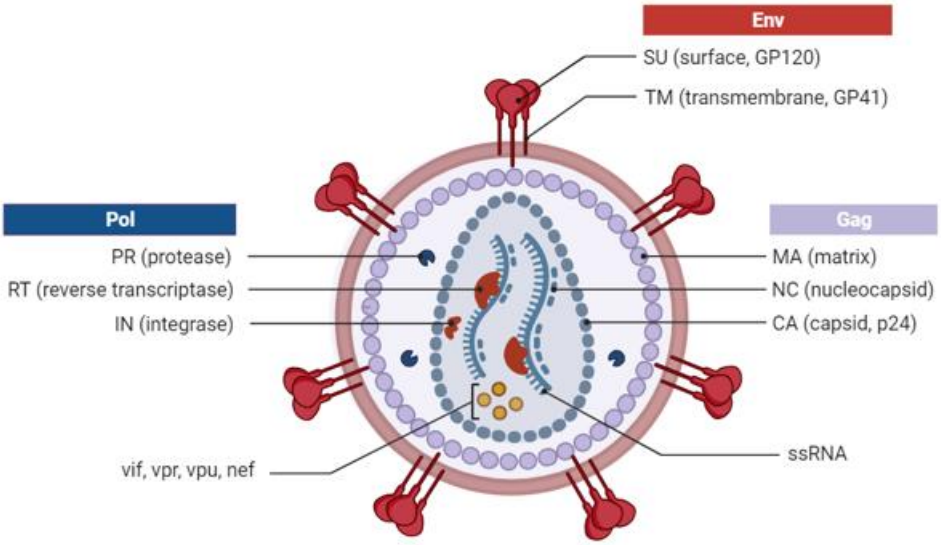


**Figure 3** HIV-1 virion structure (Created with BioRender.com).

## 1.4 Viral genome

The HIV genome, approximately 9 kb in length, consists of two positive-sense, single-stranded RNA strands and is organized into nine open reading frames (ORFs) encoding 15 viral proteins, as reviewed in (12) (Fig. 4). Each RNA encodes 3 overlapping open reading frames encoding for *gag*, *pol*, and *env*, which are subsequently proteolyzed into individual proteins common to all retroviruses. Additionally, there are two genes encoding the regulatory proteins *tat* and *rev*, along with four genes for accessory proteins: *vif*, *vpr*, *vpu* and *nef*.

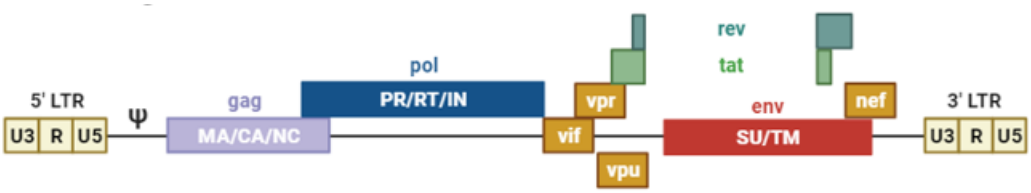


**Figure 4** HIV-1 genome and proteins organization (Created with BioRender.com).

The two RNA molecules are paired at the 5' end within a region called Ψ (psi) containing a packaging signal that facilitates the insertion of the strands into the capsid during assembly (13).

HIV is able to reverse transcribe its genome into cDNA, which is integrated into the host cell's double-stranded DNA, forming proviral DNA (or provirus). The proviral genome is flanked by long terminal repeats regions (LTR) in both ends, which are non-coding elements playing a crucial role in viral integration and transcriptional regulation (11). Particularly, the 5' LTR region acts as the promoter region for transcription of viral genes, encoding sequences for multiple transcription factors, like the nuclear factor κB (NF-κB), Sp1 and other. Moreover it contains the promoter region with the initiator site (Inr), the TATA-box sequence, and an enhancer site binding trans activating response (TAR) element, important for the transcription of integrated HIV proviral DNA (14).

## 1.5 Viral proteins

The three main HIV genes, *gag*, *pol*, and *env*, are initially translated into large polyproteins, which are then modified and cleaved into the final proteins (Fig. 4). Specifically, the four proteins derived from *gag* and the two proteins from *env* correspond to the structural components (the virion core, the envelope, and the outermost membrane); the three *pol* proteins perform essential enzymatic functions and are encapsulated inside the complete virion, along with the two RNA molecules.

In addition, Tat (transactivator protein) and Rev (RNA-splicing regulator) regulatory proteins are essential for initiating HIV replication. Meanwhile the accessory proteins, Vif (viral infectivity factor), Vpr (virus protein r), Vpu (virus protein unique) and Nef (negative regulating factor) play a role in viral replication, virus budding, and pathogenesis.

### 1.5.1 Gag proteins

The gag-pol genes are co-translated into a 180 kDa polyprotein (p180), which is subsequently cleaved into another polyprotein of 55 kDa, the $p55^{Gag}$. It serves as the precursor for the structural proteins encoded by *gag* (15).

After the additional proteolytic cleavage of $p55^{Gag}$, the mature structural proteins are produced.

The **p17** or matrix (MA) protein forms the N-terminal part of $p55^{Gag}$. It is involved in targeting the Gag protein towards the plasma membrane, incorporating the Env glycoprotein into virions, and in the early events in virus internalization (16)

The **p24** or capsid (CA) protein constitutes the core of the precursor p55; it also plays a pivotal role in the viral assembly and maturation and during the first steps of viral lifecycle (15).

The **p7** or nucleocapsid (NC) protein is characterized by the presence of CysX2-Cys-X4-His-X4-Cys (CCHC) that act as the zinc fingers domains. It binds to the Ψ region present in LTRs, thereby promoting encapsidation (17), (18).

The **p6** is a small protein located in the C-terminal region of $p55^{Gag}$ and its main role is to bind Vpr during assembly (19). Its function is likely associated with the budding and release of new viral particles (20).

### 1.5.2 Pol proteins

The Pol polyprotein is derived from a ribosomal frameshift on $p55^{Gag}$, leading to the formation of the 160-kD Gag-Pol fusion polyprotein, known as p160 Gag-Pol (21). The pol gene codes for the main viral enzymes: the protease (PR), the reverse transcriptase (RT), and the integrase (IN).

The **protease** plays a pivotal role in the assembly and maturation of viral proteins. It acts as a homodimer, cleaving the p55Gag and Gag-Pol precursors following dimerization (12).

The **reverse transcriptase** is structurally a heterodimer, composed of a major subunit (p66) and a minor subunit (p55). The catalytic activity of the enzyme resides in the p66 subunit, while the p55 subunit, although enzymatically inactive, plays a role in stabilizing the structural conformation required for its function (22), (23). This enzyme is a defining feature

of all retroviruses, as it can convert a single strand of RNA into a double strand of DNA (cDNA or provirus), a crucial step for integrating the viral genome. Therefore, it exhibits DNA polymerase activity using both RNA and DNA templates. Additionally, it possesses ribonuclease H activity, responsible for degrading the RNA segment of RNA-DNA hybrids generated during viral reverse transcription (22).

The **integrase** facilitates the integration of the provirus, originating from reverse transcriptase, into the host genome. The core of the protein exhibits a similar structure to that of RNase H and consists of the catalytic triad motif that binds the Zn ion in the active site, promoting integration. The C-terminal domain forms nonspecific bonds with DNA. Viral integration is an essential step for the establishment of viral reservoir, a pool of latently infected cells ready to produce new virus (24).

### 1.5.3 Env proteins

Through alternative splicing events, the *env* gene gives rise to the Env polyprotein or gp160 (25). In contrast to Gag and Gag-Pol precursors, which are cleaved by the viral protease, the Env precursor undergoes processing by a cellular protease in the Golgi apparatus, resulting in the formation of the structural envelope proteins: the surface glycoprotein gp120 (SU) and the transmembrane glycoprotein gp41. These proteins associate to form hexamers, creating protrusions known as spikes on the surface of the virion, which then initiate the host-virus interaction (26), (27).

The **gp120** is responsible for receptor binding and comprises two domains: five internal conserved regions (C1-C5) and five external variable regions (V1-V5). The C1 and C5 domains bind the gp41, while the C2-C3-C4 domain form a hydrophobic core within the molecule structure. Instead, V3 domain is involved in the co-receptor recognition mechanism, mediated by conformational changes that occur following the binding of the glycoprotein to the primary receptor (28). Depending on the receptor binding, the virus establishes tropism either for T lymphocytes (CXCR4) or the macrophage lineage (CCR5) (29).

The **gp41** consists of three main domains: the ectodomain, catalysing the fusion between viral and cellular membranes during virus penetration; the anchoring domain, securing the SU/TM complex to the host membrane and a cytoplasmic tail (25).

At the end of the normal cellular protein maturation process, gp120 and gp41 undergo glycosylation, a crucial step for the virus's infectivity. During the budding phase from the plasma membrane, these proteins are incorporated into the mature virion (28).

### 1.5.4 Regulatory proteins

**Tat** (Transactivator of transcription) is a small 14-16 kDa protein, encoded by two exons located at the 3' end of the viral genome. The primary function of Tat is to transactivate viral RNA transcription. This is achieved through the binding of Tat's basic domain to a region within the 5' LTR (TAR), thereby increasing the number of transcripts from the viral genome at the LTR level (30). Several studies have demonstrated that Tat can recruit the active form of the transcription elongation factor (P-TEFb), composed of the cyclin T1 subunit and the cyclin-dependent kinase (Cdk9). The latter phosphorylates the C-terminal domain of RNA polymerase II, enhancing its processivity and promoting the formation of complete transcripts (31). Observations have indicated that Tat also enhances the transcription initiation rate by being involved in chromatin structure modification events (29). In addition, Tat protein exhibits pleiotropic effects by modulating the expression of numerous cellular genes, cell survival, proliferation, and angiogenesis (32). Importantly, Tat can also act as an extracellular particle when secreted by infected cells, interacting with non-infected cells in a paracrine manner (33). Due to its involvement in a variety of processes, Tat represents an excellent target for both gene therapy and vaccination.

The **Rev** (Regulator of virus expression) protein plays a crucial role in the nuclear export of mRNA containing introns. The N-terminal region of the protein contains a sequence rich in arginine, serving both as a nuclear localization signal (NLS) and an RNA-binding domain (RBD). The C-terminal domain, rich in leucine, houses the nuclear export signal (NES) (34). Rev carries out its function by initially binding to the RRE element of viral messengers that do not undergo splicing. Subsequently, it recruits CRM1 and other cellular proteins, including Ran-GTP. This complex is exported out of the nucleus, and in the cytoplasm, it dissociates, releasing intact viral RNA (35).

### 1.5.5 Accessory proteins

**Vif** (Viral Infectivity Factor) is a highly conserved protein found in lentiviruses and is produced during the final stages of the viral replicative cycle. Its activity is closely linked to the host restriction factor APOBEC3 (A3) (36). In particular, it plays a crucial role in

generating highly infectious mature virions, as it facilitates the degradation of antiviral A3 proteins through the host ubiquitin-proteasome pathway, enabling viral immune evasion (37).

**Vpr** (Viral protein R) is a protein of approximately 14 kDa, and its main function is to transport the viral nucleocapsid complex into the nucleus, where it is subsequently integrated into the host genome. This process is facilitated by an unconventional nuclear localization signal (NLS) (38). Moreover, Vpr is known to play multiple roles at different stages of the HIV-1 viral life cycle. It induces cell cycle arrest at the G2/M phase, enhances viral activity by regulating apoptosis (39), and accomplishes this by hijacking E3 ubiquitin ligases. Consequently, Vpr targets multiple cellular proteins for proteasomal degradation, leading to a global remodelling of the cellular proteome (40).

**Vpu** (Viral protein U) is a membrane-associated protein, predominantly expressed on intracellular membranes, including the endoplasmic reticulum (ER), trans-Golgi, and endosomal compartments. One of its main functions is to recruit newly synthesized CD4 from the endoplasmic reticulum and mediate their degradation through the proteasome. This prevents the formation of the CD4-Env complex, thus facilitating the normal assembly of the virion (41).

**Nef** (Negative regulatory factor) is a 27 kDa myristoylated protein primarily found in the cytoplasm of infected cells, with partial recruitment to the cell membrane. It is expressed in the early phase of infection and is required for efficient viral pathogenesis *in vivo*. In fact, Nef plays a fundamental role in virus replication, infectivity and in the progression of AIDS (42), (43).

The main characteristics and functions of Nef will be elucidated in detail in the following paragraphs

## 1.6 HIV-1 replication cycle

The HIV-1 life cycle consists of several events involving both viral and cellular factors. It is generally divided into two phases: the *early* phase, which encompasses all events from target cell recognition to provirus integration into the cellular genome, and the *late* phase, during which transcriptional and protein synthesis events occur, culminating in the formation of new virions. These virions are released through budding, becoming mature and infectious (Fig. 5) (44).

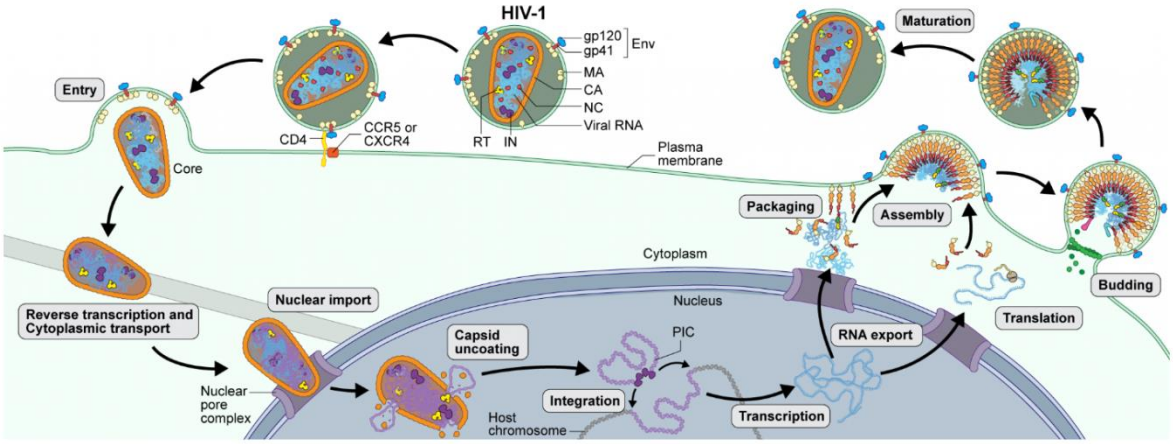


**Figure 5** Schematic overview of the HIV-1 replication cycle (*https://scienceofhiv.org/wp/life-cycle/*).

### 1.6.1 Early phase

#### *Entry and Uncoating*

The initial stages of infection involve intricate interactions, some of which are nonspecific, between viral proteins and cellular factors. The virus establishes its first contact with the cellular membranes through electrostatic forces, resulting from the interaction between Env and various cell attachment molecules, such as the α4β7 integrins, the intracellular adhesion molecules (ICAM) and the negatively charged heparin sulfate proteoglycans (45). This interaction allows the virus to anchor itself to the target cell. The primary recognition event occurs between the surface glycoprotein, gp120, and the CD4 receptor, expressed on various cell types, including T lymphocytes, monocytes/macrophages, dendritic cells, and the microglia of the central nervous system.

The binding between gp120 and the N-terminal region of CD4 induces a conformational change in the variable domains V1/V2 of gp120, and subsequently, in the V3 domain. The V3 domain modifications determine the tropism of HIV for the specific co-receptor, either CCR5 or CXCR4 (46).

Following co-receptor binding, a conformational change in gp41 occurs, exposing a hydrophobic domain known as the fusion peptide (47). This peptide comprises two helical regions: an N-terminal (HR-N) and a C-terminal (HR-C). In the assembled trimer, these two regions come together to form a six-helix bundle (6HB) binding domain. This domain holds the membranes close, creating a fusion pore, and subsequently, complete membrane fusion occurs, resulting in the release of the viral core into the cytoplasm (48) (Fig. 6).

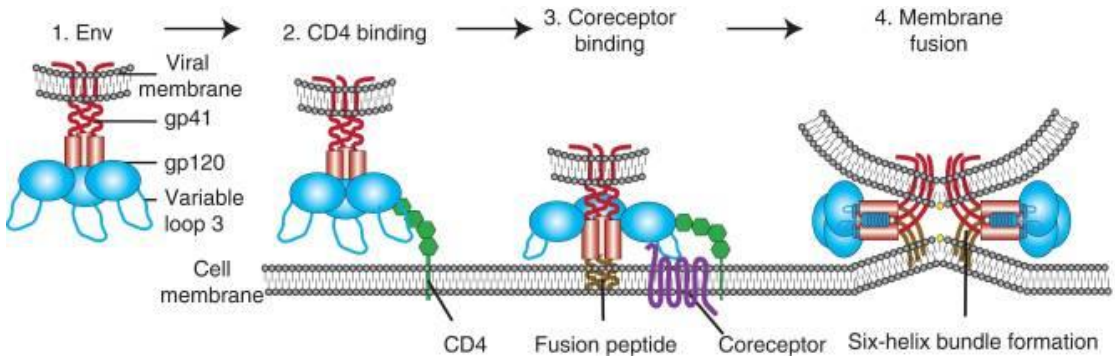


**Figure 6** Overview of cell binding and entry (47).

In addition to traditional cell-free virus infection, an alternative mechanism for the viral spread involves cell-to-cell transfer of virions. This method requires close proximity between cells carrying the virus and uninfected target cells. This entry pathway is more expedient and efficient than the fusion of cell-free virions, bypassing the initial attachment steps and allowing the virus to effectively evade the humoral immune response (49).

Regardless of the pathway, the entry process concludes with the release of the viral capsid into the cytoplasm. A successful infection relies on the precise dissociation of the capsid protein (CA) from the HIV-1 core (50). Subsequently, the nucleocapsid is released into the cytoplasm (*uncoating*).

Recent live-cell imaging, combined with fluorescently tagged markers, reveals that uncoating occurs in the cytoplasm within the first thirty minutes after entry (51).

***Reverse transcription and nuclear import***

The reverse transcription process converts a single-stranded RNA (ssRNA) template into double-stranded DNA (dsDNA or cDNA or proviral DNA), essential for integration into the host cell's genome. The reaction is catalysed by the reverse transcriptase enzyme (RT) that has two primary activities: DNA/RNA-dependent DNA polymerase and RNase H. These activities work in tandem to synthesize the new DNA strand and cleave portions of genomic RNA from the DNA/RNA duplexes (23) (Fig. 7).

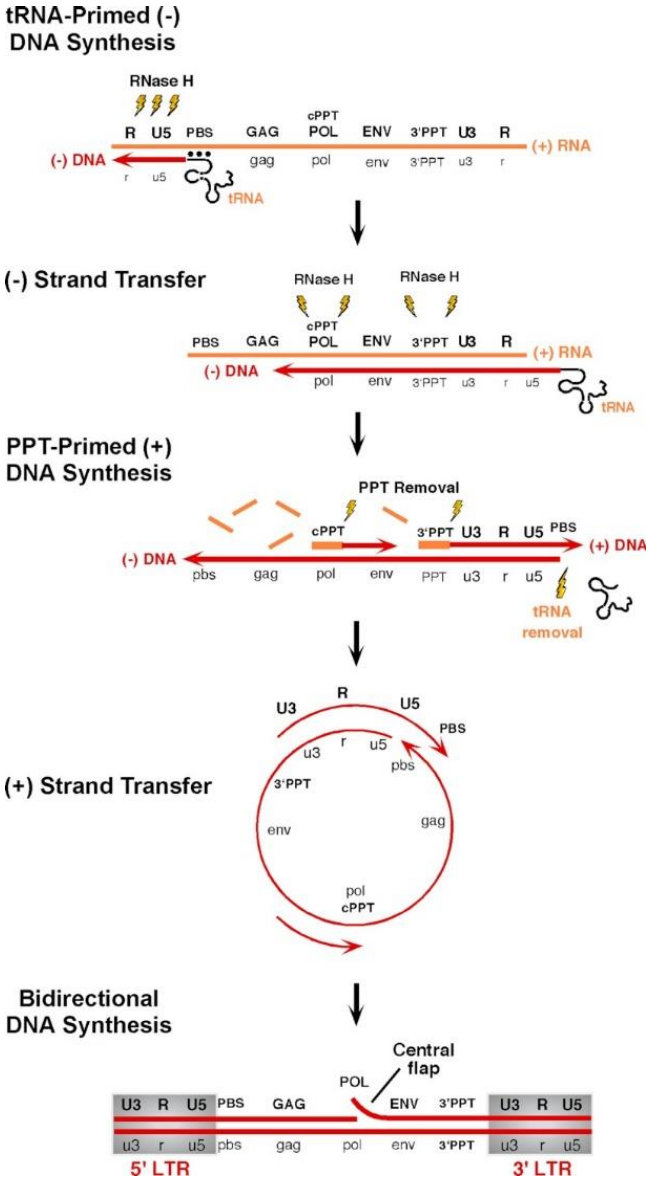


**Figure 7** Reverse transcription process of HIV-1 (23)

The process begins with the annealing of $tRNA^{Lys}$ to the primer binding site (PBS) region, located at the 5' end of the viral genome. This site acts as a primer for reverse transcriptase, initiating the synthesis of the negative-DNA strand (-) and resulting in the formation of an RNA/DNA hybrid. Through the RNase H activity, the RNA strand of the hybrid is degraded.

The ssRNA genome features distinct ends marked by a specific motif, comprising a repetitive region (R) that is identical for both the 5’ and 3’ ends and a unique region that differs between the 5’ end (U5) and the 3’ end (U3). Following annealing to the R sequence at the opposite end of the template RNA, the newly synthesized cDNA is translocated from the 5’ end to the 3’ end, where the synthesis of the (-) strand resumes. The RNA molecule is not degraded in correspondence of a small purine-rich segment (PPT) which are resistant to RNase H activity and serves as a template to form the second positive-DNA strand (52). After the degradation of the tRNA primer at the 3’ end of the (-) DNA strand, a second strand transfer takes place. This transfer moves the incomplete (+) DNA from the 3’ to the 5’ of the DNA template, resulting in the complete synthesis of a double-stranded DNA (cDNA). The cDNA is longer than the viral RNA due to the duplication of the U3-R-U5 regions, leading to the formation of the Long Terminal Repeats (LTRs) (53).

In the last phase of the reverse transcription process, the reverse transcription complex (RTC), consisting of the newly formed cDNA associated with integrase (IN), capsid proteins, and some cellular proteins, transitions into the pre-integration complex (PIC), which is subsequently transported into the nucleus (52). The nuclear import is mediated by the nuclear localization signals (NLS) of the MA protein, which interact with importins, and the unconventional NLS of Vpr and IN, facilitating direct contact with the nuclear pore.

***Integration***

The integration process, consisting of the insertion of the cDNA in the host cell genome, occurs in the nucleus and is the hallmark of retrovirus replication. This process begins within the PIC as the complex is translocated from the cytoplasm to the nucleoplasm and is catalysed by the integrase (IN) enzyme, involving several cellular factors that influence the selection of integration sites.

The enzyme cleaves both the viral cDNA and the cellular genome. In particular, some nucleotides at the 3' end of the viral cDNA are removed, generating free CA-OH ends that insert into the cut produced in the cellular genome, resulting in a hybrid duplex molecule (54).

Finally, the remaining unpaired nucleotides at the 5' viral end are eliminated, and through ligation, the ends are linked, forming the HIV-1 *provirus* (55), (56). This provirus can either be transcriptionally active or enter latency, contributing to the viral *reservoir*.

The integration site plays a crucial role in determining the fate of the provirus and is influenced by various factors, including chromatin structure, cell cycle phase, sequence specificity, and cellular elements. Viral transcription occurs when integration takes place in permissive chromatin regions. Conversely, in non-permissive regions, transcription is silenced, potentially contributing to the formation of latent viral reservoirs (57). Other factors that may induce latency include the absence or low expression of Tat and/or Rev and minimal promoter stimulation. Additionally, several cellular proteins, such as histone deacetylase (HDAC) and the antiviral factor found in from CD8+ cells, can lead to the suppression of infection in the infected cell (58).

It is well-established that HIV typically integrates its genome within actively transcribed regions; therefore, the activated CD4+ T cells are the primary target of productive infection. While the majority of these cells succumb to the infection, some may transition to a quiescent state. In this state, the virus is integrated and latent, unable to establish a productive infection and evading both immune defences and therapy. Consequently, the viral reservoir mainly comprises quiescent memory CD4+ T cells, which, in turn, can reactivate and lead to the production of infectious virus (59), (60). For this reason, the viral reservoir represents one of the most significant obstacles to the HIV eradication.

Lastly, the integration can result in defective products, including circular forms like 1-LTR and 2-LTR. The formation of 2-LTR circles is driven by the activity of the cellular repair system, while 1-LTR circles can arise from defective reverse transcription, auto-integration from circular form rearrangement, or homologous recombination between 2-LTR circles (61), (62).

### 1.6.2 Late phase

#### *Transcription and Translation of viral genome*

Integration marks the transition from the early to late phase of HIV-1 life cycle, involving the transcription and translation of viral proteins, as well as the assembly and release of new virions (63).

Transcription initiates from the LTRs, specifically from the U3 region that shares sequence homologies with control regions of cellular genes. The promoter in this region exhibits low basal activity; hence, several elements take place to enhance transcription efficiency and RNA polymerase II processivity (64). The first mRNAs produced are those encoding Tat, Nef, and Rev proteins that require complete alternative splicing before leaving the nucleus. Subsequently, the mRNAs of the Env, Vpu, Vif, and Vpr proteins are transcribed, undergoing a partial splicing process. Finally, the mRNAs encoding the structural polyproteins, Gag and Gag-Pol, along with the mRNAs representing the new viral genome, are transcribed. However, these transcripts undergo no splicing process and are the last to exit the nucleus.

The nuclear export of viral mRNA is orchestrated by Rev, shuttling between the nucleus and cytoplasm and binding to the Rev responsive element (RRE) present on unspliced viral messengers. Subsequently, Rev recruits CRM1 (or EXP1) and other cellular proteins, including Ran-GTP, forming the export complex that facilitates the exit of messengers from the nucleus and their proper processing in the cytoplasm, giving rise to all viral proteins (65).

In contrast to the non-spliced mRNAs, those encoding Tat, Nef, and Rev utilize endocellular pathways to exit the nucleus (66).

Once all the mRNAs reach in the host cell's cytoplasm, they are translated into their respective proteins that contribute to the formation of the new viral particle.

***Virus assembly, budding and maturation***

After the synthesis of viral proteins, the assembly of new viral particles occurs. The Gag polyprotein coordinates essential events in this phase, including membrane anchoring, Gag-Gag interactions, viral RNA encapsidation, association with Env, and the final budding process.

The assembly begins with the migration of Gag, in the form of small oligomers, at the inner leaflet of the cell's plasma membrane (67). The process continues with the encapsidation of viral RNA, also mediated by Gag. HIV-1 incorporates two identical copies of RNA into the virion, which bind at a region near the 5' end, known as DIS (dimer initiation signal). This dimerization, occurring at both the plasma membrane and in the cytoplasm, serves as one of the recognition signals for virion assembly (68). NC also contributes to the multimerization of Gag, a key step in viral assembly (69).

The translocation of the Env polyprotein to the plasma membrane, conversely, is independent of Gag. Env undergoes post-translational modifications following passages through the rough endoplasmic reticulum (RER) and subsequently the secretory pathway, ultimately reaching the membrane. During this transit, Env is cleaved into its functional trimers, gp120 and gp41, by cellular proteases. The mechanism leading to Env incorporation is not yet completely understood, but it may be facilitated by the interaction between the cytoplasmic tail of gp41 and the MA domain of Gag (67).

The progression to virion budding begins as Gag moves to the lower region of the plasma membrane, exposing the Env trimers, and arranges itself within still immature spherical-shaped particles (Fig. 8).

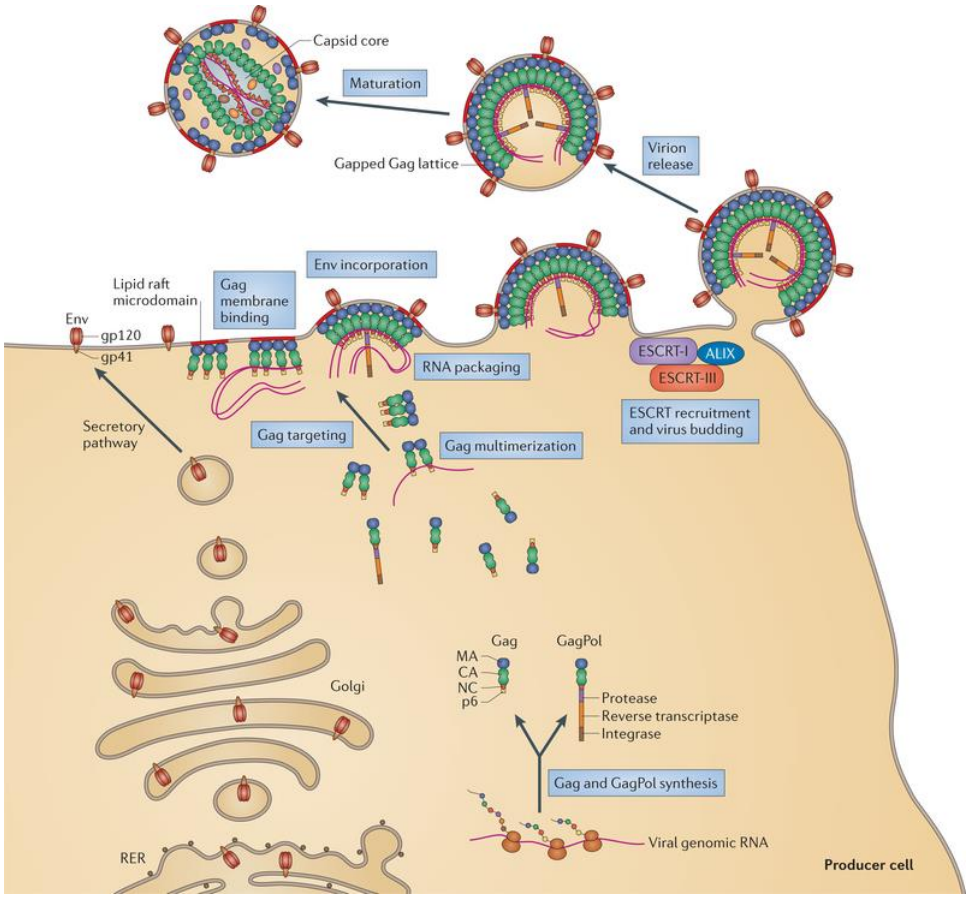


**Figure 8** The late stages of the HIV-1 replication cycle (67).

The final step of viral assembly corresponds to the release of the immature viral particle from the membrane of the host cell through a process known as *budding*. The release is orchestrated by specific domains of the $p6^{Gag}$ protein, that induce a constriction in the virion protrusion, leading to the budding of the virion from the infected cell (Fig. 8).

To achieve maturation and, consequently, infectivity, the viral protease plays a pivotal role by cleaving the Gag and Gag-Pol polyproteins (70). This step is essential for releasing all mature proteins. Notably, the liberation of CA induces conformational changes, enabling the viral core to adopt its characteristic conical shape. The mature viral particle becomes infectious and, thus, capable of initiating a new replicative cycle.

## 1.7 HIV-1 transmission and pathogenesis

According to the Centers for Disease Control and Prevention, HIV is transmitted through direct contact with infected blood, amniotic fluid, semen, pre-ejaculate, vaginal fluids, rectal fluids, and breast milk, involving mucosal tissue, blood, or damaged skin. Transmission can occur through unprotected sexual intercourse, sharing contaminated needles or syringes, mother-to-child transmission during childbirth or breastfeeding, and less commonly, through blood transfusions or organ transplants from infected donors (71). Presently, around 85% of new infections result from sexual transmission (4). Factors that enhance the infectiousness of an individual with HIV include elevated virus levels in plasma or genital secretions, as well as the presence of other sexually transmitted infections (72).

The persistent HIV replication in the host leads to a gradual depletion of the immune system, culminating in Acquired Immune Deficiency Syndrome (AIDS) and eventual death in the absence of antiretroviral therapy. The clinical progression unfolds in three main phases: primary infection (acute), late infection (chronic), and the advanced AIDS phase (Fig. 9). The pathogenesis of HIV-1 infection results from the intricate interplay among the virus life cycle, the host cellular environment, and immune responses, involving both cell-mediated and immune-mediated reactions. This dynamic interaction influences the complex trajectory of the disease from initial infection to the profound immunosuppression characteristic of advanced AIDS (9).

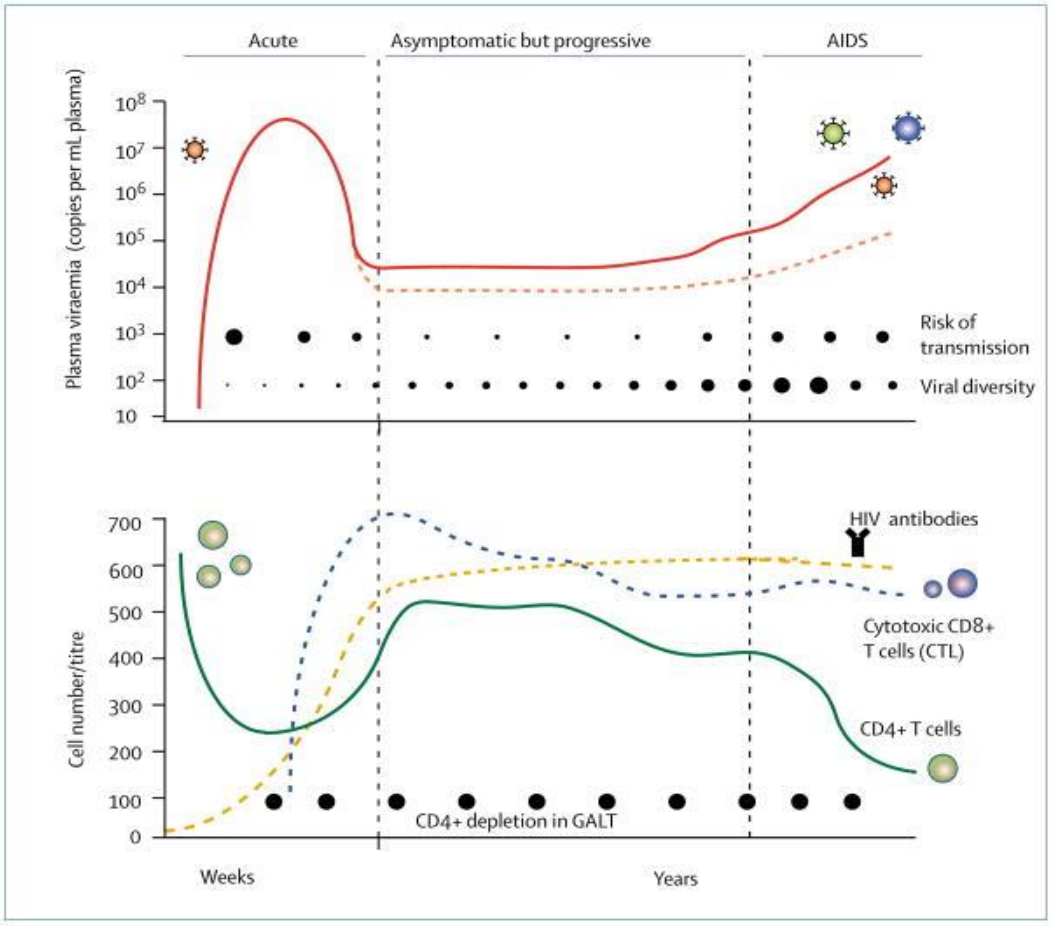


**Figure 9** Clinical course of HIV-1 infection (9)

Primary HIV infection encompasses the period between the virus's entry into the organism and the development of non-neutralizing antibodies against it, known as seroconversion (9).

The initial approximately two-three weeks represent the "window period" of the infection, characterized by viral replication and dissemination in the body, especially in the mucosa-associated lymphoid tissue. Infected individuals typically remain asymptomatic: there is an ongoing immune response within the body, however the seroconversion may not yet has occurred (9). The acute phase is characterized by a significant increase in plasma viremia, reaching approximately $10^6$-$10^7$ copies of viral RNA/ml. Concurrently, there is an elevation in the numbers of infected CD4+ T-lymphocytes and virions in both the bloodstream and lymph nodes, with the secondary amplification occurring in the gastrointestinal tract, spleen, and bone marrow, resulting in extensive infection of susceptible cells (9). In close temporal relation to the resulting peak of viremia, clinical symptoms such as fever, arthralgia, myalgia, and a skin rash can manifest. During the peak of viremia and in the subsequent three months,

immunocompetent individuals develop an immune response, including the production of antibodies against viral proteins (9). Simultaneously, a cell-mediated response is activated involving cytolytic CD8+ lymphocytes and CD4+ T helper cells targeting antigens expressed by infected cells (73). As a result, there is a gradual depletion of CD4+ T lymphocytes, while the number of CD8+ T cells undergoes a rapid increase, resulting in an inverted CD4/CD8 ratio (<1) (7). After approximately 6-8 weeks, the acute phase is followed by an intense reduction in viremia, reaching a level defined as the "set point". This reduction is attributed to both the immune system's partial control of the infection and the reduction of T-lymphocytes. Regarding CD4+ T cells, there is a rapid decline in this T-cell subtype that stabilizes once viremia reaches its peak. Subsequently, there is a partial recovery of CD4+ T cells, establishing a delicate balance between viral replication and the immune response but no eradication of the viral infection occurs (7).

Chronic infection, also defined as clinical latency, can vary widely in duration, extending to several years. Clinical latency does not correspond to viral latency; despite the absence of clinically identifiable symptoms related to HIV infection, the virus continues to actively replicate in the cells of lymphoid tissues, particularly in the gut-associated lymphoid tissues (GALT) (7), (9) . The replication of the virus is countered by the host's antiviral response, characterized predominantly by the development of neutralizing antibodies against gp120 (occurring after approximately 3 months), T cells, and natural killer (NK) cells (9). However, one of the hallmarks of HIV-1 is its ability to evade immune system and to be a fast-evolving virus. Thus, antibodies are not able to protect the host in the long term (74).The rate of progression toward the final phase of the disease varies widely among infected individuals. Typically, in the absence of therapy, after approximately 10 years of infection, an imbalance between the immune system and viral replication emerges (9). This is marked by a significant increase in plasma viremia and a reduction in CD4+ lymphocytes. When the count of CD4+ T lymphocytes drops below 200 cells/µl of plasma, it is considered advanced AIDS, characterized by a severely depleted immune system incapable of mounting an effective response. This vulnerability exposes individuals to various opportunistic infections, both bacterial and viral, ultimately leading to the death of the infected individual (75).

Multiple factors influence the pathogenesis of HIV, including the type of target cell. It is important to note that, although CD4+ T lymphocytes are the primary target of the virus, other cell types, such as CD8+ T lymphocytes, natural killer (NK) cells, dendritic cells (DCs),

and monocytes/macrophages, can also be infected (76). Dendritic cells promote virus dissemination through the formation of infectious synapses. While the virus cannot establish a productive infection within these cells, it is not degraded. HIV also selectively targets monocytes, which, upon migrating to tissues, differentiate into macrophages. Once infected, they better evade the host's immune defences, establishing a persistent infection and serving as a primary viral reservoir. Moreover, these cells have the capability to migrate to various tissues and organs, including the brain. Due to these characteristics, infected macrophages play a pivotal role in in HIV pathogenesis, especially concerning its chronicity and widespread dissemination (77).

As previously discussed, the hallmark of HIV-1 infection is the progressive depletion of both naïve and memory CD4+ T-lymphocyte populations. However, this reduction in CD4+ T cells is not solely attributed to the direct impact of the virus but also results from the intense and persistent activation of the immune system, leading to a state of chronic inflammation (9), (77).

Two distinct categories of patients, characterized by atypical infection patterns, have been identified based on virological and immunological parameters: *elite controllers* (ECs) and *post-treatment controllers* (PTCs). These individuals exhibit an ability to control viral infection, although the specific viral and host mechanisms involved remain unclear (78), (79).

*Elite controllers* are defined by the ability to spontaneously suppress plasma viremia for prolonged periods without antiretroviral therapy. They represent approximately 1% of the infected population and are characterized by a higher number of CD4+ T lymphocytes, resulting in a slower progression of HIV infection. Despite significant variability among patients, genetic and immunologic parameters have been identified to effectively characterize this group. In particular, on a genetic basis, there is an overexpression of protective HLA alleles, such as HLA-B57, HLA-B27, and HLA-B*5801 (80). Immunologically, this group is characterized by the presence of polyfunctional CD8+ T-cells exhibiting superior inhibition of HIV-1 (78).

Contrastingly, *post-treatment controllers* are HIV+ individuals who received early treatment, diagnosed during the detectable acute phase. They underwent prolonged antiretroviral therapy for approximately 4 years. Following the cessation of treatment, they can sustain plasma viremia below the detectable limit for an extended period before experiencing a viral rebound.

PTCs frequently exhibit symptomatic acute retroviral syndrome and high viral loads, in contrast to elite controllers, which likely contribute to their early diagnosis and ensuing early antiretroviral treatment. The presence of protective HLA-class I allele variants is not decisive in post-treatment controllers, except for the HLA-B*35 variant, associated with a more rapid disease progression. The efficacy of CD8 T-lymphocytes in inhibiting HIV-1 replication is relatively reduced in PTCs compared to ECs. Additionally, the expression of a specific set of immunoglobulin-like receptors, known as KIR, on the surface of NK-cells, seems to limit viral replication. Among these, KIR3DL1 expression has been linked to a slower disease progression, and NK-cells in this patient group exhibit higher IFNγ production, thereby imparting greater control over the virus (79).

## 1.8 HIV diagnosis

A timely and accurate diagnosis of the infection is crucial not only for the benefits derived from starting an early antiretroviral therapy but also for minimize the risk of further transmission. The current guidelines from the US Centers for Disease Control (71) and European Centre for Disease Prevention and Control (81) recommend employing a fourth-generation antigen–antibody assay for screening and diagnosis: the ability to detect both antigens and antibodies in the same test offers the advantage of identifying the infection even in the absence of antibody production, as observed during the window period, or in some cases of immunocompromised patients. Positive samples must be confirmed using a Recombinant ImmunoBlot Assay (RIBA). The virological diagnosis is further confirmed by quantitative analysis, utilizing RT qPCR assays (Reverse transcriptase-quantitative polymerase chain reaction), to detect the presence of HIV-RNA in plasma (viremia or viral load). Furthermore, the HIV viral load acts as a prognostic marker, enabling the prediction of the infection's clinical progression risk and the evaluation of the extent of therapeutic response (82).

An additional virological analysis involves the search of proviral DNA extracted from peripheral blood mononuclear cells (PBMCs). Proviral DNA testing is typically conducted in children born to HIV-positive mothers, since conventional screening tests may yield false positives, due to the transfer of maternal antibodies from the placenta to the fetus.

*Timing* of the infection is another important aspect in the context of HIV diagnosis, especially for epidemiological purposes. For this reason, the avidity test was implemented. The method is able to measure the bond strength between antibodies (IgG class) and the corresponding antigen, which increases over time during HIV infection.

Consequently, using a denaturing reagent (urea, guanidine) that acts on the Ag-Ab binding, it is possible to distinguish between recent (low avidity, < 6 months) and previous infections (high avidity, > 6 months) (83).

The Italian guidelines (82) also recommend to perform a drug resistance test, based on sequencing methods, for all newly diagnosed HIV+ individuals, naïve to antiretroviral therapy (ART). This is crucial for assessing transmitted primary drug resistance, to ensure an accurate therapeutic approach and to maintain a prolonged virological suppression, as well as immune and clinical homeostasis. The drug resistance test is also performed in cases of treatment failure due to the emergence of therapy-resistant mutant variants.

Finally, the immunological diagnosis is based on lymphocyte count: the CD4+ T cells act as a prognostic marker linked to the clinical progression of HIV-1 infection. A low percentage of CD4+ T-lymphocytes is associated with a more rapid disease progression and impacts therapy efficacy. In people living with HIV (PLWH) under stable antiretroviral therapy, the recovery of CD4+ T-cells is connected to CD4+ nadir value, aging, and co-infections (84), (85). Another crucial parameter is the CD4+/CD8+ ratio, considered an index of immune system restoration (86). Prior to therapy administration, PLWH typically exhibit an inverse ratio, which is restored only in a few cases (87).

## 1.9 Antiretroviral therapy

The AntiRetroviral Therapy (ART) has emerged as a groundbreaking and transformative approach in the management of HIV infection and represents a pivotal milestone in the medical landscape. The therapeutic strategy involves the use of a combination of different antiretroviral drugs to suppress and maintain viral replication under undetectable levels (≤ 20 copies/ml) and restore the CD4 cells count, mitigating the risk of clinical complications and reducing the likelihood of transmission. Thanks to ART, HIV infection shifted from a once fatal diagnosis to a chronic yet manageable condition (88). Although ART successfully

suppresses active viral replication, it falls short in eliminating the viral reservoir, allowing latently infected cells to persist over time. Indeed, it is important to emphasize that discontinuation of therapy can reactivate the latent virus in the reservoirs, leading to a new cycle of productive infection and a subsequent rebound of viremia (88). Latency represents a critical obstacle to complete infection eradication, driving ongoing research efforts focused on modelling new molecules and strategies. Therefore, the primary objective is to supplement current therapy with innovative approaches capable of effectively purging the viral reservoir and achieving the ultimate goal of eradicating HIV-1 infection.

Moreover, in some cases, treated patients may develop drug resistance, due to the virus's rapid genetic evolution. HIV employs this strategy to evade not only immune system control but also the therapeutic effects of ART in blocking certain stages of the viral lifecycle. For this reason, it is crucial to carefully assess the appropriate therapeutic regimen to ensure better adherence to the treatment and, at the same time, minimize potential side effects (89).

Currently, ART is initiated immediately after diagnosis (82). The TEMPRANO study (90) has demonstrated that an early start, facilitated by the improved tolerability and safety of modern drugs, ensures limited reservoir filling, slows the progression of the disease, and preserves the immune system from damage. Moreover, a recent study by Leyre et al. has confirmed that starting ART as soon as possible ensures a rapid clearance of the pool of cells that are early targets during acute infection (91).

ART encompasses various drugs that target the specific step of the virus' replication cycle. Using a combination of drugs, rather than just one, enhances treatment effectiveness and reduces the risk of treatment failure. Today, therapeutic regimens typically include an integrase inhibitor as the 'anchor drug,' supplemented by other inhibitors of viral enzymes (71), (82).

*Nucleoside Reverse Transcriptase Inhibitors (NRTIs)* are analogues of structurally modified nucleosides or nucleotides and act by blocking RT in the early stages of replication, following the virus's entry into the cell. These molecules are activated by cellular kinases through phosphorylation, and once converted into the active triphosphate form, they compete with natural nucleotides for binding to reverse transcriptase. Upon incorporation into the growing DNA strand, they induce premature termination (acting as chain terminators) or alter its function. This class of molecules is often referred to as the 'backbone' in a first-line HIV

treatment combination (72). Drugs belonging to this class include: Zidovudine (known as AZT, it's the first drug approved for antiretroviral therapy), Tenofovir Disoproxil Fumarate (TDF), Emtricitabine, Abacavir, and Lamivudine. Tenofovir is associated with a gradual and consistent decline in kidney and bone function, with the rare occurrence of Fanconi syndrome as a potential complication (92). Tenofovir alafenamide fumarate (TAF) is a newly formulated prodrug of tenofovir, exhibiting reduced kidney and bone toxicity. TAF may have greater penetration into lymphoid tissues (the primary site of HIV) compared to TDF (72).

*Non-Nucleoside Reverse Transcriptase Inhibitors (NNRTIs)* are non-competitive compounds highly selective for reverse transcriptase. They operate through an allosteric mechanism at the enzyme's active site, binding to the hydrophobic pocket of the p66 subunit of RT without phosphorylation. This induces a conformational change that inhibits the enzyme function. These molecules are potent, safe, and easy to produce. When used in adherent patients as part of three-drug regimens, these drugs have demonstrated remarkable effectiveness (72). Currently, both first-generation drugs (Nevirapine, Efavirenz) and second-generation drugs (Rilpivirina e Doravirina) are in use.

*Protease Inhibitors (PIs)* act in the final phase of the replication cycle by blocking the protease enzyme, essential for proteolytic cleavages on the Gag and Gag-Pol polyproteins. As a result, the new viral particles are non-functional and unable to infect other cells. These drugs are rapidly metabolized by the liver and are often co-administered with molecules that inhibits these metabolic pathways (Ritonavir or Cobicistat, defined as 'boosters') (72).

*Integrase Strand Transfer Inhibitors (INSTIs)* act at the nuclear level preventing the integration of the DNA strand into the host cell's genome. Blocking integration not only halts the production of infectious viral particles but also can hinder the formation and persistence of reservoirs (72). They are characterized by a very high genetic barrier, and are well-tolerated and safe.

*Fusion Inhibitors* explicate their function outside the cell, targeting the viral transmembrane glycoprotein gp41. The first drug of this class is Enfuvirtide, which blocks the conformational change that leads gp41 to its active form. Several studies have demonstrated that Enfuvirtide remains effective against strains resistant to reverse transcriptase and protease inhibitors (93).

*Entry inhibitors* are a class of antiretroviral drugs that prevent HIV from entering host cells by interfering with the interaction between the viral gp120 protein and host cell entry receptors

and co-receptors. Maraviroc is been the first drugs approved in this class, which acts by inducing a conformational change in the CCR5 co-receptor, rendering it inactive.

Fostemsavir is a recent addition to the arsenal of approved drugs as an attachment inhibitor (94). It acts in the early phase of the HIV life cycle by blocking the conformational changes of gp120. Trial results have revealed not only good safety and efficacy but also the absence of cross-resistance to other currently licensed classes of antiretrovirals. This makes it a promising new treatment option for individuals with multidrug resistance who are at risk of disease progression and death. However, it's worth noting that polymorphisms in the gp120 sequence, more frequently observed in the non-M group, could potentially lead to the onset of drug resistance (95).

## 1.10 HIV-1 Nef: a multifunctional protein

The accessory Nef protein is uniquely expressed by primate lentiviruses (HIV-1, HIV-2 and SIV). Nef is located in the cytoplasm of infected cells and is partially recruited to the cell membrane. It is translated from a multiply spliced mRNA which generates a protein of 27–35 kDa, abundantly expressed during the early stage of the viral life cycle (96).

Nef was originally identified as an open reading frame (ORF) that partially overlaps with the 3'-long terminal repeat of HIV-1 and was named based on early evidence suggesting it acted as a "negative factor" for HIV-1 replication (97). However, contrary to this initial characterization, Nef plays significant roles in HIV-1 pathogenesis by actively promoting viral replication and spread *in vivo*, as well as facilitating immune escape for HIV-infected cells, as reviewed in (42).

Studies with Rhesus macaques infected with SIVmac showed that a large deletion in *nef* greatly attenuated viral replication and failed to progress to simian AIDS (43). In contrast, research conducted in Rhesus monkeys unequivocally demonstrated the crucial role of an intact *nef* gene in achieving high virus loads and the development of an AIDS-like illness in animals infected with the SIV (43). Later on, significantly flawed *nef* genes were identified in several long-term slow/non-progressors (LTNPs) with HIV-1 infection (98–100). All these individuals exhibited low viral loads and generally sustained consistent CD4+ T cell counts for over a decade after infection. Nevertheless, a subset of these individuals exhibited signs of immunodeficiency following extended asymptomatic periods (101), (102). Additionally, a minority of adult and the majority of infant macaques progressed to simian AIDS after infection with *nef*-defective SIV mutants (103). Significantly, the induction of an AIDS-like syndrome in transgenic mice is observed with the exclusive expression of HIV-1 Nef directed by the CD4 promoter, highlighting a direct involvement of Nef in HIV-1 pathogenesis (104), (105). This evidence suggests that, while Nef is not absolutely required for disease progression, it significantly expedites the progression to immunodeficiency.

The NMR structure analysis enabled the identification of four main regions of Nef: a flexible myristoylated N-terminal anchor domain, a loop containing a proline-rich region, a conserved well-ordered globular core structure, and a C-terminal flexible loop (or disordered loop) (Fig. 10). The N-myristoylation of Nef, along with a stretch of basic amino acids near the N-terminus, is required for its association with the cellular membrane and is crucial for all of its

biological activities (106). Further, myristoylation may also play a role in preventing Nef from multimerizing (107). The significant amount of flexible surface contribute to Nef's ability to interact with a large number of cellular partners, many of which are associated with the membrane (108). Additionally, the presence of the protein within virion particles could be attributed to Nef's ability to associate with cellular membranes (109).

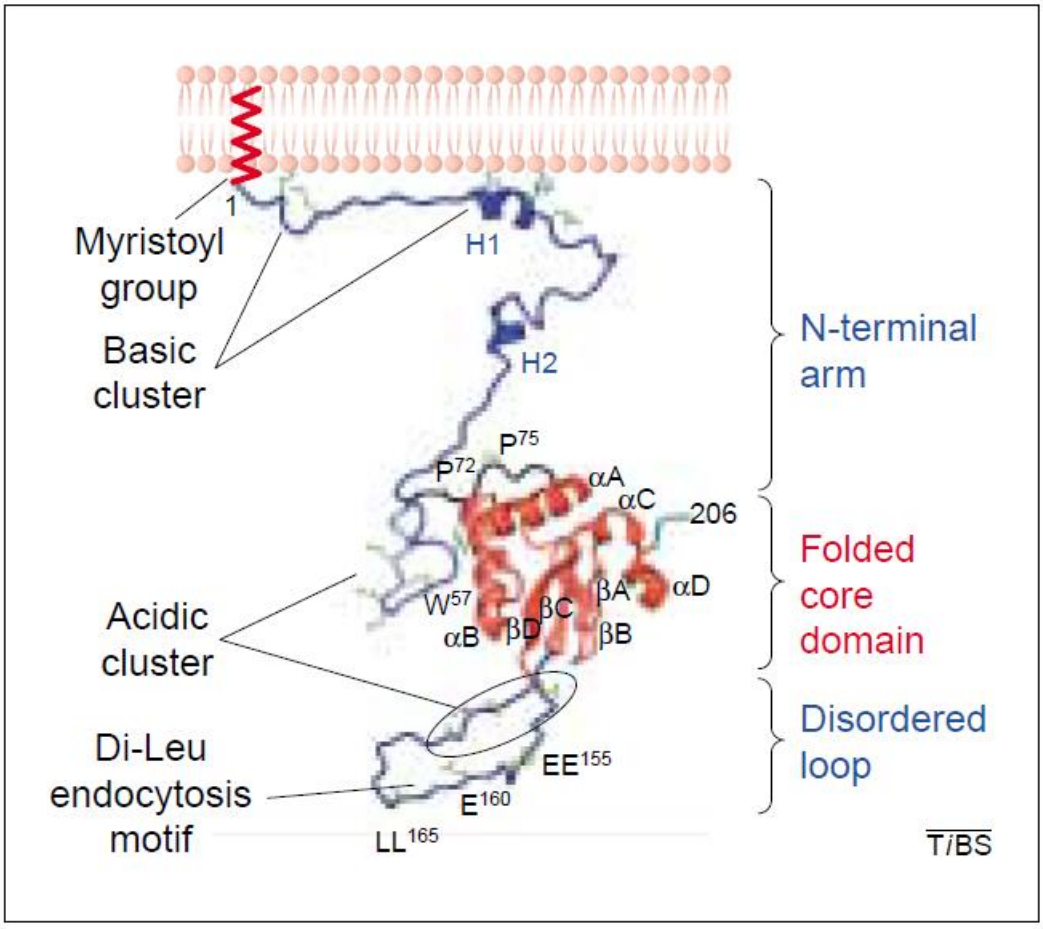


**Figure 10** A model of full-length Nef, anchored to the cellular membrane, built based on the NMR structures (110).

Arguably, the most striking aspect of Nef lies in its multifunctionality. It does not exhibit any known enzymatic or biochemical activities but exerts various cellular functions by interacting with a plethora of host factors. The most extensively characterized activities of Nef result from its ability to engage with the cellular vesicular trafficking machinery and thus perturbing cell signalling (111).

### 1.10.1 Modulation of cell-surface receptors by Nef

The HIV-1 Nef is recognized for orchestrating the modulation of critical cell surface proteins essential for the immune synapse, constituting a pivotal viral strategy to regulate cell communication and behaviour, thereby establishing persistent infection (112). A distinctive feature of Nef resides in its ability to manipulate the intracellular trafficking machinery, finely tuning the expression of cell-surface proteins. This manipulation results in diverse effects on the surface expression of various proteins. Nef upregulates the surface expression of TNF, LIGHT (113), DC-SIGN (114), and immature (invariant chain-associated) major histocompatibility complex class II (MHC-II) (115). In contrast, Nef downregulates the surface expression of several other proteins, including CD3 (for SIV and HIV-2) (116), (117) tetherin/BST2 (for SIV) (118), CD8 (119), CD28 (120), CXCR4 (121), CCR5 (122), CCR3 (123), CD1 (124), CD80/CD86 (125), CTLA-4 (126) and mature (antigenic peptide-loaded) MHC-II (115).

Among its well-defined functions, Nef proficiently downregulates major histocompatibility complex I (MHC-I) and CD4 proteins, reviewed in (127). These regulatory processes are genetically separable and involve distinct mechanisms mediated through the endocytic adaptor protein complexes, AP-1 (128) and AP-2 (129), necessary for hijacking the proteins into the intracellular endo-lysosomal compartment. It was recently identified (130), (131) that Nef counteract the host restriction factors serine incorporators (SERINC) 3 and 5, by downregulating the molecules from the cell surface using a mechanism involving AP-2, contributing to the amplification of viral infectivity (132).

AP-1 and AP-2 are members of the heterotetrameric adaptor protein (AP) complexes, crucial components of clathrin-coated vesicles (CCVs). These vesicles play pivotal roles in trafficking within the endocytic and late secretory pathways, orchestrating precisely regulated routes of protein transport from various cellular locations, including the plasma membrane, *trans*-Golgi network (TGN), and endosomes. Their primary function is to deliver cargo to specific recipient compartments, predominantly endosomes or lysosomes, reviewed in (133). Nef manipulates vesicle trafficking dynamics by modulating the actions of adaptors like AP-1 and AP-2, along with other accessory proteins, leading to alterations in cargo recruitment selectivity and promoting CCV formation. Consequently, Nef effectively hijacks the vesicle

trafficking machinery, influencing the movement of cellular components within the cell and potentially impacting various cellular processes, reviewed in (134) (Fig. 11).

This control over cellular processes underscores Nef's key role in the intricate interplay between the virus and host cell machinery, setting the stage for further exploration into its multifaceted functions.

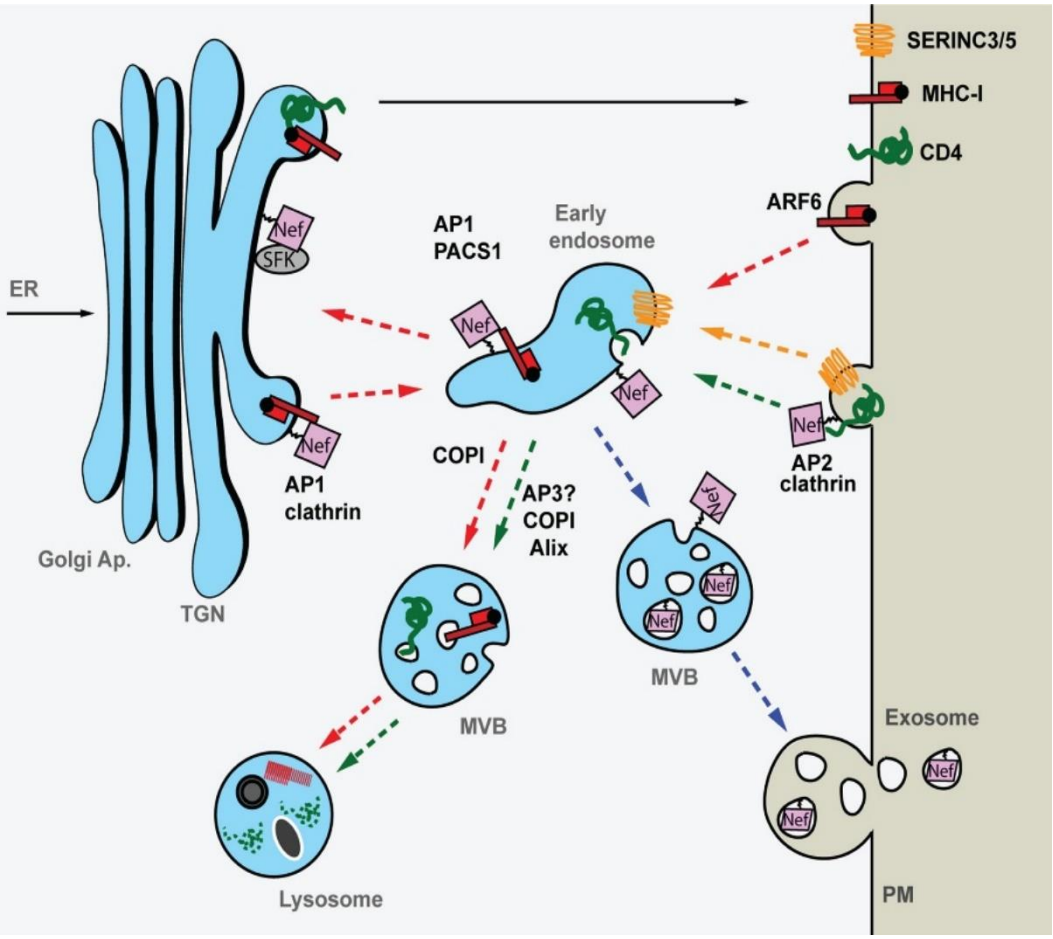


**Figure 11** Schematic representation of the protein trafficking pathways involved in MHC-1, CD4, and SERINC3/5 downregulation by HIV-1 Nef (134).

### *1.10.1.1 MHC-I downmodulation*

The MHC-I molecules play a crucial role in the immune system by delivering short endogenous peptides to the surface of antigen-presenting cells, enabling CD8+ (cytotoxic) T lymphocytes (CTLs) to recognize these epitopes. In the context of infected cells, viral peptides undergo processing and are presented on the cell surface, triggering the activation of CTLs and facilitating viral clearance. Thus, the antigen presentation mediated by MHC-I is an

indispensable pathway in adaptive immunity (135), (136). Due to its high expression levels in the early stages of infection, Nef is exceptionally well-suited to disrupt antigen presentation by sequestering MHC-I molecules in intracellular compartments via AP-1, directing them towards lysosomal degradation instead of plasma membrane presentation (133). This mechanism allows Nef to evade the destruction of newly infected cells by cytotoxic T lymphocytes (CTLs).

Peptides are transported into the ER lumen via the antigen processing transporter (TAP), where nascent MHC-I molecules fold. ER chaperones facilitate MHC-I-TAP interactions and peptide transfer. After loading, the MHC-I-peptide complex detaches from TAP, traveling through the ER and Golgi to the plasma membrane (133). Under physiological conditions, the endocytosis of MHC-I occurs by a clathrin-independent pathway and MHC-I does not engage with clathrin adaptors. However, in HIV-infected primary T cells, Nef promotes a direct interaction between the MHC-I cytoplasmic tail and the μ1 subunit of the clathrin adaptor complex AP-1 at the *trans*-Golgi network (128), (137).

The key elements of Nef crucial for MHC-I downregulation comprise an N-terminal α-helix, an acidic cluster (62EEEE65), a poly-proline cluster (PxxP) repeat located at the junction of the N-terminal loop and the folded core, and the residue Asp123 (138), (139).

The crystal structures of the HIV-1 Nef, MHC-I cytoplasmic tail (CD), and the μ1-C-terminal domain (CTD) complex reveal a cooperative assembly, mimicking the binding of physiological Tyr motifs to the μ1-CTD. In this configuration, a β sheet of μ1-CTD surrounds residues 314 to 332 of the MHC-I tail, with stabilization provided by Nef at positions 62EEEE65 and 72PxxP75. Additionally, extensive electrostatic interactions, mediated by specific Nef residues, were identified in this structure (133). The recruitment of AP-1 to specific microdomains on a donor membrane is dependent on the activity of the small GTPase Arf1. Nef enhances the membrane association of AP-1 in an Arf1-dependent manner, and the activity of Arf1 is crucial for stabilizing the Nef-dependent interaction between MHC-I and AP-1 (140), thereby preventing anterograde trafficking toward the plasma membrane.

The host PACS-1 and PACS-2 (phosphofurin acidic cluster sorting) proteins have been suggested as alternative pathways essential for Nef-induced downregulation of MHC-I. Specifically, Nef is recruited to the trans-Golgi network by PACS-1, where it activates Src-family kinases specific to the host cell lineage, such as Hck in macrophages and Lyn in T

cells. This kinase activity initiates a signalling cascade, increasing levels of membrane phosphatidylinositol (3,4,5)-trisphosphate through phosphoinositide 3-kinase. Consequently, the small GTPases Arf1 and Arf6 are activated, leading to the endocytosis of cell-surface MHC-I. Once internalized, MHC-I is sequestered in vesicles along with Nef and AP-1, preventing its recycling back to the plasma membrane (127).

Finally, Nef demonstrates a specific ability to downmodulate MHC-I HLA-A and HLA-B allotypes, while leaving HLA-C and HLA-E unaffected. This selectivity is attributed to a YSQA sequence in the cytoplasmic tail of HLA-A and HLA-B molecules, acting as a Nef binding site, which is absent in the other two types. Given that HLA-A and HLA-B play a primary role in presenting antigens to CTLs, and the expression of HLA-C and HLA-E inhibits natural killer cell-mediated lysis, it is proposed that Nef's selectivity enables infected cells to evade CTL-mediated killing while avoiding detection by NK cells (134).

Previous studies have shown that Nef's capacity to downregulate MHC-I in primary alleles varies significantly (141), (142), (143), and many aspects of this interplay in viral pathogenesis remain unclear.

#### *1.10.1.2 CD4 downmodulation*

The CD4 protein is a 55 kDa type I transmembrane glycoprotein, constituting a part of the T cell receptor on MHC class II-restricted cells, including helper/inducer T-lymphocytes and cells of the macrophage/monocyte lineage. Importantly, it functions as the primary cellular receptor for both HIV and SIV (112).

Structurally, CD4 consists of an N-terminal extracellular/luminal domain, a membrane-spanning region, and a short cytoplasmic tail (CT), which associates with the Src family protein tyrosine kinase, $p56^{lck}$, in T cells (144). In these cells, the physiological role of CD4 is to act as a co-receptor alongside the T-cell antigen receptor/CD3 complex in recognizing antigenic peptides bound to MHC-II molecules on antigen-presenting cells (APCs). CD4 plays a crucial role in stabilizing interactions between T cells and APCs and transduces a signalling cascade essential for immune responses. Upon T-cell activation, $p56^{lck}$ dissociates from the CD4 CT, leading to phosphorylation and subsequent internalization of CD4 via CCVs (145), (146).

Nef removes CD4 from the cell surface by enhancing its endocytosis through recruitment to the clathrin AP-2 complex and directing the receptor to lysosomes for degradation (147). The

persistent reduction in CD4 surface levels induced by Nef serves a dual purpose: preventing superinfection (148) and facilitating the release of viral progeny. This mechanism avoids harmful CD4-Env interactions within the producer cell (149), (150). The observed ability of Nef to downregulate CD4 is closely linked to viral pathogenesis (150), (151).

Nef-mediated endocytosis of CD4 does not rely on the phosphorylation of the CD4 cytoplasmic tail, distinguishing it from the process during normal T-cell activation (152). Nef associates with the endocytic clathrin adaptor AP-2 at the plasma membrane, forming a complex through the α:σ2 hemicomplex. This interaction leads to the accumulation of CD4 in emerging clathrin-coated vesicles (CCVs), initiating the endocytosis of CD4 via CCV-mediated mechanisms (153), (154).

Extensive mutational analysis has revealed three crucial domains within the conserved 27-amino acid central loop of Nef that play a key role in mediating interactions with AP-2. The dileucine motif (160LL165)and the newly identified hydrophobic motif (M168/L170) were predicted to engage with the σ2 subunit, while an acidic motif (174DD175) was proposed to interact with a basic patch in the α subunit (155–158).

The crystal structure revealed that most residues in Nef's central loop directly interact with AP-2. Meanwhile, D175 indirectly participates and aids in stabilizing the loop's conformation. These findings propose a model wherein Nef docks to the plasma membrane, bound to the complete AP-2 tetramer in an open conformation. In this model, the myristoylated N-terminus of Nef, including the 57WL58 motif,  is exposed, allowing contact with the membrane (159). Additionally, segments of the Nef central loop and membrane-proximal regions of AP-2 create a concave structure. This suggests that multivalent interactions among Nef, CD4, and AP-2 likely coordinate the assembly of this ternary complex (134).

Furthermore, Nef also directly binds to the CT of CD4. The specific determinants within the CD4 tail facilitating this interaction are not well-defined. However, a cluster of hydrophobic amino acids (M407 and/or I410) near the membrane and a dileucine motif (413LL414) are known to influence CD4-Nef association and the effectiveness of endocytosis. Moreover, the Nef N-terminal motif 57WL58 has been identified as mediating binding to the CT of CD4. Despite these insights, demonstrating the binding of Nef to CD4 *in vitro* remains challenging and is believed to have low affinity (160–162). This suggests that additional factors may contribute to stabilizing the Nef-CD4 interaction within cells.

Accelerated endocytosis is not the exclusive mechanism employed by Nef to sequester CD4 away from the plasma membrane. Interestingly, CD4 molecules internalized by Nef exhibit inefficient entry into a retrieval pathway from early endosomes (EE) back to the plasma membrane, redirecting them instead to lysosomes. It is probable that Nef commandeers both recycling and degradative pathways, leading to a prolonged depletion of CD4 (134).

While the pathways employed by Nef to downregulate CD4 and MHC-I molecules initially differ, both mechanisms involve Nef-induced formation of Clathrin-coated vesicles that bud either from the trans-Golgi network (Nef/AP-1-mediated MHC-I downregulation) or the plasma membrane (Nef/AP-2-mediated CD4 downregulation) and are directed to early endosomes (EE). The reduction in CD4 and MHC-I expression levels mediated by Nef can be restored by treatment with lysosomal inhibitors, indicating that Nef targets these receptors for lysosomal degradation (134).

Despite several research studies have shown a significant capacity of Nef to downregulate CD4 (141), (143), (163) the variability of the viral protein and its broad spectrum of action in downregulating CD4 still leave many questions unanswered about this function, particularly in the context of primary alleles.

#### *1.10.1.3 Mechanism of SERINC5 counteraction by HIV-1 Nef*

It has long been known that one of the most significant Nef function in HIV-1 pathogenesis is to enhance the infectivity of newly produced virus particles within the HIV-1 producer cell (164). However, only recently was the Nef target most crucial to infectivity enhancement identified as the host surface protein SERINC5, and to a lesser degree SERINC3 (130), (131).

The serine incorporator (SERINC) protein family constitutes a group of transmembrane carrier proteins conserved in all eukaryotes, from yeast to mammals, likely involved in lipid metabolism. They are thought to regulate the incorporation of the polar amino acid serine into cell membranes, thereby facilitating the biosynthesis of phosphatidylserine and sphingolipids (165), however, the exact nature of their molecular functions remains unclear. Five SERINC genes are present in the human genome, encoding homologous proteins with a similar predicted transmembrane topology (166). Among these, using complementary approaches, two recent groundbreaking studies have identified independently SERINC3 and 5 as host cell restriction factors against retroviral replication, targeted by Nef (130), (131). By comparing the transcriptomes of various types of producer cells, the Pizzato's group identified SERINC5

as the transcript that exhibits the strongest correlation with the dependence of Nef for virus infectivity. SERINC5 was observed to associate with virus particles and inhibit infectivity, but this effect was only evident in the absence of Nef (130). Simultaneously, through a comparison of the proteomes of cell-free virions produced in the presence and absence of Nef and glycoGag from murine leukemia virus, the Göttlinger's group revealed an enrichment of SERINC3 in Nef-defective virus particles. Additionally, SERINC5 was identified once again as the SERINC protein exhibiting the most potent inhibitory activity against viral infectivity (131).

SERINC5 is highly expressed in multiple tissues, including lymphoid lineages, suggesting its potential antiviral role against lymphotropic and myelotropic viruses like HIV, MLV, and EIAV, which have developed counteracting factors. Notably, only the larger SERINC5 splice isoform (SERINC5-001), encoding a 10-transmembrane domain protein, demonstrates significant expression and antiviral activity (167). The proposed model for SERINC5 activity in retrovirus infectivity suggests that the incorporation of SERINC5 into a virion particle hinders the delivery of the viral core to target cells. Nef, through mediating the endocytosis of SERINC5, counteracts its inhibitory effects by preventing its incorporation into virions.

A hallmark of SERINC5 is its capability to associate with virion particles. Although the mechanism remains unclear, it has been observed to preferentially localize within detergent-resistant domains of the plasma membrane, where virus budding could occur. This suggests that incorporation into virions might be a passive mechanism enhanced by colocalization with budding virions (168). Moreover, whether virion incorporation of SERINC5 is mandatory for its impact on infectivity remains unclear. However, a linear correlation between its level of incorporation into virions and the inhibition of infectivity strongly suggests that virus-associated SERINC5 plays a role in inhibiting particle infectivity (169). The specific step of the virus penetration process affected by SERINC5 and the molecular mechanism of this inhibition remain obscure Nevertheless, viral particles harboring the host restriction factor exhibit a reduced ability to deliver viral genetic material into the cytoplasm of target cells, likely due to impaired virus-cell fusion (170).

Concomitant with Nef's ability to exclude SERINC5 from virions is its capacity to downmodulate SERINC5's cell-surface expression. The reduction in SERINC5 surface expression is associated with its accumulation in late endosomes, indicating that the restriction factor undergoes endocytosis when Nef is expressed (166).

Clathrin-mediated endocytosis and AP-2 are essential for Nef to remove SERINC5 from the cell surface. The Nef determinants involved in this process are the same as those known to be crucial for CD4 downregulation, relying on the Nef dileucine motif (164LL165) and the conserved 57WL58 (169), indicating a dependency on AP-2 (130), (131). Nevertheless, SERINC5 lacks canonical AP-2- or Nef-interacting motifs, as suggested by bimolecular fluorescence complementation. The sensitivity of SERINC5 to Nef downregulation is localized to its largest intracellular loop (loop 4), particularly in two hydrophobic residues, L350 and I352 (171).

It has been suggested that the counteraction of SERINCs by Nef is also contingent on dynamin-2 (Dyn2), as indicated by a mutation at Nef D123. Dyn2 coimmunoprecipitates with Nef and is crucial for the enhancement of HIV-1 infectivity by Nef. However, there is currently no structural or biochemical confirmation of a direct Dyn2-Nef interaction using purified proteins. The Nef D123 mutation impairs the ability to counteract SERINC5 (172). Nevertheless, Nef D123 has been structurally implicated in AP-1 μ1-associated downregulation of MHC-I and in the dimerization of Nef (137). This suggests that establishing the full dependence of SERINC5 antagonism on a direct interaction with Dyn2 requires additional evidence.

After internalization, SERINC5 localizes to Rab5-positive early endosomes, Rab7-positive late endosomes, and Rab11-positive recycling endosomes. The first two suggest routing towards lysosomal degradation, in line with observations that SERINC5 is ultimately directed to lysosomes for degradation (132). The specifics transition from Clathrin-coated vesicles to the degradative lysosomal sorting pathway are not fully elucidated, but the involvement of ALIX and other endosomal sorting complexes required for transport (ESCRTs) is likely (133).

Moreover, the ability of Nef to antagonize SERINC5 varies greatly among primary alleles and subtypes, particularly due to the impact of naturally occurring Nef polymorphisms (173), (174), (175)and varies in magnitude between different HIV-1 isolates (176). Therefore, the impact of this counteraction on viral pathogenesis and the underlying mechanism remain not fully understood.

### 1.10.2 Nef's new frontier: the interaction with ACOT8

As previously described, Nef is a raft-associated protein, anchored to the cell membrane by its N-terminal myristoylation (177). The post-translational modification induces alterations in the viral protein's tertiary and quaternary structure (178), (179). In its myristoylated form, Nef primarily exists as a compacted monomer, adopting a 'closed' conformation in the cytosolic fraction. Upon association with the membrane and incorporation of myristate into the lipid bilayer, it shifts to an 'open' conformation, facilitating access to various cellular partners (110). However, myristoylation alone is not enough for lipid binding, suggesting that more complex interactions are required for Nef to undergo migration and associate with the membrane (177). In this context, it is known that Nef interacts with the human thioesterase 8 (ACOT8) (180), (181).

ACOT8 is a predominantly peroxisomal enzyme belonging to the acyl-CoA thioesterases (ACOT) family and is involved in lipid metabolism. The human ACOT8 gene is located on chromosome 20q13.12 and codes for a 319 aa residues protein of approximately 35 kDa (182). Due to the serine-lysine-leucine (SKL) peroxisomal targeting signal it localizes to peroxisomes. ACOT8 metabolizes medium- or long-chain fatty acids into their respective free fatty acids and coenzyme-A (CoASH), implying its partecipation in regulating intraperoxisomal acyl-CoA/CoASH levels to optimize fatty acid flux through β-oxidation (183). However, the role of ACOT8 in lipid metabolism is not fully elucidated. It is known that overexpression of ATCOTs leads to increased depalmitoylation of numerous membrane proteins (184), (185). Palmitoylation is a modification found exclusive in membrane-associated proteins, and plays a crucial role in various cellular processes. These include protein trafficking across membranous compartments, modulation of protein-protein interactions (186), vesicular transport (187), signal transduction, and the anchoring of proteins into the membrane (188). In this context, ACOTs could potentially influence the expression levels of proteins modified at their cysteine residues by fatty acids (palmitoylated), including MHC-I, CD4, Hck, and Lck, which are particularly relevant to Nef functions (189).

Additionally, lipid rafts, crucial sites for HIV-1 particle budding, depend on the hydrolysis of long-chain fatty acyl-CoA for correct budding of Coat Protein Complex I (COP-I) coated vesicles, with the β-COP subunit being a target that interacts with Nef (190).

Nef is the only viral protein known to bind to ACOT8. It has been identified that key residues for Nef/ACOT8 interaction include Asp108, Leu112, Phe121, Pro122, and Asp123 in HIV-1

Nef-LAI (191). Moreover, the expression of ACOT8 has been shown to induce the relocalization of Nef to peroxisomes in 3T3 cells. Notably, the colocalization of Nef and ACOT8 in peroxisomes is contingent upon the C-terminal peroxisomal targeting sequence of ACOT8 (191), (192).

Serena et al. demonstrated, through *in silico* modelling, and subsequently confirmed via coimmunoprecipitation and colocalization analysis, that the regions Arg45-Phe55 and Arg86-Pro93 in ACOT8 are involved in the association with Nef. Furthermore, the interaction was disrupted by the K91S mutation, suggesting a pivotal role for the Lys 91 in this association (193). Of particular interest in this model is the observation that ACOT8 Arg53 establishes electrostatic interactions with Nef-LAI Asp108. This prediction gains further support from the intriguing finding that in Nef-SF2, which does not interact with ACOT8, the residue corresponding to Nef-LAI Asp108 is substituted with glutamic acid (193). Notably, this substitution interferes with the formation of salt bridges with ACOT8 Lys91, underscoring the significant role of this residue situated in the central core of Nef. These data support the hypothesis that the Nef/ACOT8 association may enhance Nef stability, potentially preventing its proteasome-mediated degradation.

Furthermore, additional evidence suggests the potential involvement of ACOT8 in Nef-mediated downregulation of CD4 and MHC-I, as indicated by the presence of mutational residues crucial for both activities (194).

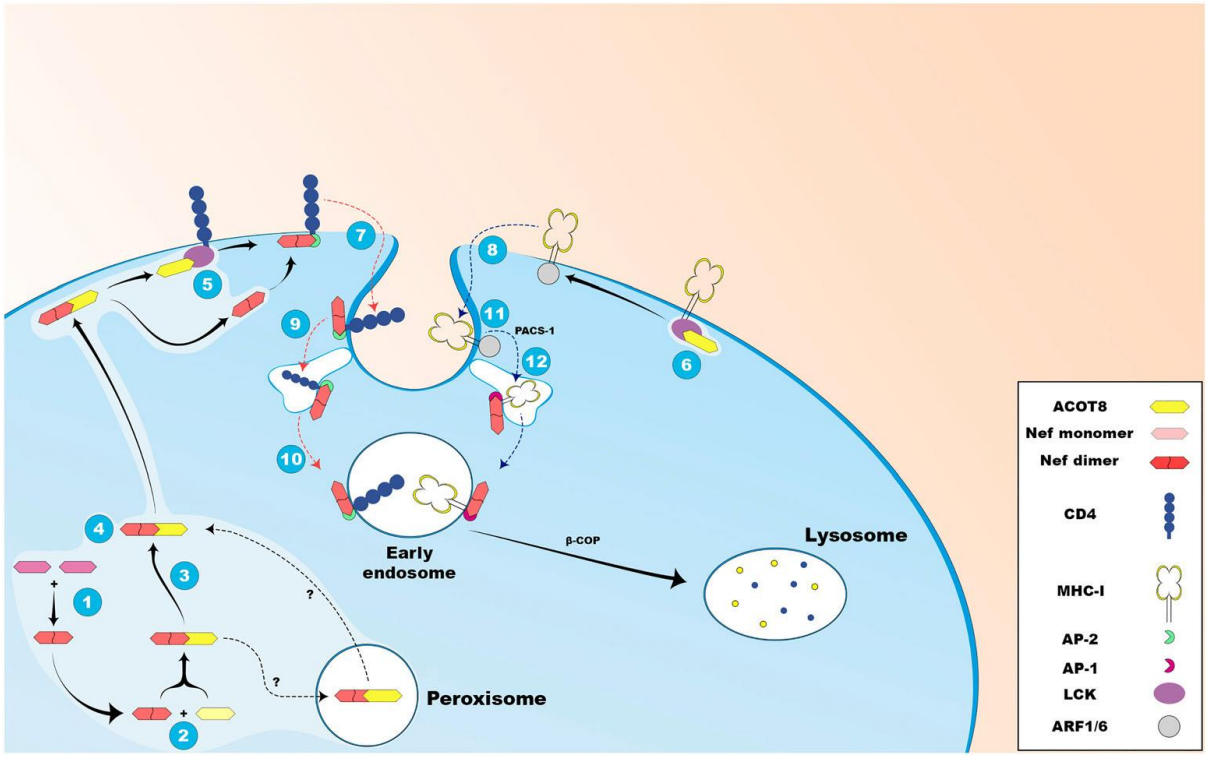


**Figure 12** Schematic representation of possible physiological roles of ACOT8 protein in the HIV Nef functions (194).

Moreover, some hypotheses suggest that the ACOT8-Nef interaction could also impact other events related to AIDS clinical symptoms, including metabolic complications observed in AIDS (e.g., hypertriglyceridemia), as reviewed in (194).

Overall, the biological role of the Nef/ACOT8 interaction has not yet been fully elucidated and could involve various aspects of lipid metabolism related to Nef functions. Furthermore, it is crucial to note that no evidence has yet highlighted the presence and role of this interaction in primary *nef* alleles.

# 2 Aim of the project

The accessory protein Nef of HIV-1 plays one of the most intriguing and least understood roles in HIV infection. The crucial involvement of Nef in virus spread and disease progression *in vivo* is now well established, highlighting its pivotal role in the HIV pathogenesis.

Nef's multifunctionality stems from its adeptness at interacting with an extensive array of host factors, enabling it to modulate key cellular processes and subvert immune surveillance. Of particular interest are Nef's interactions with the cellular vesicular trafficking machinery, which allow it to finely tune the expression of critical cell surface receptors involved in immune recognition and communication. Among these, the most well studied Nef functions include cell-surface downregulation of the HIV-1 receptor MHC-I and CD4, essential for immune synapse formation, antigen presentation, and immune activation. Moreover, recent studies have uncovered Nef's ability to counteract the host restriction factors SERINC5, further emphasizing its pivotal role in enhancing viral infectivity. Especially due to the high variability of Nef sequence, several underlying aspects of Nef-mediated downregulation processes remain unclear.

Amidst the complexity of Nef's interactions with host cellular machinery, one of the most interesting aspects is its interaction with ACOT8, a key player in lipid metabolism. The implications of this interaction remain largely unexplored but emerge as potential links in Nef-mediated viral pathogenesis. Moreover, the absence of information regarding this interaction in primary alleles leaves numerous aspects unresolved, underscoring the need for further investigations not fully understood.

In order to explore incompletely understood aspects of Nef's primary biological functions, the principal aim of this project was to investigate the impact of primary *nef* alleles on the modulation of cell-surface receptors MHC-I, CD4, and SERINC5, as well as the interaction with ACOT8. Furthermore, it sought to assess whether genetic variability within the HIV-1 M group influences Nef's functional activities.

For this purpose, the functionality of primary *nef* alleles was examined in an ART-naïve cohort of HIV-1 positive individuals with various viral subtypes within the M group at the Microbiology Laboratory of IRCCS Policlinico di S. Orsola in Bologna.

The functional analysis was carried out at Institute for Medical Virology and Epidemiology of Viral Diseases – University Hospital of Tübingen (Germany).

The study aimed to investigate Nef's capability to downregulate cell surface receptors using *in vitro* flow cytometry analysis. Additionally, it was conducted a comprehensive examination of the major naturally occurring polymorphisms in Nef to elucidate the principal functional motifs involved in its function. Furthermore, the research delved into the pathogenetic mechanisms by exploring inter-relationships among various Nef functions and their association with baseline viral load. Finally, the investigation sought to uncover the unknown interaction between primary *nef* alleles and ACOT8 through co-immunoprecipitation assays, shedding light on the genetic determinants involved in this interaction.

Therefore, this thesis endeavored to understand elusive aspects of Nef's intricate activity, providing insights into key mechanisms in HIV pathogenesis.

# 3 Materials and Methods

## 3.1 Sample collection

Primary *nef* alleles were obtained from a cohort of 26 HIV-1 positive individuals with known date of seroconversion, untreated at the time of sample collection. Clinical plasma samples were collected at the Microbiology Laboratory of IRCCS Policlinico di S. Orsola in Bologna and stored at -80°C. The study was approved by the local Ethical Committees of Area Vasta Emilia Centro of Emilia-Romagna (CE-AVEC, protocol number 489/2018/Sper/AOUBo), all individuals provided written informed consent before being enrolled in the study.

Eligibility criteria included: (a) age >18 years, (b) primary diagnosis of HIV-1 infection with well-characterized infectious subtype (identified during diagnostic procedure) and (c) naïve to antiretroviral therapy (ART).

Finally, subjects were divided into 5 groups based on viral subtype as follow: 6 (subtype B), 6 (subtype F1), 5 (subtype G), 5 (subtype C), 4 (subtype CRF02_AG).

## 3.2 Molecular biology techniques

### 3.2.1 Viral RNA extraction

RNA was extracted from plasma samples by using the NUCLISENS® EASYMAG® System (Biomerieux) according to the manufacturer's protocol. Briefly, 1 ml of plasma sample was mixed with a lysis buffer containing a chaotropic agent (GuSCN). Subsequently, the isolation process was initiated by adding Magnetic Silica to the lysate, followed by several washing. Finally, the RNA was eluted from the Magnetic Silica, concentrated in a volume of 40 µl of the elution buffer. The RNA was quantified by Qubit Fluorometer (Thermo Fisher Scientific) and stored at -80°C until further downstream application.

### 3.2.2 Nested RT-PCR

Each HIV-1 *nef* gene was amplified by nested reverse transcriptase-polymerase chain reaction (RT-PCR). The viral RNA was reverse transcribed into cDNA and amplified in the first-round RT-PCR using the SuperScript™ IV One-Step RT-PCR System (Invitrogen™, Thermo Fisher Scientific) and the outer primers Fw_nef1 and Re_nef1. Of note, Re_nef1 were designed to be

subtype-specific (Table 1). 500 ng of total RNA were used in a 50 µl PCR reaction mix. The reaction mix included: 25 µl of 2X Platinum Super$^{Fi}$ RT-PCR Master Mix, 1.5 µl of each forward and reverse primer (10 µM, respectively), and 0.5 µl of SuperScript IV RT Mix. The PCR reaction was performed at the following conditions: 50°C for 30 minutes, 98°C for 2 minutes, 40 amplifications cycles of 98°C for 10 seconds, 56°C for 10 seconds, 72°C for 40 seconds and 72°C for 5 minutes.

The PCR product was quantified by Qubit Fluorometer and amplified in the subsequent nested PCR using the DreamTaq PCR Master Mix (2X) (Thermo Fisher Scientific) and the inner degenerate primers Fw-clone_nef and Re-clone_nef (Table 1). These primers were constructed to include the EcoRI restriction site and a 5' region with 20 bp that is homologous to the sequence of the linearized vector backbone used in the subsequent cloning strategy. 1 µg of DNA were used in a 50 µl PCR reaction including: 25 µl of 2X Dream Tac PCR Master Mix and 1 µl of each forward and reverse primer (10 µM, respectively). The PCR reaction was conducted as follows: 94°C for 3 minutes, 35 amplification cycles of 94°C for 30 seconds, 61°C for 30 seconds, 72°C for 1 minute and 72°C for 10 minutes. The PCR product was stored at -20°C until further analysis.

**Table 1** List of primers

| **Name** | **Sequence 5' to 3'** |
|---|---|
| Fw_nef1 | CCRCCRMTTGAGAGACTT |
| Re_nef1 (subtypes B-F1) | GCCACTCCCCAGTCCCG |
| Re_nef1 (subtype G) | AGGCAAGCTTTATTGAGGC |
| Re_nef1 (subtype C) | TGACCACTCCCAGTCCCG |
| Re_nef1 (subtype CRF02_AG) | GCCACTCCCCA ACTCCG |
| Fw-clone_nef | CGAGCTCAAGCTTCGAATTCACATA CCTASAAGAATMAGAC |
| Re-clone_nef | TACCGTCGACTGCAGAATTCCAGGC CACRCCTCCCTGGAAASKCCC |

Note: all primers were manually designed using SnapGene® Viewer 5.1.5. To assess their specificity, each primer was blasted and subsequently ordered from Thermo Fisher Scientific, Life Technologies Italia.

### 3.2.3 Agarose gel electrophoresis and gel extraction

The PCR products from *nef* amplification were separated by agarose gel electrophoresis. A 1.5 % agarose gel was prepared by dissolving 1.5 g of agarose (Lonza) with 100 ml of 1x TAE buffer using a microwave. After cooling, 1X of GelRed® Nucleic Acid Gel Stain (Biotium™) was added to the gel. Before loading onto the gel, DNA samples were mixed with 10X loading dye. To estimate the size of the DNA fragments, the samples were run alongside the DNA Molecular Weight Marker IV (Roche®). Electrophoresis was performed at 100 V for 30-40 minutes.

The DNA fragment of interest was excised from the agarose gel using a clean scalpel under the FastGene® Blue LED Transilluminator (Resnova) and purified with the GeneJET™ Gel Extraction Kit (Thermo Fisher Scientific), following the manufacturer's instructions. DNA was eluted twice in 25 µl of elution buffer and quantified by Qubit Fluorometer.

### 3.2.4 Restriction enzyme digestion

For cloning purpose the purified DNA samples and the vector backbone were digested using the EcoRI (10 U/µL) restriction enzyme (Thermo Fisher Scientific). 3 µg of purified DNA/vector backbone, were mixed with 3 µl of the restriction enzyme and 3 µl of the 10X buffer EcoRI in a 30 µl reaction volume at 37°C for 3 hours.

For digestion control, 1 µg of plasmid DNA was double-digested with 0.5 µl of FastDigest NdeI and FastDigest Kpn2I (Thermo Fisher Scientific). The digestion mix was then combined with FastDigest Restriction Green Buffer in a 15 µl reaction volume and incubated at 37°C for 15 minutes.

After digestion, the whole reaction mixture was loaded into the agarose gel, and electrophoresis and gel purification were performed as previously described (section 3.2.3).

### 3.2.5 SLiCE cloning

Nef amplicons were cloned into pIRES2-eGFP expression vector using the Seamless Ligation Cloning Extract (SLiCE) Method (195), (196). The pIRES2-eGFP and the SLiCE cloning materials were kindly provided by Prof. Massimo Pizzato, University of Trento. This system exploits a recombinase activity present in *E. coli* JM109 lysates to catalyse homologous recombination between short homologous sequences in the linearized vector and the PCR product. The SLiCE reaction was set up according to the Table 2 and then incubated for 9 minutes at 37°C:

**Table 2** Seamless Ligation Cloning Extract (SLiCE) reaction

| Component | Quantity |
|---|---|
| Vector backbone (pIRES2-eGFP) | 20 ng |
| Insert (*nef* amplicons) | 15 ng |
| SLiCE lysate | 1 µl |
| 10x SLiCE buffer | 1 µl |
| PEG4000 | 0.5 µl |
| Nuclease-free water | Filled up to 10 µl |

Immediately after incubation, the reaction was transferred to ice and used for bacterial transformation.

### 3.2.6 Bacterial transformation

Bacterial transformation was performed by adding 5 µl of the ligation mixture to 50 µl of XL-1 Blue Competent Cells. The bacteria were incubated on ice for 30 minutes, heat-shocked at 37°C for 1.5 minutes, and then placed on ice for 2 minutes before adding 500 µl of 1x LB medium without antibiotics. This was followed by an incubation step at 37°C under vigorous shaking for 1 hour. A 100 µl aliquot of the suspension was plated on pre-warmed LB agar plates containing kanamycin for the selection of correctly transformed bacteria, and incubated at 37°C overnight (o/n).

### 3.2.7 Mini prep

To confirm successful cloning, a single colony of each *nef* clone was picked and inoculated in 5 ml LB medium supplemented with kanamycin, followed by an incubation step at 37°C under vigorous shaking o/n. The liquid culture was centrifuged at 2000 rpm for 10 minutes, and the supernatant was discarded. The plasmid DNA extraction was performed using the PureYield™ Plasmid Miniprep System (Promega), following the manufacturer's protocol. In short, the cells were initially lysed, followed by neutralization, and then centrifuged at maximum speed for 3 minutes. Subsequently, the supernatant was transferred into a purification column and, followed by 2 washing steps. Finally, the plasmid DNA was eluted in 30 µl of elution buffer and quantified by Qubit Fluorometer.

All obtained *nef* constructs were stored at -20°C until further use.

### 3.2.8 Retransformation and Midi prep

To enhance the yield of plasmid DNA, all *nef* clones and other plasmids used in the following experiments were retransformed into chemically competent *E. coli* cells (NEB10). 1 µl of plasmid DNA was added to 10 µl of NEB10 and incubated on ice for 30 minutes, followed by a heat-shock at 42°C for 45 seconds. Subsequently, the cells were allowed to rest on ice for an additional 5 minutes, and 250 µl of LB medium without antibiotic was added. The mixture was then incubated at 37°C and 450 rpm for 1 hour. Finally, 150 µl of the cell suspension was plated onto LB agar plates containing 50 µg/ml Kanamycin and incubated at 37°C overnight. To prepare an o/n culture, a single colony was picked and inoculated in 100 ml of LB medium supplemented with 50 µg/ml Kanamycin. The inoculated culture was incubated at 37°C under vigorous shaking overnight. Cells were harvested by centrifugation at 4000x g for 15 minutes and plasmid DNA was isolated using the PureYield$^{TM}$ Plasmid Midiprep System (Promega) following the manufacturer's instructions.

The concentration and purity of all clones were measured using the NanoDrop™ 2000 spectrophotometer (Thermo Fisher Scientific). Correctness of the plasmid was confirmed by restriction digestions (section 3.2.4). Sequencing was then employed to confirm the correct insertion and the integrity of the *nef* open reading frames.

## 3.3 Sequencing

All *nef* clones were validated by Sanger sequencing provided by Eurofins Genomics. A total DNA amount of 100 ng in 20 µl for each clone was mixed with 5 µl of the Fw-Nef1_seq and 5 µl of the Re-Nef2_seq primers (10 µM, respectively) shown in Table 3. The sequencing results were analysed using the UniProt online tool, SerialCloner software, and BioEdit v 7.2.5 software.

**Table 3** List of sequencing primers

| **Name** | **Sequence 5' to 3'** |
|---|---|
| Fw-Nef1_seq | CGCAAATGGGCGGTAGGCGTG |
| Re-Nef2_seq | CGCACACCGGCCTTATTCC |

## 3.4 Cell biological methods

### 3.4.1 Cell culture

HEK293T cells (from AG Schindler, Prof. Michael Schindler, Universitätsklinikum Tübingen, Germany) were cultured in Dulbecco's Modified Eagle Medium (DMEM) (Gibco, ThermoFisher Scientific) supplemented with 10% (v/v) fetal calf serum (FCS) (Gibco, ThermoFisher Scientific) and 1x penicillin/streptomycin (P/S) (100 x; Sigma-Aldrich) at 37°C with 5% $CO_2$. Passaging was performed every three days when confluence reached 80-90%. Therefore, medium was removed, cells were washed once with Phosphate Buffered Saline (PBS) (Gibco, ThermoFisher Scientific) and incubated with Trypsin/EDTA (0.05%; Sigma-Aldrich) at 37°C until cells detached. Cells were resuspended in fresh DMEM and splitted with a ratio of 1:6 – 1:8.

Jurkat T cell (kindly provided by Prof. Christine Goffinet, Institute of Virology, Charité-Universitätsmedizin Berlin, Germany) were cultured in RPMI medium (Gibco, ThermoFisher Scientific) supplemented with 1x L-Glutamine (200 mM; Gibco, ThermoFisher Scientific), 1x MEM Non-Essential Amino Acids Solution (MEM NEAA) (100X; Gibco, ThermoFisher Scientific), 10% (v/v) FCS and 1x P/S at 37°C with 5% $CO_2$. The cells were maintained at a concentration of 0.5-1x$10^6$ cells/ml and split every three days.
Cells were counted, if necessary using a Neubauer-improved counting chamber.

### 3.4.2 Transfection of adherent cells

For functional analysis of primary *nef* alleles, cloned *nef* constructs (pIRES2-Nef-eGFP) were transfected into HEK293Ts cells. The transfection controls used in all experiments are listed in Table 4.

**Table 4** List of plasmids

| Name | Source |
|---|---|
| Nef C | Prof. Massimo Pizzato |
| $Nef^{FS}$ | Prof. Massimo Pizzato |
| PBJ5-SERINC5-iFLAG-HA | Prof. Massimo Pizzato |
| pcDNA empty vector | AG Schindler |
| pCG NA7nefHIV-1IRESGFP | AG Schindler |
| pCG NL43nef3-IRESGFP | AG Schindler |
| mScarletACOT8 | AG Schindler |

To assess the expression levels of Nef and the Nef-mediated downregulation of endogenous MHC-I, HEK293T were transfected with primary *nef* constructs and controls. $Nef^{FS}$ (generated by introducing a frameshift in the $Nef^{Lai}$ sequence) and the empty pIRES2-eGFP vector were used as negative control, $Nef^{C}$ was used as positive control. The day before transfection, HEK293Ts were seeded at a density of 125,000 cells/0.5 ml in a 24-well plate and incubated at 37°C with 5% $CO_2$. Prior to transfection, a medium change was carried out. The transfection mixture is detailed in Table 5.

**Table 5** Transfection mixture for Nef-mediated MHC-I downregulation

| **Component** | **Quantity** |
|---|---|
| pIRES2-Nef-eGFP/controls | 0.5 µg |
| Carrier pcDNA | 0.5 µg |
| 2 M $CaCl_2$ | 3.1 µl |
| Nuclease-free sterile water | Filled up to 25 µl |
| 2x HBS | 25 µl |

Due to the unavailability of a properly-working antibody for the detection of endogenously expressed SERINC5, artificial overexpression of tagged proteins was necessary to study the mechanism of Nef counteraction. For this reason, the expression level of SERINC5 was evaluated using a plasmid expressing a modified SERINC5 harboring an internal FLAG epitope within the fourth extracellular loop (PBJ5-SERINC5-iFLAG-HA), conveniently detectable with an anti-FLAG antibody (176). To assess Nef-mediated downregulation of SERINC5 in an overexpression context, HEK293T were co-transfected with primary *nef* constructs and PBJ5-SERINC5-iFLAG-HA. Previously described plasmids were used as controls. The day before transfection, HEK293Ts were seeded at a density of 125,000 cells/0.5 ml in a 24-well and incubated at 37°C with 5% $CO_2$. Prior to transfection, a medium change was carried out. The transfection mixture is detailed in Table 6.

**Table 6** Transfection mixture for Nef-mediated SERINC5 downregulation

| **Component** | **Quantity** |
|---|---|
| pIRES2-Nef-eGFP/controls | 1 µg |
| SERINC5-iFLAG-HA | 1 µg |
| 2 M $CaCl_2$ | 3.1 µl |
| Nuclease-free sterile water | Filled up to 25 µl |
| 2x HBS | 25 µl |

The interaction between Nef and ACOT8 was investigated by using the coimmunoprecipitation (Co-IP) assay in a mScarletACOT8 overexpression context. Prior to the Co-IP, HEK293T cells were co-transfected with primary *nef* constructs and a mScarletACOT8 plasmid, which expresses an ACOT8-mScarlet fusion protein. In addition to the previous controls, two other controls expressed in a different backbone were included: pCG NL43nef3-IRESGFP (presenting a premature stop codon and expressing GFP) used as a negative control, and pCG NA7nefHIV-1IRESGFP (co-expressing the lab-adapted strains NA7nef and GFP) used as a positive control. The day before transfection, HEK293Ts were seeded at a density of 450,000 cells/2 ml in a 6-well plate and incubated at 37°C with 5% $CO_2$. Prior to transfection, a medium change was carried out. The transfection mixture is detailed in Table 7.

**Table 7** Transfection mixture for Nef-ACOT8 Co-IP

| **Component** | **Quantity** |
|---|---|
| pIRES2-Nef-eGFP | 2 µg |
| mScarletACOT8 | 2 µg |
| 2 M $CaCl_2$ | 13 µl |
| Nuclease-free sterile water | Filled up to 100 µl |
| 2x HBS | 100 µl |

All transfection mixtures were prepared in a 1.5 ml Eppendorf tube by adding DNA, $CaCl_2$, and filling up with sterile water. Each mixture was briefly vortexed and spun down. Subsequently, 2X HBS (detailed in Table 10) was slowly added dropwise under constant vortexing at the lowest speed. After incubation for 15 minutes on room temperature, the transfection mix was distributed dropwise into the respective well, and plates were swirled to ensure equal distribution. Finally, medium was changed 16 hours post transfection (hpt) and fluorescence was checked. Cells were harvested by centrifugation 48 hours after transfection.

### 3.4.3 Electroporation of suspension cells

In order to assess Nef-mediated endogenous MHC-I and CD4 downregulation in Jurkat T cells, electroporation was carried out. Cells were electroporated by using the Neon™ transfection system (Invitrogen) according to the manufacturer's protocol. For each electroporation, 200,000 cells were washed twice with PBS and centrifuged at 1800 rpm for 8

minutes. The cells were resuspended in 10 µl of PBS supplemented with magnesium and calcium and added to a sterile 1.5 ml Eppendorf tube containing 2 µg of plasmid DNA and gently mixed. The cell/DNA mixture was electroporated with 1600V, 10ms, 3 pulses. Subsequently, cells were transferred to 0.5 ml pre-warmed RPMI medium supplemented with 5% (v/v) FCS without antibiotic, and cultured in 24-well plates for 24 hours at 37°C with 5% $CO_2$. At 24 hours post-electroporation (hpe), fluorescence was checked, and cells were harvested for flow cytometry analysis.

## 3.5 Biochemical methods

### 3.5.1 Preparation of cell lysates

All working steps were performed with pre-cooled reagents, on ice and in 4°C cooled centrifuges. Protease inhibitor was added freshly to the lysis buffer. For lysis of HEK293Ts, cells were washed once with cold PBS before being detached. Cells were then washed for 5 minutes at 500x g and the pellet was frozen away. Following the freezing step, cells were thawed and lysed using RIPA lysis buffer supplemented with 1x Protease inhibitor cocktail (25x, Roche). The cells were resuspended and incubated for 30 minutes on ice with continuous shaking. Finally, cell lysates were centrifuged at maximum speed for 10 minutes, the supernatant was collected and transferred to a new 1.5 ml tubes. Lysates were prepared for SDS-Page and Western Blot analysis by adding the appropriate volume of 6 x SDS loading day and subsequent boiling at 9 °C for 10 min. Samples were stored at -20°C until further use.

### 3.5.2 SDS-page and western blot analysis

Proteins from cell lysates, along with a molecular weight marker for reference, were separated on a 12 % SDS-Page. Therefore, polyacrylamide gels were prepared according to Table 10 , placed into a complete electrophoresis unit (Biorad), which was filled with 1x SDS running buffer (Table 10). Subsequently, 12 µl of protein samples and 5 µl of Page Ruler$^{TM}$ prestained protein ladder (Sigma Aldrich) were loaded. Electrophoresis was conducted at a low voltage (80 V) for the stacking gel and at a higher voltage (100-120 V) for the separating gel. The separated proteins were transferred onto a nitrocellulose membrane for 90 minutes at 80 V using a tank blot system (Biorad). Membranes were blocked with 5% skim milk in 1x TBS-T for 1 hour and then incubated at 4 °C with the primary antibody (listed in Table 8, diluted in

5% milk in TBS-T). After washing the membranes 3 times with 1x TBS-T for 15 minutes each, membranes were incubated for one hour at RT, in the dark, with the respective secondary antibody (listed in Table 8, diluted in 5% milk in TBS-T), followed by three washing steps with 1x TBS-T. Protein detection was achieved using the Li-COR Odyssey® Infrared Imaging System (Li-COR).

### 3.5.3 Co-IP assay

The coimmunoprecipitation (Co-IP) assay was carried out using the RFP-Trap Agarose beads, kindly provided by Prof. Ulrich Rothbauer, University of Tübingen, Germany. It consists of nanobodies coupled to agarose beads against the Red Fluorescent Protein (RFP), facilitating the immunoprecipitation of RFP-fusion proteins from cell extracts.

All steps were performed at 4°C. After 48 hours, the co-transfected cells were harvested and lysed with 250 µl of cold non-denaturing lysis (Table 10) buffer for 30 minutes on ice with continuous shaking. Lysates were sonicated twice for 5 seconds and then frozen at −20°C for at least 1 hour. Cellular debris was removed by centrifugation at full speed for 10 minutes at 4°C. Afterward, 20 µl of the clear lysate were prepared as input fraction and boiled at 95°C for 10 minutes with the 6x SDS-sample buffer. The lysate was transferred into a new 1.5 ml tube and mixed with 300 µl of dilution buffer (Table 10) supplemented with a 1x Protease inhibitor cocktail (stock: 25x, Roche).

Before protein binding, the beads were equilibrated in dilution buffer. In this step, 25 µ of bead slurry were gently transferred into a 1.5 mL reaction tube, and 500 µl of ice-cold dilution buffer (Table 10) was added. The beads were sedimented by centrifugation at 2,500x g for 5 minutes at 4°C, and the supernatant was discarded. The protein binding step was initiated by adding diluted lysate to the equilibrated beads. The mixture was rotated end-over-end for 1 hour at 4°C. Subsequently, the beads were sedimented by centrifugation as previously described. The supernatant was discarded, and the beads were washed with 500 µl of wash buffer, undergoing sedimentation by centrifugation for three times. During the last washing step, the beads were transferred to a new tube, resuspended in 80 µL of 2x SDS-sample buffer, and boiled at 95°C for 5 minutes to dissociate the immunocomplexes from beads. Finally, the beads were sedimented by centrifugation, and the supernatant was analysed using Western blotting.

**Table 8** List of primary and respective secondary antibodies for Western Blot

| Name/Clone | Species/Isotype | Clonality | Dilution | Source |
|---|---|---|---|---|
| Anti-HIV-1 Nef (antiserum) | Rabbit | Polyclonal | 1:1000 | NIH AIDS Reagent Program |
| Anti-GAPDH Clone W17079A | Rat IgG2a, κ | Monoclonal | 1:10000 | BioLegend |
| Anti-ACOT8 Clone C-3 | Mouse IgG1 | Monoclonal | 1:1000 | Santa Cruz Biotechnology |
| alpha Tubulin Clone B-7 | Mouse IgG2a κ | Monoclonal | 1:10000 | Santa Cruz Biotechnology |
| Goat anti-Rabbit IgG (H+L) Dylight 650 | Goat | Polyclonal | 1:15000 | Invitrogen |
| IRDye 800CW Goat anti Rat IgG(H+L) | Goat | Polyclonal | 1:15000 | Li-COR |
| Anti-Mouse IgG (H+L) Dylight 650 | Goat | Polyclonal | 1:15000 | Invitrogen |

## 3.6 Flow Cytometry

### 3.6.1 Immunostaining of surface proteins

Flow cytometry analysis was performed to examine the endogenous surface expression of MHC-I and CD4, and the expression of SERINC5-iFLAG using the MACSQuant® VYB Flow Cytometer (Miltenyi Biotec). All antibodies listed in Table 9 were labeled with specific

fluorophores and were initially titrated for panel optimization, population identification, and expression level measurements.

Cells were transferred into a 96-well U-bottom plate and centrifuged at 1800 rpm, 4°C for 5 minutes. The supernatant was discarded, and the cells were washed twice with 150 µl of cold FACS buffer (Table 10), followed by centrifugation. The fixation step involved adding 100 µl of 2% PFA, incubating for 15 minutes at room temperature in the dark. Subsequently, the cells were washed three times with 150 µl of cold FACS buffer and centrifuged. The supernatant was discarded, and cells were resuspended in 50 µl of a labeled specific-antibody staining solution diluted in FACS buffer. For the respective dilutions see Table 9. Unstained controls and respective single-stained controls were included. The antibody staining solution was incubated for 1 hour at 4°C in the dark. Cells were then washed twice, as described above, and resuspended in 150 µl of ice-cold FACS buffer. Subsequently, they were analysed using the MACSQuant. The results were examined using the FlowJo™ software.

**Table 9** List of antibodies for Flow Cytometry

| Name/Clone | Species/Isotype | Clonality | Dilution | Source |
|---|---|---|---|---|
| PE anti-human HLA-A,B,C<br>Clone W6/32 | Mouse IgG2a, κ | Monoclonal | 1:50 | BioLegend |
| Brilliant Violet 421™ anti-human CD4<br>Clone OKT4 | Mouse IgG2b, κ | Monoclonal | 1:50 | BioLegend |
| Purified anti-DYKDDDDK Tag (FLAG tag)<br>Clone L5 | Rat IgG2a, λ | Monoclonal | 1:2000 | BioLegend |

### 3.6.2 Analysis of flow cytometry data

Following the sample acquisition, FlowJo™ software was employed for the subsequent analysis of flow cytometry data. Cell morphology assessment was conducted through the FSC and SSC scatter, with subsequent gating for single cells based on a height-to-area ratio closest to 1. When evaluating the expression of specific surface markers, cells were positive if their signal exceeded that of the respective negative control. The comparison between different

conditions involved assessing the percentage of marker-positive cells and/or the geometric mean of fluorescence intensity across a specific population.

Nef expression was determined by GFP fluorescence. This was achieved as *nef* alleles were cloned upstream of an IRES2-eGFP cassette, allowing for the selective identification of Nef-expressing cells through gating on GFP signals.

Accordingly, the residual surface expression level of each molecule was measured as Median Fluorescence Intensity (MFI) and shown as a percentage normalized to that of the negative control $Nef^{FS}$ strain. A normalized value of 100% indicates expression levels equivalent to that of the $Nef^{FS}$, representing no Nef activity. Percentages below 100% and above 100% indicate expression inferior or superior to those of $Nef^{FS}$, respectively. Thus, the Nef-mediated downregulation of MHC-I and CD4 was normalized to those of the $Nef^{FS}$ using the following equation: $[MFI_{sample}\ (GFP+)/MFI_{sample}\ (GFP-)]/[MFI_{FS}\ (GFP+)/MFI_{FS}\ (GFP-)]$, while Nef-mediated SERINC5 downregulation was normalized using the following equation: $[MFI_{sample}\ (GFP+)]/[MFI_{FS}\ (GFP+)]$. Where MFI (GFP+) and MFI (GFP−) refer to the MFI of MHC-I, or CD4, or SERINC5-iFLAG expression in the Nef-expressing (GFP positive [GFP+]) and Nef-nonexpressing (GFP negative [GFP−]) gates, respectively. Similarly, $MFI_{sample}$ and $MFI_{FS}$ refer to the MFI for each primary *nef* allele and $Nef^{FS}$, respectively.

## 3.7 List of homemade buffers, solution and media

**Table 10** List of homemade materials

| Buffer/solution/medium | Composition |
|---|---|
| 50x TAE | 2 M Tris base<br>1 M acetic acid<br>50 mM EDTA disodium salt<br>Fill up to 1 l with $ddH_20$ |
| 2x HEPES buffered saline (HBS) | 275 mM NaCl<br>10 mMKCl,<br>1.4 mM Na2PO4<br>42 mM HEPES<br><br>11 mM glucose<br>Adjusted to pH 7.05<br>Fill up to 100 ml with $ddH_20$<br>Sterilize by filtration |
| RIPA lysis buffer | 10 mMTris-HCl (pH 8.0)<br>1 mM EDTA<br>0.5 mM EGTA<br>140 mM NaCl<br>0.1% sodium deoxycholate<br>0.1% SDS<br>1% Triton X-100<br>Final pH 7.4<br>Fill up to 100 ml with $ddH_20$ |
| 6x SDS-sample buffer (Laemmli) | 2% bromophenol blue<br>30% glycerol<br>10% SDS<br>0.5M Tris, pH 6.8 (gel stacking buffer)<br>0.6 M DTT<br>Fill up to 50ml with $ddH_2O$<br>Store at -20°C |
| Stacking gel | 130 mM Tris (pH 6.8)<br>17% (v/v) acrylamide<br>1% SDS<br>1% APS<br>0.2% (v/v) TEMED<br>in $ddH_2O$ |
| Separating gel | 275 mM Tris (pH 8.8)<br>33% (v/v) acrylamide<br>1% SDS<br>1% APS<br>0.16% (v/v) TEMED<br>in $ddH_2O$ |
| 10x SDS-PAGE Running buffer | 250 mM Tris base<br>1.92 M glycine |

| | |
|---|---|
| | 1% SDS<br>Final pH 8.3<br>Fill up to 1 l with $ddH_2O$ |
| 10x Transfer buffer | 250 mM Tris base<br>1.92 M glycine<br>Fill up to 1 l with $dH_2O$ |
| 1x Transfer buffer | 200 ml Methanol<br>100 ml 10x transfer buffer<br>Fill up to 1 l with $ddH_2O$ |
| 10x TBS | 500 mM Tris-HCl<br>1.5 M NaCl<br>Final pH 7.5<br>Fill up to 1 l with $ddH_2O$ |
| 1x TBS-T | 100 ml 10x TBS<br>1% Tween® 20<br>Fill up to 1 l with $ddH_2O$ |
| FACS buffer | PBS supplemented with 1% (v/v) of FCS |
| 4% PFA | Heat 800 ml of 1x PBS up to 60°C<br>40 g PFA<br>Cool down the solution<br>Fill up to 1 l with 1x PBS<br>Filtrate the solution<br>Final pH 6.9 |
| 2% PFA | 4% PFA diluted in FACS buffer |
| Non-denaturating Lysis buffer | 10 mM Tris–HCl<br>5 mM EDTA<br>150 mM NaCl<br>1% Triton X-100<br>Final pH 7.5<br>Fill up to 200 ml with $ddH_20$ |
| Dilution buffer/wash buffer | 10 mMTris/Cl<br>150 mM NaCl<br>0.5 mM EDTA<br>adjust the pH at 4°C<br>Final pH 7.5<br>Fill up to 200 ml with $ddH_2O$ |
| LB medium | 5 g NaCl<br>5 g Yeast extract<br>10 g Peptone<br>Filled up to 1 ml with $ddH_2O$<br>Sterilized by autoclaving |
| LB agar | 5 g NaCl<br>5 g Yeast extract<br>10 g Peptone<br>20 g Agar<br>Filled up to 1 l with $ddH_2O$<br>Sterilized by autoclaving |

# 4 Results

## 4.1 Primary individuals-derived *nef* alleles

### 4.1.1 Study subject characteristics

The study subjects were selected from a cohort of HIV-1 positive people consisted of 26 ART-naïve individuals with an age range of 20 to 76 years, and with a predominance of men (65%) over women (35%). The subjects were categorized based on the HIV-1 viral subtype distinguishing five groups: B, F1, G, C, and CRF02_AG.

The clinical information of the subjects, detected during the diagnostic procedure and summarized in Table 11, included:

- A known seroconversion date with identification of the **Infection Timing**, determined through the avidity test. This test allowed to identify in the cohort 15% of recent infections (< 6 months) and 85% of previous chronic infections (> 6 months).
- Baseline **Viral Load quantification (cp/ml)** for each subject before the initiation of ART.
- Immunological values, including the CD4 count (**CD4 cells/mmc**) and the **CD4+/CD8+ ratio**. (Note: Values indicated with 'x' were not recorded at the time of specimen collection and therefore this data is unavailable).
- Baseline **Drug Resistance Test** results for the principal HIV drug classes: Protease Inhibitors (PIs), Nucleoside Reverse Transcriptase Inhibitors (NRTIs), Non-Nucleoside Reverse Transcriptase Inhibitors (NNRTIs), and Integrase Strand Transfer Inhibitors (INSTIs). This analysis identified, sensitivity (S), resistance (R), reduced sensitivity (RS), and not detection (ND) for each drug class.

**Table 11** Sample selection and respective individual characteristics

| | | | | | | | | HIV Drug Resistance Test | | | |
|---|---|---|---|---|---|---|---|---|---|---|---|
| **Sample** | **HIV-1 Subtype** | **Age** | **Gender** | **Infection Timing** | **Baseline Viral Load (cp/ml)** | **CD4 cell/mmc** | **CD4+/CD8+ (range 1.00-2.70)** | **PIs** | **NRTIs** | **NNRTIs** | **INSTIs** |
| Nef 1 | B | 52 | W | < 6 months | 1260942 | 27 | 0.21 | S | S | R | S |
| Nef 2 | | 31 | M | > 6 months | 19203 | 405 | 0.34 | S | S | R | S |
| Nef 3 | | 67 | W | > 6 months | 147143 | 36 | 0.07 | S | S | S | S |
| Nef 4 | | 76 | M | < 6 months | 2229676 | 176 | 0.26 | S | S | S | S |
| Nef 5 | | 66 | W | > 6 months | 1430925 | 58 | 0.13 | S | S | S | S |
| Nef 6 | | 43 | W | > 6 months | 806154 | X | 0.24 | S | S | S | S |
| Nef 7 | F1 | 54 | W | > 6 months | 235795 | X | 0.05 | S | S | S | S |
| Nef 8 | | 35 | M | > 6 months | 302836 | 336 | 0.25 | S | S | S | S |
| Nef 9 | | 30 | M | > 6 months | 222446 | 672 | 0.69 | S | S | S | S |
| Nef 10 | | 59 | M | > 6 months | 206539 | 742 | 1.15 | S | S | S | S |
| Nef 11 | | 36 | M | > 6 months | 205500 | 1188 | 0.85 | S | S | S | S |
| Nef 12 | | 34 | M | > 6 months | 52411 | 940 | 1 | S | S | S | S |
| Nef 13 | G | 29 | M | > 6 months | 6808 | 806 | 0.65 | S | S | S | S |
| Nef 14 | | 30 | M | < 6 months | 401834 | 1808 | 1.33 | S | S | S | S |
| Nef 15 | | 31 | M | > 6 months | 23299 | 534 | 1.03 | S | S | S | S |
| Nef 16 | | 31 | W | > 6 months | 43209 | X | X | S | S | S | ND |
| Nef 17 | | 33 | W | < 6 months | 224318 | 661 | 0.53 | S | S | S | ND |
| Nef 18 | C | 20 | M | > 6 months | 39369 | X | X | S | S | S | ND |
| Nef 19 | | 29 | M | > 6 months | 7115 | 752 | 0.77 | S | S | S | ND |
| Nef 20 | | 27 | M | > 6 months | 37912 | X | X | S | S | S | S |
| Nef 21 | | 32 | W | > 6 months | 51589 | 279 | 0.32 | S | S | S | S |
| Nef 22 | | 32 | M | > 6 months | 549975 | 37 | 0.04 | S | S | RS | S |
| Nef 23 | CRF02_AG | 23 | M | > 6 months | 44359 | 378 | 0.31 | S | S | S | S |
| Nef 24 | | 57 | M | < 6 months | 51076 | 571 | 0.38 | S | S | S | S |
| Nef 25 | | 46 | W | > 6 months | 45284 | 500 | 0.97 | S | S | S | ND |
| Nef 26 | | 21 | M | > 6 months | 110045 | 310 | 0.25 | S | S | S | S |

### 4.1.2 From primary *nef* alleles to expression constructs

To assess the functional activity of primary *nef* alleles *in vitro*, *nef* amplicon from HIV-1-positive individuals was isolated from baseline plasma RNA using a nested reverse transcriptase PCR (RT-PCR), which involved two sets of degenerate amplification primers. Subsequently, the obtained *nef* amplicons were cloned into a pIRES2-eGFP expression vector upstream of the IRES2-eGFP cassette, using the SLiCE method. The simultaneous expression of eGFP and Nef from the same RNA allowed for the efficient gating of fluorescent cells that expressed the viral factor (176). 26 primary *nef* alleles were obtained, and a single clone per sample was analysed for further functional tests.

### 4.1.3 Alignment and Sequence analysis of *nef* alleles

All previously obtained *nef* clones were validated using Sanger sequencing, and their sequences were aligned with the consensus sequence HIV-1 Nef Lai (GenBank accession number: K02013.1). The analysis, shown in Fig. 9, revealed an intact open reading frame (ORF) for 24 out of the 26 primary *nef* alleles investigated. Of note, samples Nef 12 and Nef 22 exhibited a truncated amino acid sequence.

Among the 24 samples with an intact ORF, the pattern of sequences variation was not evenly distributed throughout the length of the primary Nef proteins. The N-terminal myristoylation motif, crucial for Nef's association with cellular membranes and for virtually all of its biological activities (108), was found to be intact in all samples. Moreover, it has been observed that residues W124 and P136, crucial for the structural integrity of the Nef protein (197), were highly conserved in all primary alleles. 50% of the sequences, excluding those from subtype CRF02_AG, exhibited insertions of amino acids in the length variable region, recognized as the protein interaction site (198), which includes amino acid residues 12-39 (AA 12-39).

The 72PxxP75 motif, and the residue Asp123, identified to play a crucial role in the recognition of the AP-1 complex and, consequently, for MHC-I downregulation (138), (139), were highly conserved in all primary *nef* alleles, regardless of subtype. Contrastingly, the 62EEEE65 motif, which mediates the interaction with PACS-1 (199), exhibited variability in 75% of the samples, equally distributed within the subtypes, and particularly prevalent in subtype G where all samples displayed variations in the site.

The molecular determinants governing CD4 and SERINC5 downregulation primarily include the di-leucine motif (164LL165), which is crucial for AP-2 recruitment (159). This motif resulted preserved in all primary *nef* alleles under study. Nevertheless, the endocytic signal 160Exxx, in conjunction with the di-leucine motif (108), was highly variable in all samples. In particular, the polymorphism S163C in this site, previously associated with an increased Nef activity to counteract CD4 and SERINC5 (200) (175), was found in 50% of the samples, but completely absent in subtype B and CRF02_AG. Furthermore, the N-terminal 57WL58 motif, also crucial for the downregulation of the two receptors, was highly conserved, except for samples Nef 3 and Nef 18, which exhibited the substitutions L58V and W57Q, respectively.

The polymorphism H116N, selectively impairing Nef-mediated CD4 and SERINC5 downregulation functions (174), was found in 46% of the samples, with a higher prevalence observed in subtype B and C. The residue R178, crucial for AP-2 recruitment (129), displayed significant variability, and the R178G mutation, associated with a reduced capacity to downregulate SERINC5 (175), was found in 29% of the primary alleles, excluding subtype F1.

Finally, it was observed that the residues D108, D111, L112, F121, P122, D123, and W124, crucial for Nef/ACOT8 interaction (191), (192), (193), were highly conserved in all primary alleles, except for residue D108, which was found to be mutated in 50% of the samples, across all subtypes. Notably, subtype B exhibited the lowest percentage (20%) of mutations among them.

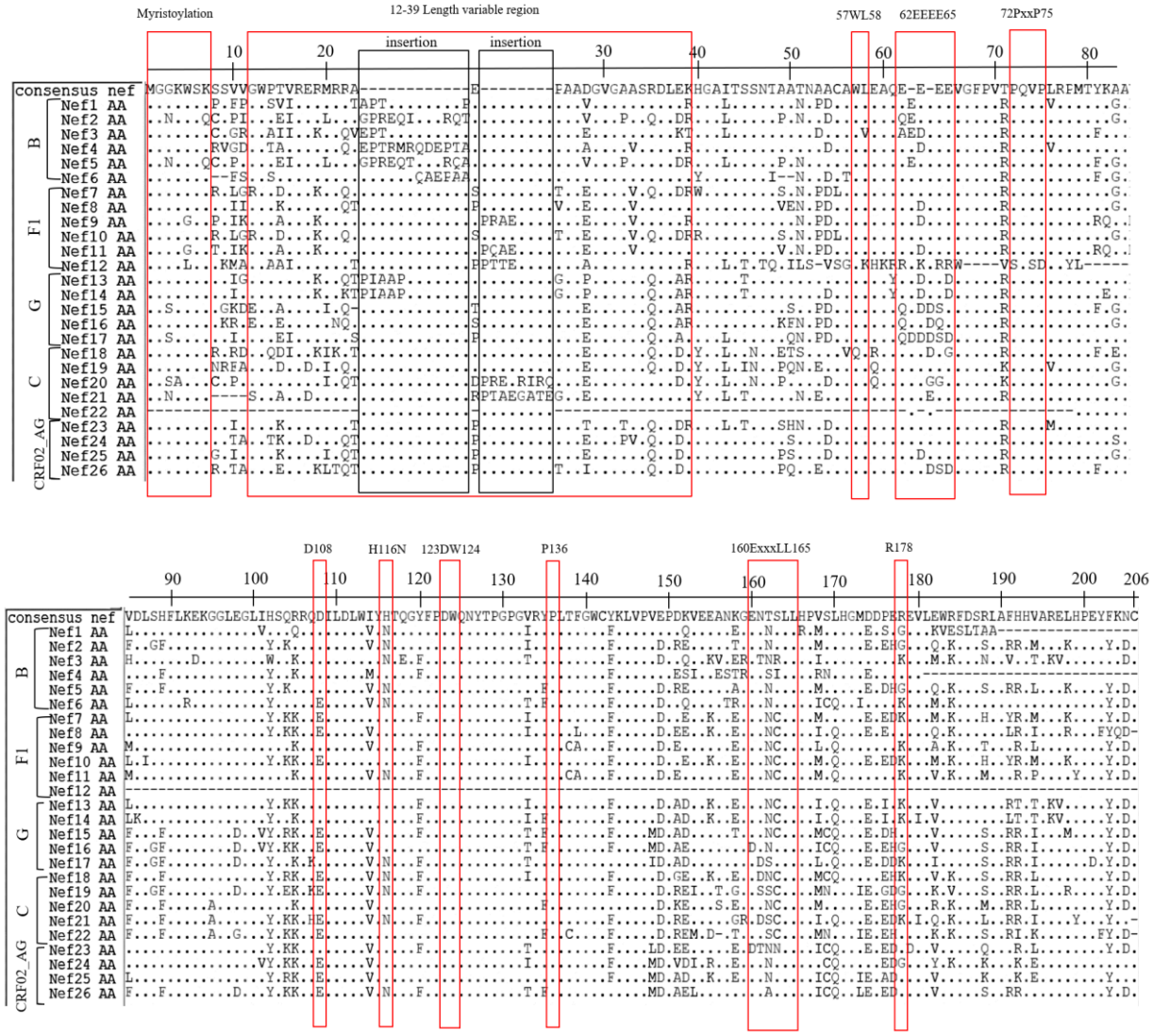


**Figure 13 Sequence alignment of individuals-derived nef alleles**. Amino acid sequence alignment of the Nef proteins analysed using BioEdit v 7.2.5 software. Consensus nef indicates the HIV-1 Nef Lai sequence (GenBank accession number: K02013.1) and serves as a reference. Red boxes indicate the position of functionally relevant residues and motifs.

### 4.1.4 Expression and detection of *nef* alleles

In addition to obtaining the representative Nef sequence for each HIV-1 positive person, the limited steps for further functional analysis involve determining whether the expression of the clonal constructs can be detected and assessing whether they are expressed at a comparable level. Therefore, the steady-state Nef protein expression of the constructs was assessed by Western Blot analysis. Briefly, HEK293T cells were transfected with primary *nef* alleles and various controls. The controls included: the empty vector pIRES2-eGFP, $Nef^{C}$ as a positive control, and $Nef^{FS}$ (with a frameshift in the $Nef^{Lai}$ sequence) as a negative control, both expressed into the pIRES2-eGFP vector. In addition, two other controls expressed in a different backbone were included: pCG NL43nef3-IRESGFP (presenting a premature stop codon and expressing GFP) as a negative control, and pCG NA7nefHIV-1IRESGFP (co-expressing the lab-adapted strains NA7nef and GFP) as a positive control. Subsequently, levels of Nef expression were detected by Western Blot analysis and GAPDH was used to normalize for equal loading (Figure 14 A, lower panel).

As depicted in Fig. 14 A, Nef was expressed in all primary alleles that had an intact open reading frame, apart from Nef 12 and Nef 22, which was expected due to the disrupted ORF. Consequently, they were included in the subsequent functional analyses as negative internal controls. Primary *nef* alleles exhibited high variability in molecular weight, ranging between 27-35 kDa. Notably, Nef 2 and Nef 5, displayed an additional band visible at around 15 kDa, while Nef 20 showed only a band at 15 kDa. Nef probing revealed variable band intensities with equal loading of GAPDH, suggesting a distinct expression pattern of the primary *nef* alleles. In parallel, variable Nef expression levels was also confirmed through the detection of GFP expression in the flow cytometry analysis of the same transfected cells (Fig. 14 B).

The observed variability in band intensity may be attributed to the differential binding of the primary polyclonal antibody to genetically diverse Nef isolates.

Overall, the expression levels of the alleles were detectable but variable. However, all 26 *nef* alleles were considered for further functional analysis.

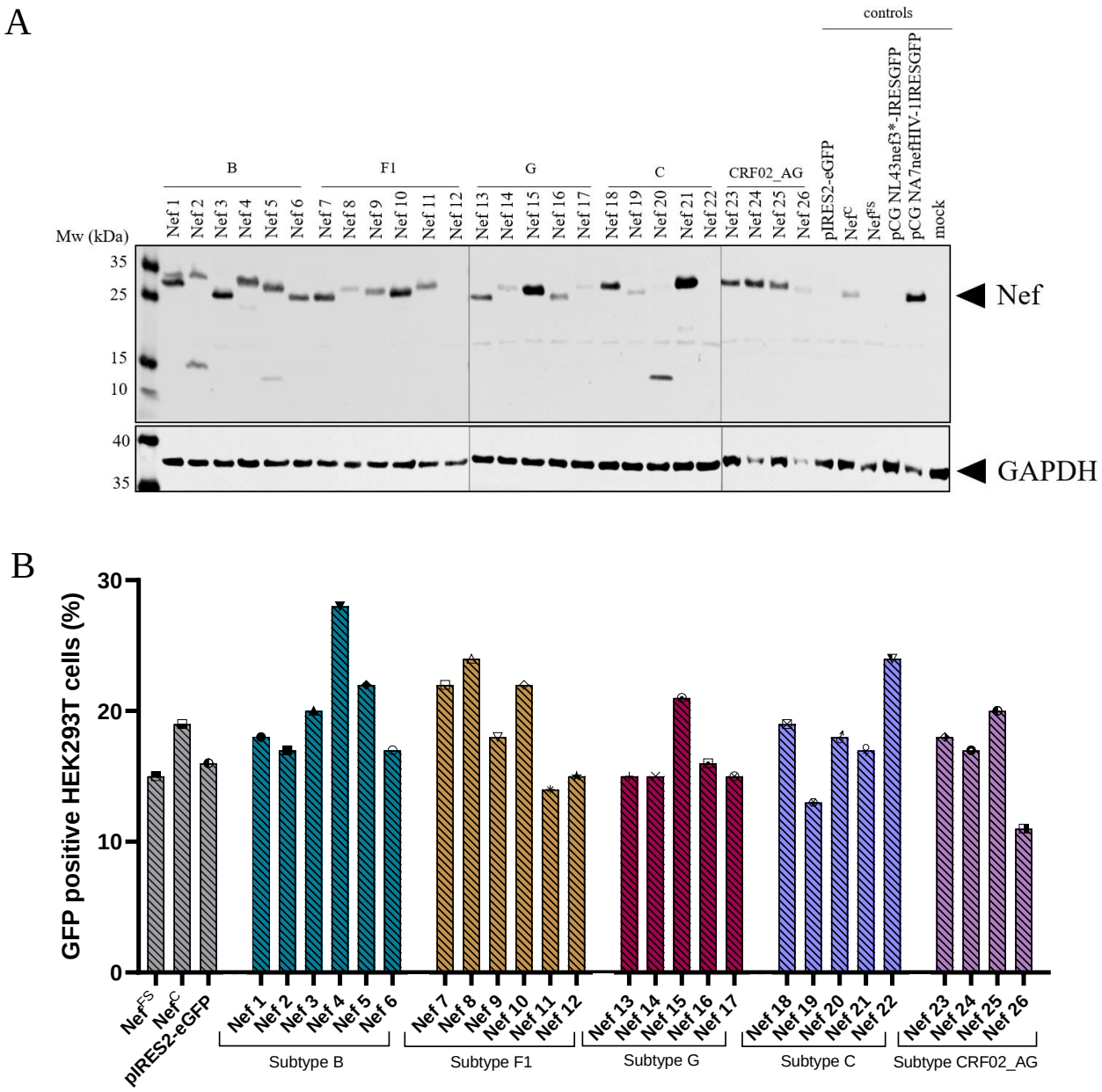


**Figure 14 Expression and detection of *nef* alleles by Western blot and Flow Cytometry**. HEK293T were transfected with *nef* alleles as well as the indicated controls. Cells were harvested at 48 hpt and A) cell lysates were analysed by immunoblotting for Nef and GAPDH expression. (Mw, molecular weight). B) Nef expression in Flow Cytometry analysis detected as GFP positive population.

## 4.2 Functional assessment of primary *nef* alleles on cell surface receptors

To analyse the functional activity of each primary *nef* allele, modulation of the cell surface receptors MHC-I, CD4 and SERINC5 were studied, since these receptors are established main targets of Nef function (128), (129), (130). As controls, $Nef^{FS}$, $Nef^{C}$, and the empty vector pIRES2-eGPF were included.

### 4.2.1 Conserved downregulation of endogenous MHC-I by primary-derived *nef* alleles

To investigate whether MHC-I downmodulation on an endogenous level is preserved in the primary *nef* alleles, HEK293T and Jurkat T cells were transfected/electroporated with the *nef* expressing constructs and the respective controls. The MHC-I levels were assessed by flow cytometry at 24 or 48 hpt, respectively and transfection efficiency was controlled by measuring the GFP signal of the backbone for each cell type.

Quantitative analysis of residual MHC-I surface expression, relative to the negative control $Nef^{FS}$, revealed a significant ($p < 0.05$) reduction in receptor expression on the surfaces of both HEK293T and Jurkat T cells for all primary *nef* alleles with an intact ORF. As expected, samples Nef 12 and Nef 22, used as internal negative controls due the truncated Nef protein, mirrored the levels observed in the $Nef^{FS}$, with no statistically significant difference ($p > 0.05$). Additionally, the majority of *nef* alleles downmodulated MHC-I to a greater extent than the positive control $Nef^{C}$.

Nef-mediated MHC-I downregulation in HEK293T cells was observable in the representative flow cytometry plots illustrated in Fig. 15 A, particularly when compared to the negative controls $Nef^{FS}$, pIRES2-eGPF, Nef 12, and Nef 22.

Nevertheless, subtle variations were observed among individual samples. In the quantitative analysis, showed in Fig 15 B, samples Nef 20 and Nef 26 exhibited the lowest MHC-I downregulation capacity (MHC-I expression > 50%). Less downregulation activity (MHC-I expression > 45%) was observed in samples Nef 8, 16, 17, 21, 23 and 24 in HEK293Ts. Contrastingly, the greatest downregulation activity in these cells was observed in samples Nef 3 and Nef 14 (MHC-I expression < 30%).

A

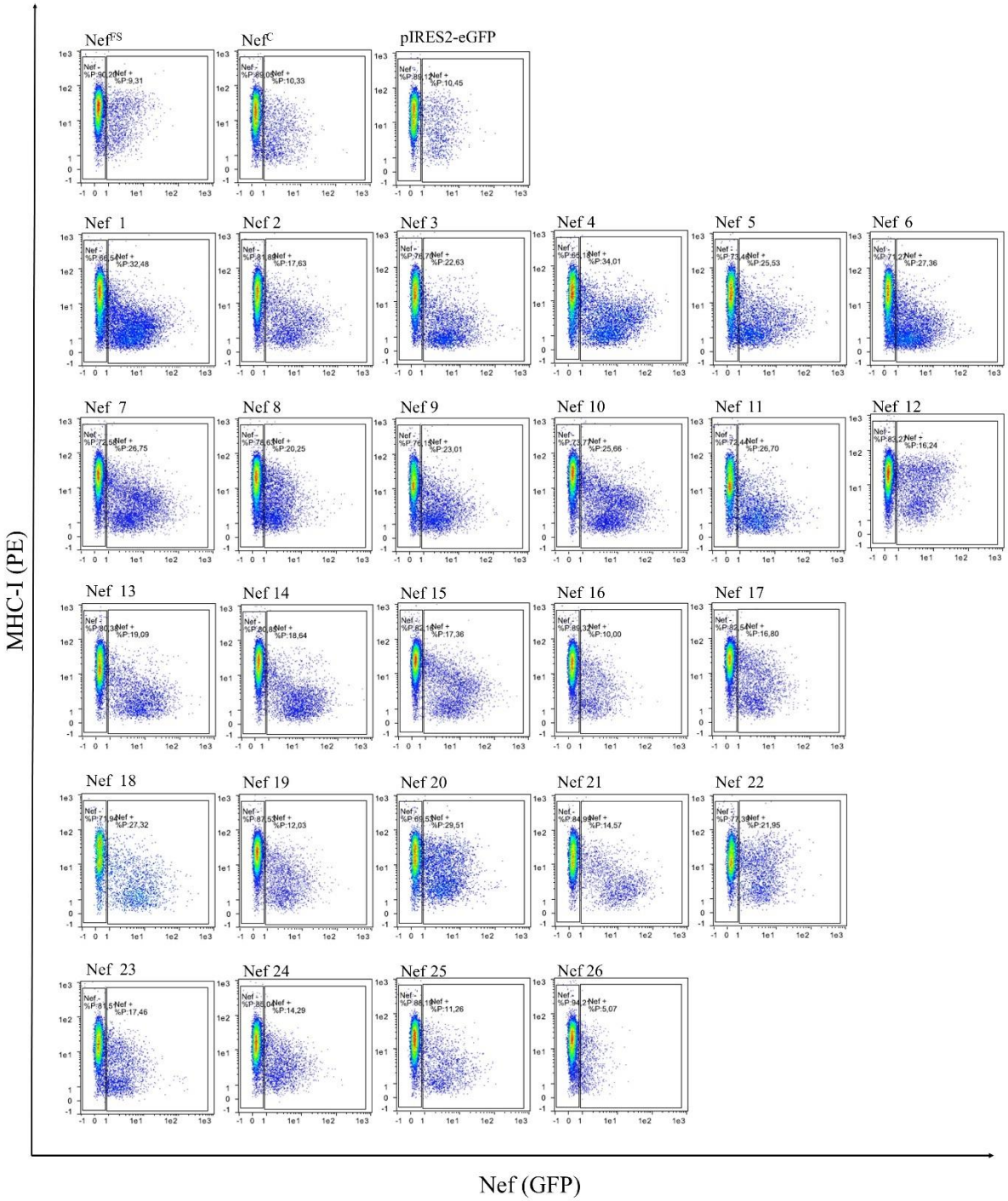
Nef^FS
Nef^C
pIRES2-eGFP
Nef 1
Nef 2
Nef 3
Nef 4
Nef 5
Nef 6
Nef 7
Nef 8
Nef 9
Nef 10
Nef 11
Nef 12
Nef 13
Nef 14
Nef 15
Nef 16
Nef 17
Nef 18
Nef 19
Nef 20
Nef 21
Nef 22
Nef 23
Nef 24
Nef 25
Nef 26
MHC-I (PE)
Nef (GFP)

B

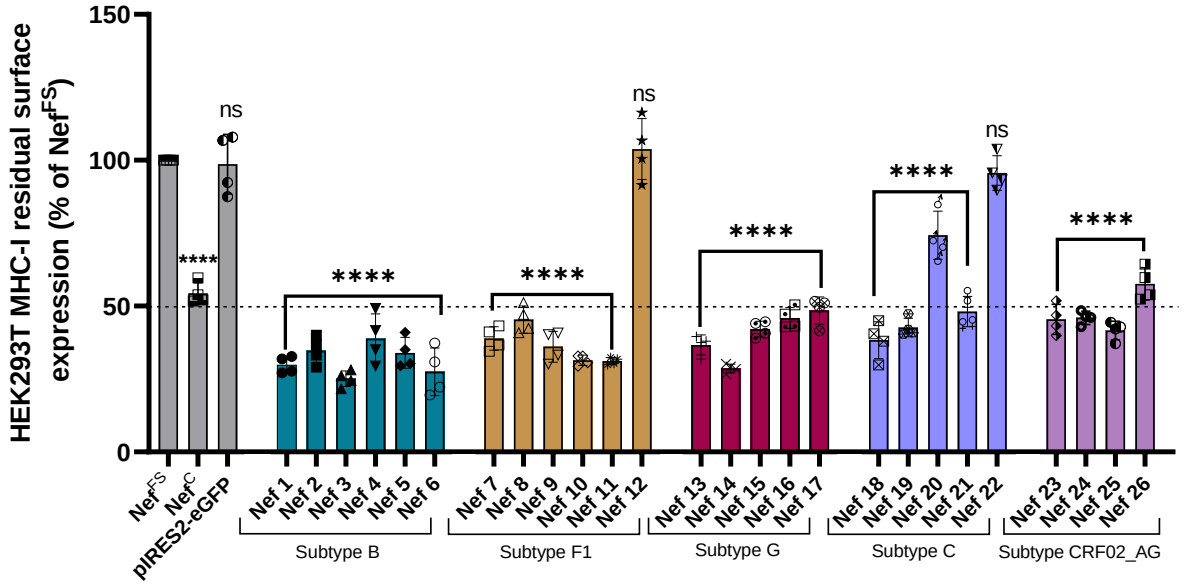


**Figure 15 Nef-mediated downregulation of MHC-I in HEK293T cells**. HEK293Ts cells were transfected with *nef* alleles and respective controls. Cells were harvested at 48 hpt and MHC-I levels were assessed by flow cytometry analysis. A) Representative flow cytometry plots of MHC-I (anti-HLA-A,B,C-PE) cell-surface expression (y-axis) in GFP-positive population (x-axis) for negative control ($Nef^{FS}$), positive control ($Nef^{C}$), empty vector (pIRES2-eGFP), and primary *nef* alleles. B) Quantitative analysis of MHC-I downregulation. The mean fluorescence intensity (MFI) of MHC-I expression in GFP-expressing cells were normalized to the MFI of the GFP negative population. The values were normalized and expressed as a percentage of $Nef^{FS}$. Significance was determined using non-parametric One-way ANOVA in GraphPad Prism v.9 (****$p < 0.0001$,***$p < 0.001$, **$p < 0.01$, ns = not significant). Data from four independent experiments are presented as mean ± standard deviation (Mean ± SD).

The flow cytometry plots representing Nef-mediated MHC-I downregulation in Jurkat T cells, as illustrated in Fig. 16 A, confirmed the previous observation in HEK293T showing visible downregulation in all *nef* alleles compared to negative controls.

The quantitative analysis, presented in Fig 16 B, underlined subtle inter-individual variations, with the lowest downregulation ability in samples Nef 20 and Nef 26 (MHC-I expression > 50%). Moreover, Nef 1, 5, 8, 9, 17, and 24 exhibited reduced downregulation activity (MHC-I expression > 45%). In contrast, Nef 3, 14, and 18 demonstrated the greatest downregulation ability (MHC-I expression < 30%),

A

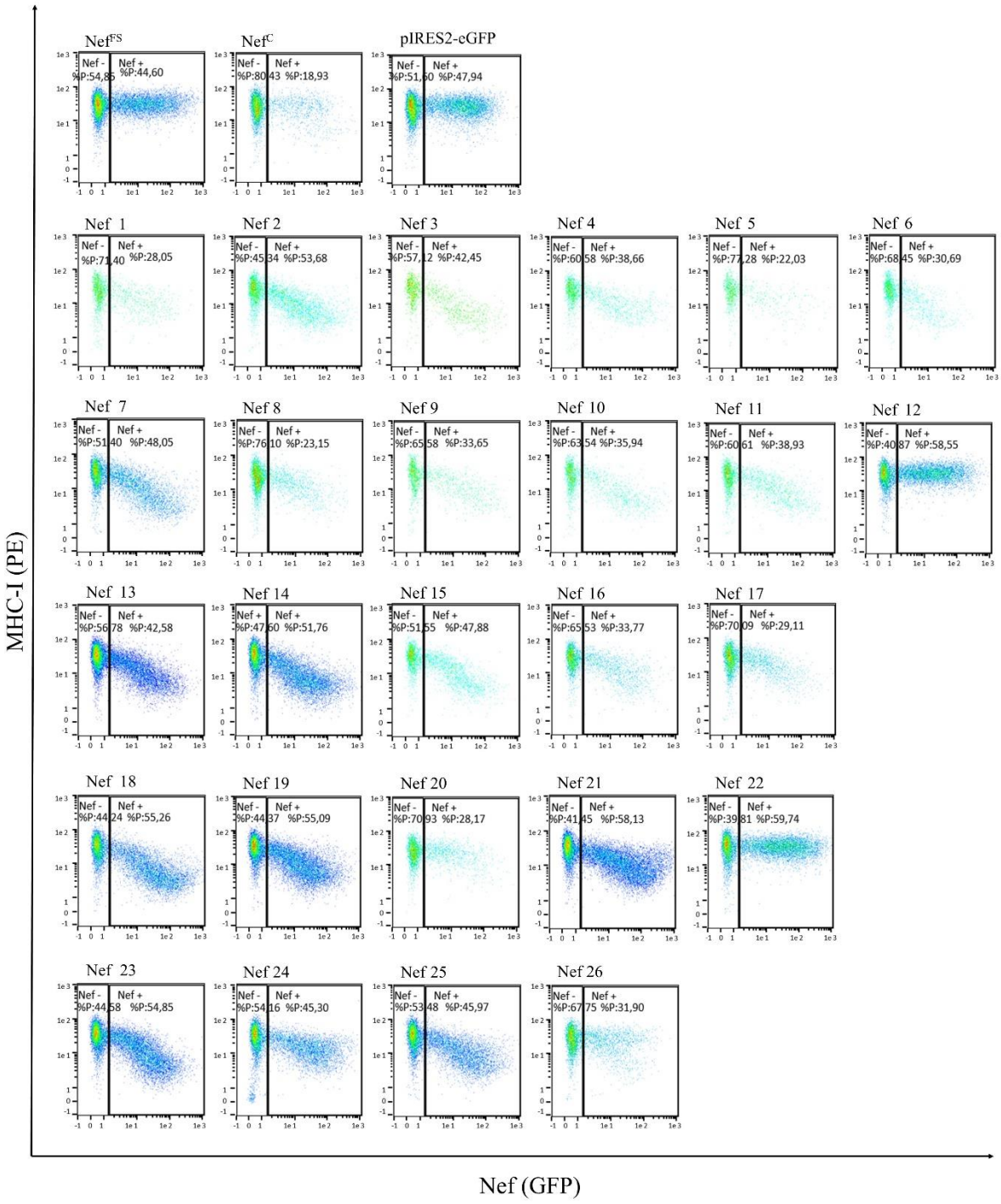
Nef^FS
Nef^C
pIRES2-cGFP
Nef 1
Nef 2
Nef 3
Nef 4
Nef 5
Nef 6
Nef 7
Nef 8
Nef 9
Nef 10
Nef 11
Nef 12
Nef 13
Nef 14
Nef 15
Nef 16
Nef 17
Nef 18
Nef 19
Nef 20
Nef 21
Nef 22
Nef 23
Nef 24
Nef 25
Nef 26
MHC-I (PE)
Nef (GFP)

B

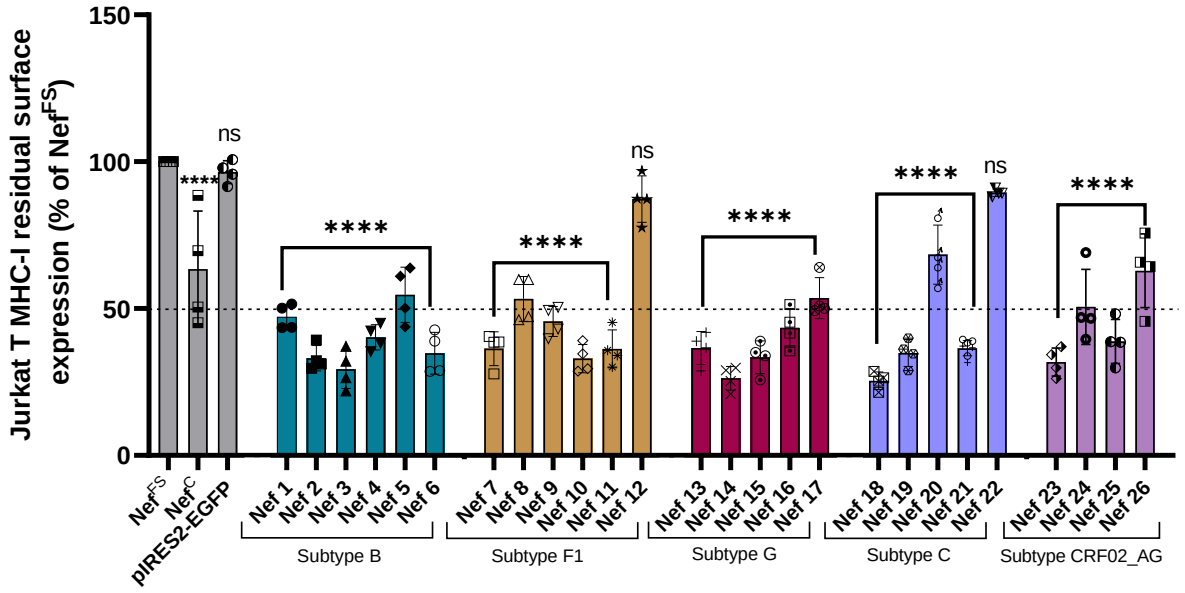


**Figure 16 Nef-mediated downregulation of MHC-I in Jurkat T cells**. Jurkat T cells were electroporated with *nef* alleles and indicated controls. Cells were harvested at 24 hpe and MHC-I levels were assessed by flow cytometry. A) Representative flow cytometry plots of MHC-I (anti-HLA-A,B,C-PE) cell-surface expression (y-axis) in GFP-positive population (x-axis) for negative control ($Nef^{FS}$), positive control ($Nef^{C}$), empty vector (pIRES2-eGFP), and primary *nef* alleles. B) Quantitative analysis of MHC-I downregulation. The mean fluorescence intensity (MFI) of MHC-I expression in GFP-expressing cells were normalized to the MFI of the GFP negative population. The values were normalized and expressed as a percentage of $Nef^{FS}$. Significance was determined using non-parametric One-way ANOVA in GraphPad Prism v.9 (****$p < 0.0001$,***$p < 0.001$, **$p < 0.01$, ns = not significant). Data from four independent experiments are presented as mean ± standard deviation (Mean ± SD).

Overall, no statistically significant differences were observed among the subtypes in both cell types. Therefore, taken together, the results imply that Nef activity in downregulating MHC-I from the cell surface remained highly conserved across different viral subtypes within the M group.

### 4.2.2 Downmodulation of endogenous CD4 by primary *nef* alleles

The ability of Nef to downmodulate endogenous levels of CD4 surface expression was investigated in Jurkat T cells, previously confirmed to express high levels of the receptor (data not shown). Jurkat T cells were electroporated with primary *nef* alleles and corresponding controls, and the CD4 expression levels were evaluated by flow cytometry at 24 hpe. Transfection efficiency was assessed by measuring the GFP signal of the backbone in the cells.

Nef-mediated downregulation of CD4 was confirmed through quantitative analysis. Primary *nef* alleles with an intact ORF significantly ($p < 0.05$) reduced the surface expression of the receptor compared to the negative control $Nef^{FS}$ . As observed with MHC-I downregulation, the internal negative controls Nef 12 and Nef 22 showed a comparable effect ($p > 0.05$) to $Nef^{FS}$. Moreover, the CD4 downregulation capacity of *nef* alleles was greater than the positive control $Nef^{C}$ for the majority of the samples.

The representative flow cytometry plots of Nef-mediated downregulation of CD4, depicted in Fig. 17 A, showed a substantial activity of all *nef* alleles compared to negative controls $Nef^{FS}$ and internal control Nef 12 and Nef 22.

Slight inter-individual differences were observed. Specifically, the quantitative analysis presented in Fig. 17 B displayed that samples Nef 1, 5, and 26 exhibited the lowest CD4 downregulation activity (CD4 expression > 50%), while samples Nef 8, 9, 17, and 20 showed reduced downregulation activity (CD4 expression > 40%) Conversely, a larger number of samples, including Nef 2, 11, 13, 14, 15, 19, 21, 23, and 25, exhibited high downregulation activity (CD4 expression < 30%).

Overall, no variations in terms of significant differences were observed in the downregulation activity of CD4 across different subtypes. Thus, in summary, flow cytometry results indicate that modulation of CD4 expression is conserved within the primary *nef* alleles.

A

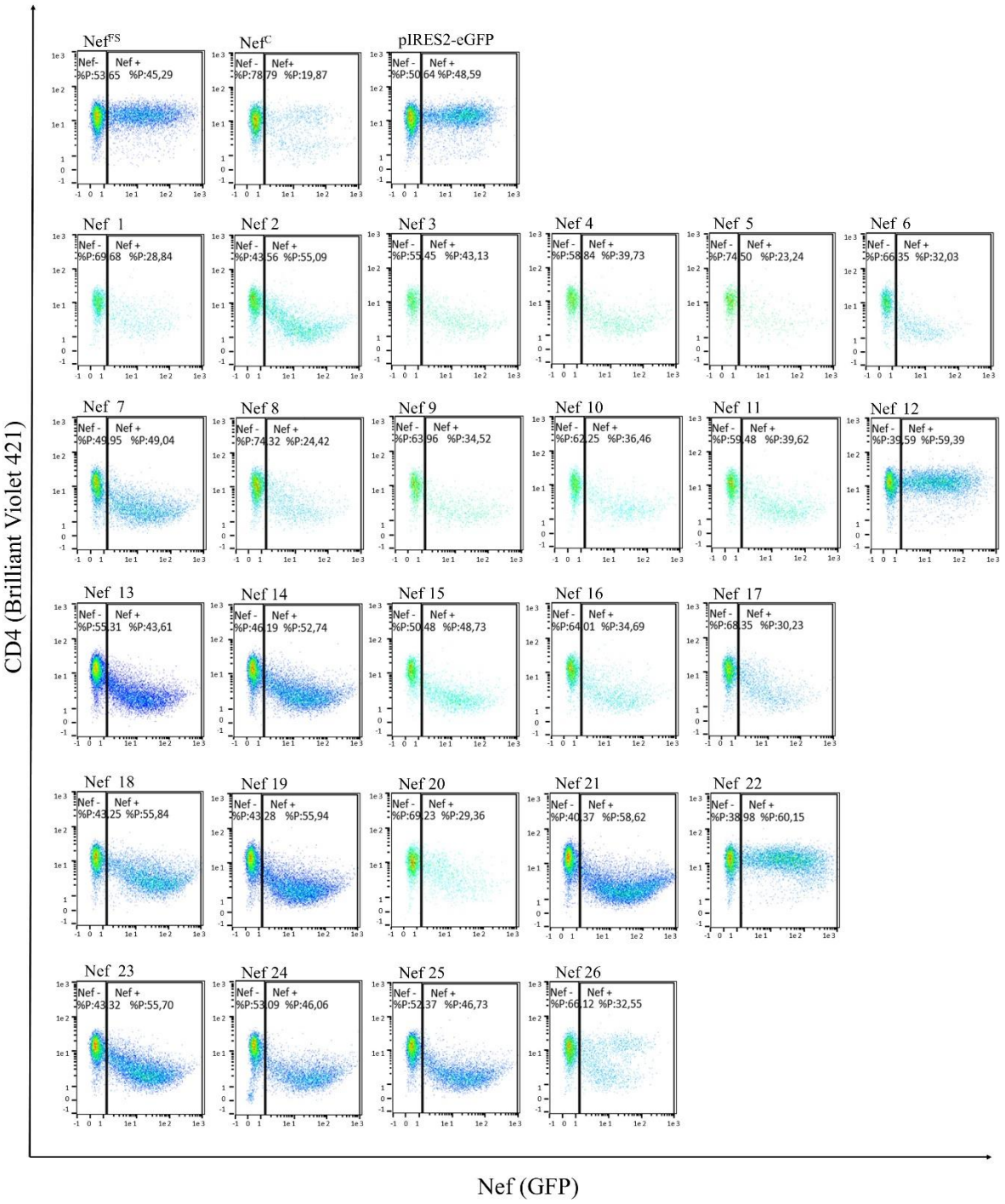
Nef^FS
Nef- %P:53,65 Nef+ %P:45,29
Nef^C
Nef- %P:78,79 Nef+ %P:19,87
pIRES2-eGFP
Nef- %P:50,64 Nef+ %P:48,59
Nef 1
Nef- %P:69,68 Nef+ %P:28,84
Nef 2
Nef- %P:43,56 Nef+ %P:55,09
Nef 3
Nef- %P:55,45 Nef+ %P:43,13
Nef 4
Nef- %P:58,84 Nef+ %P:39,73
Nef 5
Nef- %P:74,50 Nef+ %P:23,24
Nef 6
Nef- %P:66,35 Nef+ %P:32,03
Nef 7
Nef- %P:49,95 Nef+ %P:49,04
Nef 8
Nef- %P:74,32 Nef+ %P:24,42
Nef 9
Nef- %P:63,96 Nef+ %P:34,52
Nef 10
Nef- %P:62,25 Nef+ %P:36,46
Nef 11
Nef- %P:59,48 Nef+ %P:39,62
Nef 12
Nef- %P:39,59 Nef+ %P:59,39
Nef 13
Nef- %P:55,31 Nef+ %P:43,61
Nef 14
Nef- %P:46,19 Nef+ %P:52,74
Nef 15
Nef- %P:50,48 Nef+ %P:48,73
Nef 16
Nef- %P:64,01 Nef+ %P:34,69
Nef 17
Nef- %P:68,35 Nef+ %P:30,23
Nef 18
Nef- %P:43,25 Nef+ %P:55,84
Nef 19
Nef- %P:43,28 Nef+ %P:55,94
Nef 20
Nef- %P:69,23 Nef+ %P:29,36
Nef 21
Nef- %P:40,37 Nef+ %P:58,62
Nef 22
Nef- %P:38,98 Nef+ %P:60,15
Nef 23
Nef- %P:43,32 Nef+ %P:55,70
Nef 24
Nef- %P:53,09 Nef+ %P:46,06
Nef 25
Nef- %P:52,37 Nef+ %P:46,73
Nef 26
Nef- %P:66,12 Nef+ %P:32,55
CD4 (Brilliant Violet 421)
Nef (GFP)

B

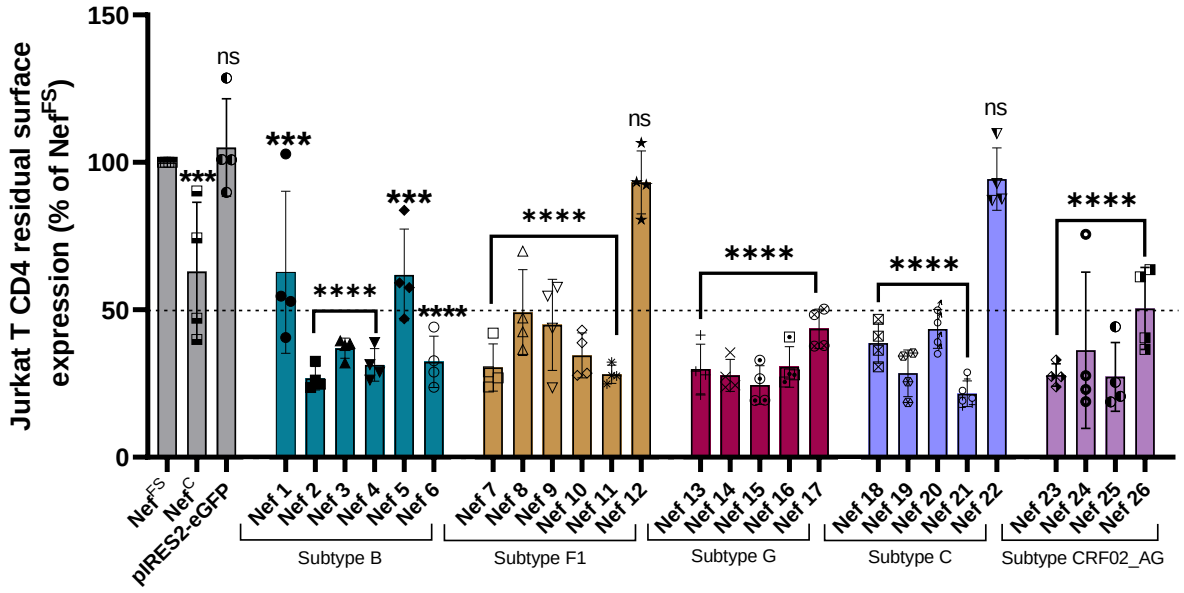


**Figure 17 Nef-mediated downregulation of CD4 in Jurkat T cells**. Jurkat T cells were electroporated with nef alleles and indicated controls. Cells were harvested at 24 hpe and CD4 level were assessed by flow cytometry. A) Representative flow cytometry plots of CD4 (anti-CD4-Brilliant Violet 421) cell-surface expression (y-axis) in GFP-positive population (x-axis) for negative control ($Nef^{FS}$), positive control ($Nef^{C}$), empty vector (pIRES2-eGFP), and primary nef alleles. B) Quantitative analysis of CD4 downregulation. The mean fluorescence intensity (MFI) of CD4 expression in GFP-expressing cells were normalized to the MFI of the GFP negative population. The values were normalized and expressed as a percentage of $Nef^{FS}$. Significance was determined using non-parametric One-way ANOVA in GraphPad Prism v.9 (****$p < 0.0001$,***$p < 0.001$, **$p < 0.01$, ns = not significant). Data from four independent experiments are presented as mean ± standard deviation (Mean ± SD).

### 4.2.3 Conserved antagonistic function of primary *nef* alleles against restriction factor SERINC5

The natural variability of SERINC5-counteracting activity in HIV-1 Nef proteins was explored by assessing the ability of primary *nef* alleles to downregulate the surface expression of the host factor in an overexpressing context. For this purpose, HEK293T cells were co-transfected with *nef* alleles and a PBJ5-SERINC5-iFLAG-HA plasmid, expressing human SERINC5 modified to expose a FLAG tag (DYKDDDDK) on the fourth extracellular loop. The residual SERINC5-iFLAG expression levels were analysed at 48 hpt by flow cytometry and the GFP signal of the backbone was used to evaluate the transfection efficiency.

Quantitative analysis showed that all primary *nef* alleles with intact ORF demonstrated a significant ($p < 0.05$) ability to reduce the surface expression of the SERINC5 restriction factor, compared to the negative control $Nef^{FS}$. The internal negative controls Nef 12 and Nef 22 confirmed the same expression of the $Nef^{FS}$ control ($p > 0.05$).

The representative flow cytometry plots in Fig.18 A confirmed the downregulation ability for each *nef* alleles compared to negative controls.

The inter-individual differences, showed in the quantitative analysis in Fig 18 B, revealed that sample Nef 18 exhibited the lowest SERIN5-downregulation ability (SERINC5-iFLAG expression > 50%). However, the majority of Nef alleles demonstrated a high capacity to counteract the host restriction factor (SERINC5-iFLAG expression < 30%). Among these, Nef 4, 9, 13, 14, 16, 19, 23, 24, 25, and 26 displayed the most pronounced downregulation (SERINC5-iFLAG expression < 20%). Notably, subtype CRF02_AG showed the most robust and conserved downregulation capability across all samples (SERINC5-iFLAG expression < 20%).

Despite these differences, no statistically significant variation occurred across different groups, therefore these findings underscore a highly conserved capacity of *nef* alleles to downregulate SERINC5, regardless of viral subtypes within M group.

A

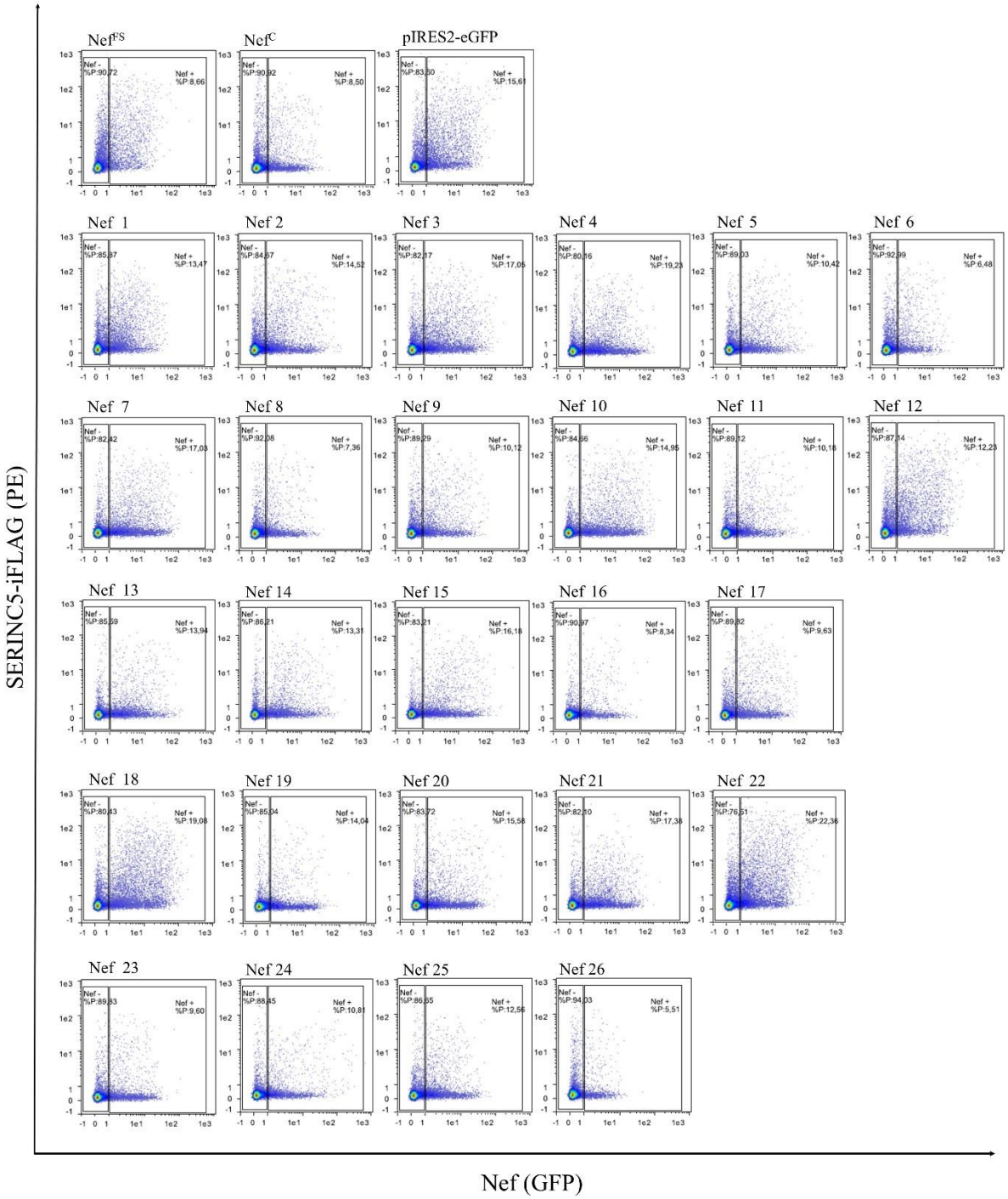
Nef^FS
Nef^C
pIRES2-eGFP
Nef 1
Nef 2
Nef 3
Nef 4
Nef 5
Nef 6
Nef 7
Nef 8
Nef 9
Nef 10
Nef 11
Nef 12
Nef 13
Nef 14
Nef 15
Nef 16
Nef 17
Nef 18
Nef 19
Nef 20
Nef 21
Nef 22
Nef 23
Nef 24
Nef 25
Nef 26
SERINC5-iFLAG (PE)
Nef (GFP)

B

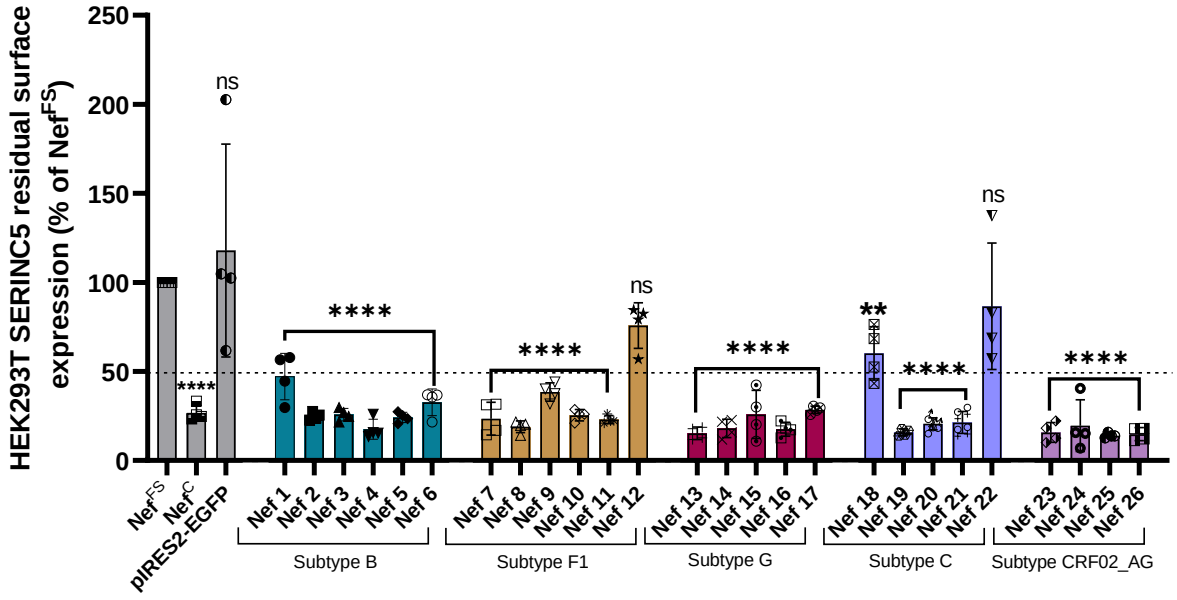


**Figure 18 Nef-mediated downregulation of SERINC5 in HEK293T cells**. HEK293Ts were co-transfected with *nef* alleles and PBJ5-SERINC5-iFLAG-HA. Cells were harvested at 48 hpt and expression levels of SERINC5 were assessed by immunostaining of extracellular FLAG-tag using flow cytometry. A) Representative flow cytometry plots of SERINC5-iFLAG (anti-FLAG Tag-PE) cell-surface expression (y-axis) in GFP-positive population (x-axis) for negative control ($Nef^{FS}$), positive control ($Nef^{C}$), empty vector (pIRES2-eGFP), and primary *nef* alleles. B) Quantitative analysis of SERINC5 downregulation. The mean fluorescence intensity (MFI) of SERINC5 expression in GFP-expressing cells were normalized to the MFI of the GFP positive population. The values were normalized and expressed as a percentage of $Nef^{FS}$. Significance was determined using non-parametric One-way ANOVA in GraphPad Prism v.9 (****$p < 0.0001$,***$p < 0.001$, **$p < 0.01$, ns = not significant). Data from four independent experiments are presented as mean ± standard deviation (Mean ± SD).

### 4.2.4 Correlation between Nef-mediated MHC-I, CD4 and SERINC5 downregulation

Even though the key genetic motifs responsible for Nef-mediated MHC-I downregulation are distinct from those governing Nef-mediated CD4 and SERINC5 downregulation (137), (159), (132), previous studies of natural Nef sequences have indicated limited correlations between specific Nef activities (200), (141,201,202). This suggest the existence of secondary or shared genetic determinants.

To investigate potential associations between functions in the 26 primary *nef* alleles, the Nef-mediated downregulation of MHC-I, CD4, and SERINC5 in their respective cell systems was correlated. Firstly, the Nef-mediated downregulation of MHC-I in HEK293T and Jurkat T cells was compared, revealing a strong correlation (Spearman r = 0.65, p = 0.0001) between both cell systems (Fig. 19 A). Additionally, CD4 downregulation and MHC-I downregulation by Nef correlated weakly (Spearman r = 0.42, p = 0.02) in HEK 293T cells (Fig. 19 B), and strongly (Spearman r = 0.77, p < 0.0001) in Jurkat T cells (Fig. 19 C), potentially influenced by the distinct cellular system. A robust correlation (Spearman r = 0.60, p = 0.0006) was observed between CD4 and SERINC5 downregulation functions (Fig. 19 D). In contrast, no correlation (Spearman r = 0.13, p 0.48) was observed between MHC-I in HEK 293T and SERINC5 (Fig. 19 E); while a slight correlation (Spearman r = 0.38, p = 0.04) occurred between MHC-I in Jurkat T cells and SERINC5 (Fig. 19 F). Notably, SERINC5 downregulation correlated more strongly with the ability of primary *nef* alleles to internalize CD4 compared with MHC-I.

These results confirmed previous observations regarding Nef activity, suggesting similarities between CD4 and SERINC5 downregulation functions, while the MHC-I downregulation activity may function more independently.

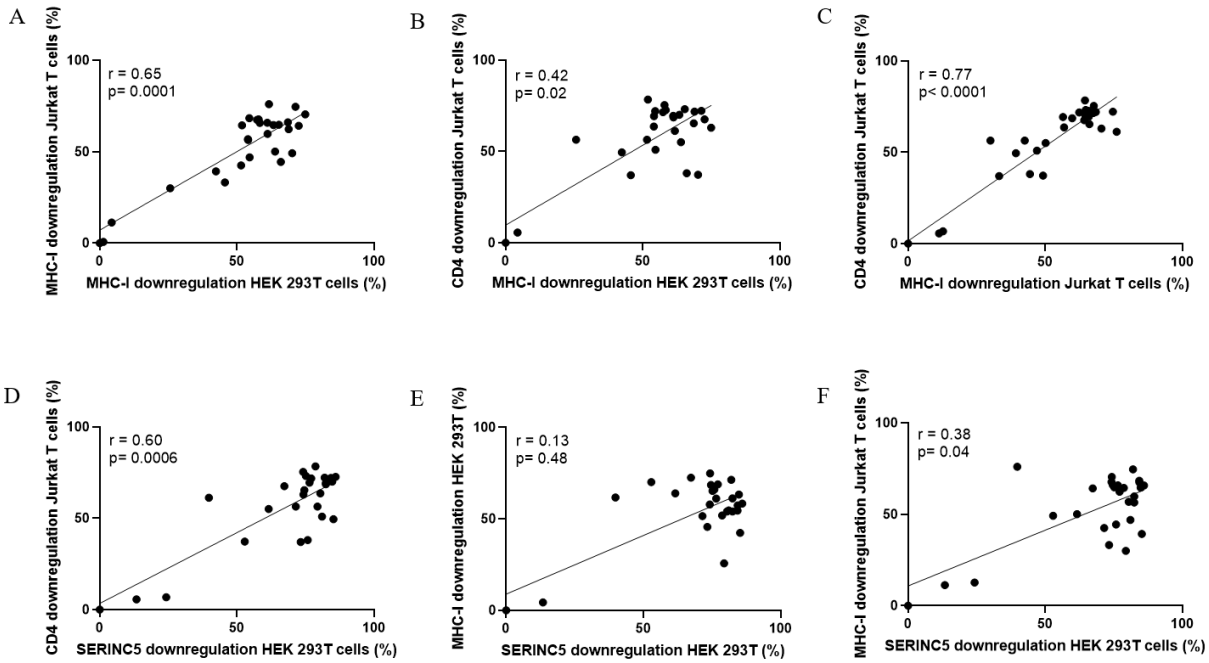


**Figure 19 Relationship between Nef functions.** Relationships are assessed using Spearman's correlation between A) MHC-I downregulation in HEK 293T cells and in Jurkat T cells, B) CD4 downregulation and MHC-I downregulation in HEK 293T cells, C) CD4 downregulation and MHC-I downregulation in Jurkat T cells, D) SERINC5 downregulation and CD4 downregulation in Jurkat T cells, E) SERINC5 downregulation and MHC-I downregulation in HEK 293T cells, F) SERINC5 downregulation and MHC-I downregulation in Jurkat T cells. All Nef functions were expressed relative to that of $Nef^{FS}$ (0% activity).

### 4.2.5 Correlation between Nef functions and Viral Load

Given the importance of CD4 downregulation in enhancing viral replication (151), (203) previous studies have observed a correlation between Nef-mediated CD4 downregulation and viral load (163). However, despite the role of SERINC5 in HIV-1 replication (130), the correlation of its downregulation and viral load was variable (204). In contrast, Nef-mediated MHC-I downregulation was identified as not directly affecting viral replication (205), and no correlation with viral load was observed in previous observations (163).

In order to investigate the impact of Nef on viral replication in primary alleles naïve to antiretroviral therapy, Nef-mediated downregulation functions were correlated with the baseline viral load (cp/ml). The only Nef function that exhibited a statistically significant correlation with baseline viral load was the downregulation of CD4 (Fig. 20 C). In fact, increased Nef-mediated CD4 downregulation ability correlating with lower viral load was observed (Spearman r = -0.47, p = 0.01). However, no relationship was found between MHC-I downregulation and viral load in both HEK 293T (Spearman r = 0.28, p = 0.15) and Jurkat (Spearman r = -0.33, p = 0.09), as well as between SERINC5 downregulation and viral load (Spearman r = -0.32, p = 0.10).

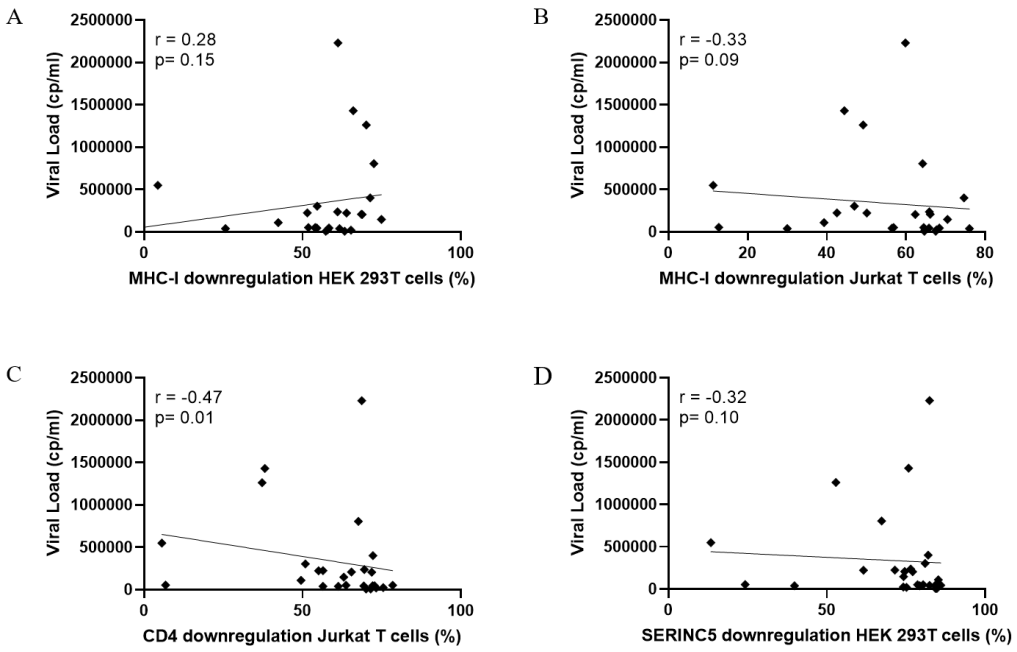


**Figure 20 Relationship between Nef functions and baseline viral load (cp/ml)**. Relationship was assessed using Spearman's correlation between A) MHC-I downregulation and viral load in HEK 293T cells, B) MHC-I downregulation and viral load in Jurkat T cells, C) CD4 downregulation and viral load in Jurkat T cells, D) SERINC5 downregulation and viral load in HEK 293T cells.

### 4.2.6 Highly variable interaction between primary *nef* alleles and ACOT8

The importance of the interaction between Nef and ACOT8 in the context of HIV-1 pathogenesis is still unclear. Furthermore, is yet to be determined whether the ability to interact with ACOT8 is a conserved function among primary *nef* alleles. To investigate the interaction between primary *nef* alleles with ACOT8, a co-immunoprecipitation assay was conducted. HEK293T cells were co-transfected with primary *nef* alleles and a mScarletACOT8 plasmid, which expresses an ACOT8-mScarlet fusion protein. The previously described plasmids pCG NA7nefHIV-1IRESGFP, pCG NL43nef3-IRESGFP, $Nef^{C}$ and $Nef^{FS}$ were included as controls. After 48-hours, cell lysates were prepared, and the Nef/ACOT8 interaction was analysed by immunoprecipitation of the mScarletACOT8 fusion protein using RFP-Trap Agarose beads.

Western blot analysis of the whole protein extracts (input), presented in Fig. 21 A, confirmed a simultaneous expression of the transfected mScarletACOT8 protein at 62 kDa and the endogenous ACOT8 at 36 kDa, along with the housekeeping tubulin. Notably, a shift in molecular weight due to the mScarlet tag was perceived. The enrichment of mScarletACOT8 in combination with the absence of endogenous ACOT8 and tubulin in the elution probe (Fig. 21 B), confirmed the successful and specific pulldown of mScarletACOT8. Furthermore, the validation of Nef expression in the whole protein extracts (input), as depicted in Fig. 21 A, echoed our previous findings. Nef was expressed in all primary alleles with an intact ORF, displaying significant variability in band intensity and height. Conversely, no expression was observed in samples Nef 12 and Nef 22 due to the disrupted ORF.

The analysis of the immunoprecipitated lysates, presented in Fig. 21 B, demonstrated that the association between Nef and ACOT8 occurred exclusively for Nef 1, Nef 3, Nef 4, Nef 5, Nef 9, Nef 11, and Nef 14. Interestingly, no interaction was detectable between ACOT8 and the $Nef^{C}$ positive control, while an association was observed between the Nef Na7 positive control and ACOT8.

Taken all together, this interaction study highlight a highly variable ability of primary *nef* alleles to interact with ACOT8, contrasting with the previously investigated functions that showed strong conservation.

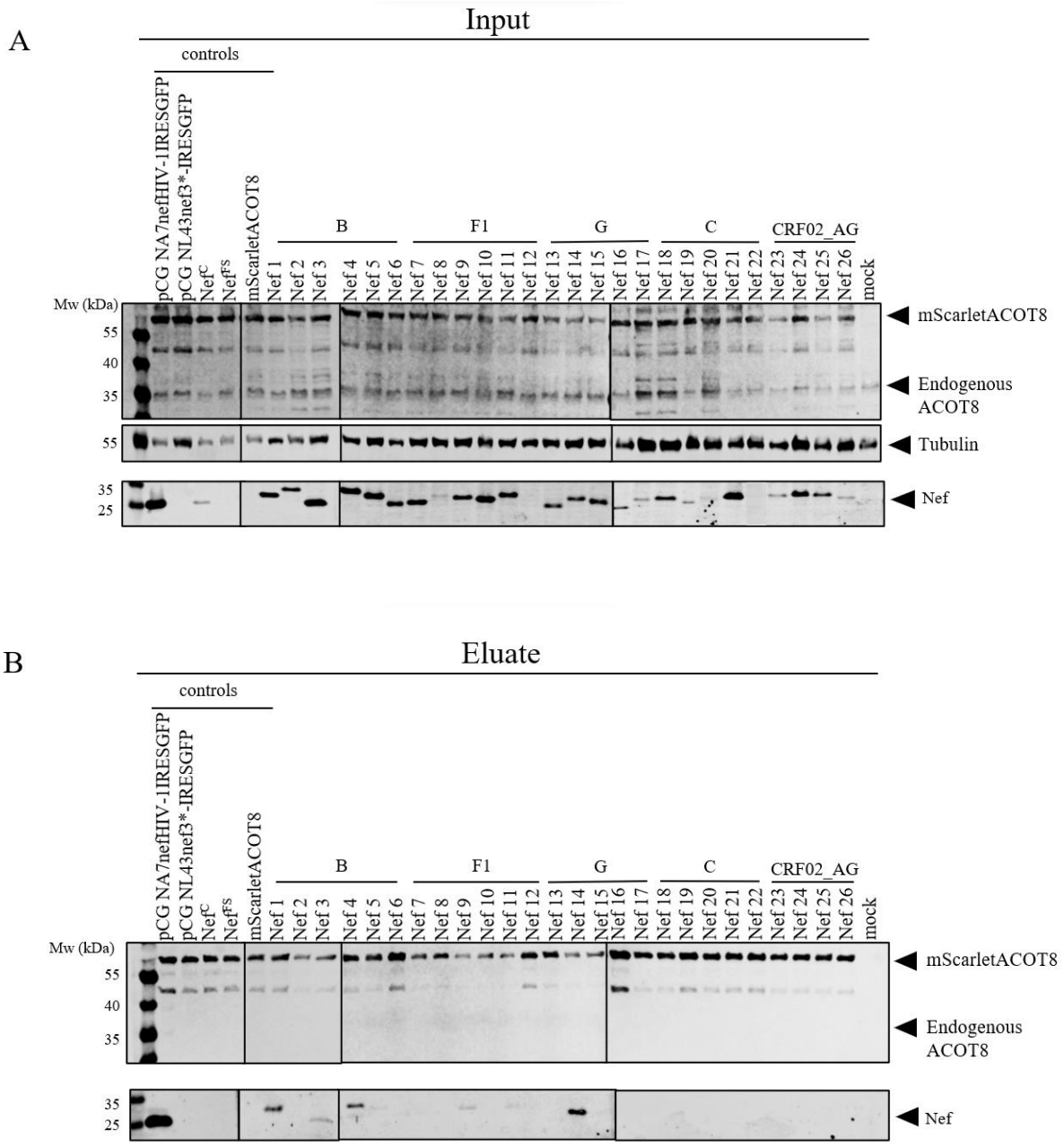


**Figure 21 Co-immunoprecipitation assay between primary *nef* alleles and ACOT8**. HEK293T were co-transfected with primary *nef* alleles and controls together with a mScarletACOT8 plasmid. After 48-hours, cells were lysed, and the mScarletACOT8 complex was immunoprecipitated with the RFP-Trap Agarose beads A) Western blot analysis of the input fraction and B) elution fraction using the indicated antibodies. N=1. (Mw, molecular weight).

# 5 Discussion

In addition to the three prototypic genes *gag*, *pol*, and *env*, which are essential and sufficient for the replication of most retroviruses, human and simian immunodeficiency viruses (HIV and SIV, respectively) contain another six open reading frames for two regulatory proteins (*tat* and *rev*) and four accessory proteins (*vif*, *vpr*, *vpu* and *nef*), that perform essential functions during the viral life cycle in the host (112), (110). Among these, the Nef protein of HIV-1, abundantly expressed early in infection, is a crucial determinant of viral pathogenesis and disease progression, believed to optimize the cellular environment for viral replication (134). It is involved in a plethora of target molecules and functions, and in particular plays a key role in immune escape of HIV-infected cells and modulating cell surface expression of several molecules, including MHC-I, CD4 and SERINC5, thus enhancing viral infectivity (127). Furthermore, Nef is described as a raft-associated protein, involving intricate interactions essential for its migration and binding to the membrane (106). Despite extensive research efforts, many aspects of the complex molecular mechanisms underlying Nef functions remain elusive and require further investigation.

Here, we investigated the impact of 26 primary individuals-derived HIV-1 *nef* alleles on the well-characterized downregulation of cell surface receptors MHC-I, CD4, and SERINC5. Subsequently, this study aimed to explore the still unclear interaction between primary *nef* alleles and ACOT8.

For this purpose, primary *nef* alleles were isolated from plasma samples of an ART-naïve cohort of HIV-positive people and with a known date of seroconversion. The baseline sampling time point, conducted before the initiation of antiretroviral therapy, allowed for the exclusion of any selective pressures induced by the treatment. Additionally, to investigate potential inter-subtype differences in Nef functions, the study subjects were grouped based on the viral subtype within the M group as follows: 6 (subtype B), 6 (subtype F1), 5 (subtype G), 5 (subtype C), and 4 (subtype CRF02_AG).

At the outset, clones generated by inserting *nef* amplicons into the pIRES2-eGFP expression vector showed an intact open reading frame in 24 out of 26 samples. Notably, no difference in the clinical data was observed in the two samples with disrupted ORF compared to the others. Within those 24 samples, high sequence variability was observed. Nevertheless, the presence

of motifs linked to Nef expression, as W124 and P136 (197), was conserved across all sequences. Additionally, the integrity of N-terminal myristoylation motif in all samples confirmed its critical role for Nef functions.

The steady-state expression of the Nef protein was confirmed for all primary alleles with intact ORF, even though they exhibited high variability in band intensity and height. Given the strong preservation of motifs linked to the structural integrity of the protein and the presence of functional activities, this differences may likely be attributed to the differential binding of the primary polyclonal antibody to genetically diverse Nef isolates and to different expression levels of the samples.

In the first functional analysis, it was demonstrated that the primary *nef* alleles with intact ORF led to a significant downregulation of the endogenous surface levels of MHC-I and CD4 receptors in both HEK293T and Jurkat T cells. Similar observations were confirmed in the context of SERINC5 overexpression, where the host restriction factor was downregulated from the cell surface by all primary *nef* alleles with intact ORF. Notably, the overexpression of SERINC5 was necessary due to the current unavailability of a properly-working anti-SERINC5 antibody for the endogenous protein. Therefore the SERINC5 downregulation was evaluated using a plasmid expressing a modified SERINC5 harboring an internal FLAG epitope within the fourth extracellular loop, conveniently detectable with an anti-FLAG antibody (176). However, it should be noted, as reported by Passos V. et al., that the modulation of the heterologous cellular factor might differ compared to the endogenous levels of SERINC5 (206).

Surprisingly, no significant inter-subtype differences were observed in the studied Nef's ability, highlighting its conserved function across HIV-1 subtypes of the M group in downregulating MHC-I, CD4, and SERINC5 from the cell surface. All together, these findings corroborate earlier observations regarding Nef's capacity to downregulate the cell surface expression of these receptors. However, the absence of inter-subtype differences contrasts with previous research that revealed variations in the ability of HIV-1 Nef to downregulate MHC-I, CD4, and SERINC5 among viral subtypes (141), (142), (173). These differences could primarily be attributed to the limited number of participants per subtype used in this study, that may not be representative of the subtype as a whole. Nonetheless, the strong conservation of the principal motifs linked to Nef functions may justify the observed

outcome. In fact, the 72PxxP75 motif, and the residue Asp123 essential for MHC-I downregulation (138), (139), as well as the di-leucine motif (164LL165) primarily involved in CD4 and SERINC5 downregulation (159), were unmutated in all primary *nef* alleles, regardless of subtype. Given the relevance of the key functional motifs in conserving Nef function, this study underscores that the downregulation of cell surface molecules mediated by Nef is closely linked to its interaction with complexes involved in vesicular trafficking machinery.

Inter-individual differences in Nef functions observed among primary alleles were examined in a more detailed analysis. Firstly, the association between the steady-state Nef proteins and the functional ability of primary alleles was explored for Nef-mediated MHC-I downregulation in HEK293T. This analysis showed that samples Nef 20 and Nef 26, that exhibited the lowest MHC-I downregulation capacity, had also low expression levels of the steady-state Nef proteins in the Western blot. A similar association was observed for samples Nef 8 and Nef 17, where the downregulation was reduced. Interestingly, this association was not seen for samples Nef 16, Nef 21, Nef 23, and Nef 24, which, despite exhibiting a reduced downregulation activity, showed high levels of the protein expression. Conversely, Nef 14, with low expression levels in Western blot, proved to be one of the most effective in downregulating MHC-I. Therefore, it is not possible to establish a direct correlation between protein expression and its functionality, primarily because the variability observed in Western blot is more likely attributed to the different detection of the polyclonal primary antibody and to different expression levels of the samples. Additionally, previous studies confirmed no correlation between Nef function and its expression (202).

These outcomes suggest that the inter-individual variability of *nef* alleles may primarily stem from Nef polymorphisms in regions involved in its functions. Specifically, variations in the AP-1 and AP-2 binding site, essential for the downregulation of surface receptors through the vesicular trafficking machinery (128), (154), (155), could play a crucial role in affecting Nef function. In support of this hypothesis, an exploratory sequence-function analysis, revealed that half of the analysed sequences exhibited large variability and insertions within the protein interaction site (AA 12-39). This site is involved in anchoring Nef to the membrane, facilitating exosome release (106), and modulating its ability to downregulate MHC-I, CD4, and SERINC5 (175), (207). Furthermore, high variability was observed in the 62EEEE65 motif, crucial for Nef's interaction with PACS-1 (199), consequently affecting Nef's ability to

downregulate MHC-I. Particularly noteworthy is the E65D mutation identified in samples Nef 17 and Nef 26, which may contribute to their diminished downregulation activity. Additionally, substantial alterations in this motif were identified in all samples belonging to the CRF02_AG subtype, which exhibited reduced MHC-I downregulation capacity.

Among the molecular determinants involved in Nef-mediated CD4 and SERINC5 downregulation, the endocytic signal 160Exxx, related to the di-leucine motif (108), exhibited high variability in primary *nef* alleles in this study. Specifically, the polymorphism S163C, associated with increased Nef activity towards CD4 and SERINC5 (200) (175), was present in the majority of samples showing high downregulation activity against these receptors. Samples Nef 4, 8, 13, 16, 23, 24, and 25, which exhibited a higher ability to downregulate SERINC5, had the H116 site unmutated, previously associated with enhanced Nef activity (174). With the exception of Nef 24, the residue R178, also associated with enhanced Nef activity (175), was predominantly found in the CRF02_AG subtype, which showed the highest activity in downregulating the host restriction factor. Lastly, Nef 18, which demonstrated the lowest SERINC5 downregulation activity, is the only sample harboring the W57Q mutation in the N-terminal 57WL58 motif, important for the downregulation of CD4 and SERINC5 (159). However, no impact of this mutation on the CD4 downregulation activity was observed.

Overall, this findings emphasized that Nef function is highly conserved among primary alleles, but the presence of specific polymorphisms may contribute to the observed inter-individual differences. However, due to the high variability in Nef sequencing among primary alleles, the presence of additional mutations or combinations thereof that compensate for the loss or gain of Nef function, and the limited number of samples, it is not possible to establish a direct correlation between mutations and the increased or decreased activity of primary *nef* alleles.

Additionally, this study revealed that the Nef-mediated MHC-I downregulation activity showed a weaker correlation with CD4 and no correlation with SERINC5, while a more pronounced correlation was observed between CD4 and SERINC5 downregulation. This reaffirmed previous evidence suggesting that the mechanisms underlying MHC-I modulation differ from those governing CD4 and SERINC5, as observed also in the functional analysis of polymorphisms. However, it leaves open the possibility of the existence of secondary or

shared genetic determinants within Nef function. Furthermore, given the importance of Nef in increasing viral infectivity and pathogenesis (151), (203), the correlation study between Nef functions and viral load was carried out in order to investigate the impact of primary alleles in viral replication. Nef-mediated CD4 downregulation correlated significantly with lower baseline viral load, highlighting Nef's pivotal role in viral infectivity, particularly during early infection stages. Interestingly, despite its strong correlation with CD4, no association was found between SERINC5 downregulation and viral load. This finding aligns with previous observations where the correlation between SERINC5 downregulation and viral load varied (204). Notably, no difference in terms of significance was observed between primary *nef* alleles with recent infection (< 6 months) and previous chronic infection (> 6 months). Nevertheless, a comprehensive analysis of Nef functions and disease markers was hindered by the unavailability of CD4 rate values for some samples. Further investigation in this regard could provide clearer insights into the relationship between Nef activity and pathogenesis.

The second Nef functional analysis revealed a surprising variability in the interaction between primary *nef* alleles and ACOT8. In particular, exclusively Nef 1, Nef 3, Nef 4, Nef 5, Nef 9, Nef 11, and Nef 14 exhibited interaction with the host protein in the Co-IP assay. Given the absence of information regarding the interaction between primary *nef* alleles and ACOT8, this study aimed to elucidate the potential functional domains involved in this interplay.

To investigate whether this variability could be attributed to specific motifs in the Nef sequence, the residues Asp108, Asp111, Leu112, Phe121, Pro122, Asp123, and Trp124, previously identified as essential for Nef/ACOT8 interaction in different HIV-1 strains (191), (192), (193), were investigated. All of these residues, with the exception of Asp108, were conserved in the sequences of primary *nef* alleles under study. Interestingly, all primary alleles demonstrating interaction exhibited an unaltered amino acid at position 108. In contrast, the majority of samples lacking interaction had a mutated amino acid at this position. Moreover, despite featuring the original amino acid Asp108, samples Nef 2, Nef 13, Nef 17, Nef 20, and Nef 23, did not show any interaction. Enigmatically, no interaction between ACOT8 and $Nef^{C}$ control was detectable, however the interaction with Nef NA7 was confirmed as reported in the aforementioned studies (193). Given the relatively low expression level of $Nef^{C}$, this raises the possibility of a methodological limitation, suggesting that for Nef proteins with low expression levels, it may be challenging to conclusively determine the presence or absence of an interaction.

All together these results suggest that the presence of Asp may be involved in the Nef and ACOT8 association, but not sufficient, given the high variability in interaction observed among primary alleles.

This research has laid the groundwork for investigating the interaction between primary *nef* alleles and ACOT8. Moreover, given deficiencies in ACOT8 have been directly linked to lipid metabolism impairment (193), studying this protein could uncover strategies to interfere with various Nef cellular functions and the HIV-1 infective life cycle.

Further studies are needed to identify the molecular determinants involved in this interaction, considering a broader spectrum of primary alleles that include a larger number of samples and a greater differentiation of viral subtypes.

# 6 Conclusions

In conclusion, this study sheds light on the complex interplay between primary individuals-derived HIV-1 *nef* alleles and host cellular factors. The extensive investigation into the multifactorial character of the viral protein, provides valuable insight into the intricate mechanisms underlying Nef-mediated modulation of cell surface receptors and the interaction with ACOT8.

The findings highlight a remarkable conservation in Nef's ability to downregulate the cell surface expression of MHC-I, CD4, and SERINC5 across the majority of primary *nef* alleles within the HIV-1 subtypes of the M group. These activities are linked with the strong conservation of key functional motifs within Nef sequences, underscoring the essential role of these elements in maintaining Nef's diverse functionalities. Despite inter-individual variations, primarily attributed to specific natural polymorphisms occurring in Nef sequence, a consistent and significantly pattern in Nef's activities is observed across the sampled cohort.

Crucially, this research demonstrates, for the first time, an interaction between primary *nef* alleles and ACOT8. In contrast to the aforementioned Nef function, this association is highly variable among the HIV-1 subtypes and might depend on amino acid residues within the central core domain of Nef.

The main limitations of the study are primarily associated with the small sample size of the cohort and the restricted number of analysed subtypes, which may not adequately represent the variability of Nef functions. Furthermore, Nef's functionality could vary across different infected cell types, necessitating further investigation to validate the findings in primary cells and other cell types beyond CD4+ T-lymphocytes. Moreover, some functions were examined in an overexpression context, implying the necessity for a more comprehensive analysis at an endogenous level to better understand the functions studied.

Overall, the study deepens our understanding of Nef biology and its significance in HIV-1 pathogenesis, setting the stage for further exploration. However, additional research encompassing a broader spectrum of primary *nef* alleles and viral subtypes is warranted to comprehensively delineate the intricate networks governing Nef-mediated viral pathogenesis.

# 7 Bibliography


1. Barré-Sinoussi F, Chermann JC, Rey F, Nugeyre MT, Chamaret S, Gruest J, et al. Isolation of a T-Lymphotropic Retrovirus from a Patient at Risk for Acquired Immune Deficiency Syndrome (AIDS). Science (1979). 1983 May 20;220(4599):868–71.

2. La Placa M. Principi di Microbiologia medica. 14th ed. 2014.

3. Gottlieb MS, Schroff R, Schanker HM, Weisman JD, Fan PT, Wolf RA, et al. Pneumocystis carinii Pneumonia and Mucosal Candidiasis in Previously Healthy Homosexual Men. New England Journal of Medicine. 1981 Dec 10;305(24):1425–31.

4. THE PATH THAT ENDS AIDS 2023 UNAIDS GLOBAL AIDS UPDATE [Internet]. Available from: http://www.wipo.int/amc/en/mediation/rules

5. Faria NR, Rambaut A, Suchard MA, Baele G, Bedford T, Ward MJ, et al. The early spread and epidemic ignition of HIV-1 in human populations. Science (1979). 2014 Oct 3;346(6205):56–61.

6. Sharp PM, Hahn BH. Origins of HIV and the AIDS Pandemic. Cold Spring Harb Perspect Med. 2011 Sep 1;1(1):a006841–a006841.

7. Maartens G, Celum C, Lewin SR. HIV infection: epidemiology, pathogenesis, treatment, and prevention. The Lancet. 2014 Jul;384(9939):258–71.

8. Visseaux B, Damond F, Matheron S, Descamps D, Charpentier C. Hiv-2 molecular epidemiology. Infection, Genetics and Evolution. 2016 Dec;46:233–40.

9. Simon V, Ho DD, Abdool Karim Q. HIV/AIDS epidemiology, pathogenesis, prevention, and treatment. The Lancet. 2006 Aug;368(9534):489–504.

10. Sierra S, Kupfer B, Kaiser R. Basics of the virology of HIV-1 and its replication. Journal of Clinical Virology. 2005 Dec;34(4):233–44.

11. Gelderblom HR. Assembly and morphology of HIV: potential effect of structure on viral function. AIDS. 1991 Jun;5(6):617–37.

12. Frankel AD, Young JAT. HIV-1: Fifteen Proteins and an RNA. Annu Rev Biochem. 1998 Jun;67(1):1–25.

13. De Guzman RN, Wu ZR, Stalling CC, Pappalardo L, Borer PN, Summers MF. Structure of the HIV-1 Nucleocapsid Protein Bound to the SL3 Ψ-RNA Recognition Element. Science (1979). 1998 Jan 16;279(5349):384–8.

14. van Opijnen T, Jeeninga RE, Boerlijst MC, Pollakis GP, Zetterberg V, Salminen M, et al. Human Immunodeficiency Virus Type 1 Subtypes Have a Distinct Long Terminal Repeat That Determines the Replication Rate in a Host-Cell-Specific Manner. J Virol. 2004 Apr;78(7):3675–83.

15. Freed EO. HIV-1 Gag Proteins: Diverse Functions in the Virus Life Cycle. Virology. 1998 Nov;251(1):1–15.

16. Ghanam RH, Samal AB, Fernandez TF, Saad JS. Role of the HIV-1 Matrix Protein in Gag Intracellular Trafficking and Targeting to the Plasma Membrane for Virus Assembly. Front Microbiol. 2012;3.

17. Summers MF, Henderson LE, Chance MR, South TL, Blake PR, Perez-Alvarado G, et al. Nucleocapsid zinc fingers detected in retroviruses: EXAFS studies of intact viruses and the solution-state structure of the nucleocapsid protein from HIV-1. Protein Science. 1992 May 31;1(5):563–74.

18. Jouvenet N, Simon SM, Bieniasz PD. Imaging the interaction of HIV-1 genomes and Gag during assembly of individual viral particles. Proceedings of the National Academy of Sciences. 2009 Nov 10;106(45):19114–9.

19. Paxton W, Connor RI, Landau NR. Incorporation of Vpr into human immunodeficiency virus type 1 virions: requirement for the p6 region of gag and mutational analysis. J Virol. 1993 Dec;67(12):7229–37.

20. Göttlinger HG, Dorfman T, Sodroski JG, Haseltine WA. Effect of mutations affecting the p6 gag protein on human immunodeficiency virus particle release. Proceedings of the National Academy of Sciences. 1991 Apr 15;88(8):3195–9.

21. Hill M, Tachedjian G, Mak J. The Packaging and Maturation of the HIV-1 Pol Proteins. Curr HIV Res. 2005 Jan 1;3(1):73–85.

22. Wang J, Smerdon SJ, Jäger J, Kohlstaedt LA, Rice PA, Friedman JM, et al. Structural basis of asymmetry in the human immunodeficiency virus type 1 reverse transcriptase heterodimer. Proceedings of the National Academy of Sciences. 1994 Jul 19;91(15):7242–6.

23. Le Grice SFJ. Human Immunodeficiency Virus Reverse Transcriptase: 25 Years of Research, Drug Discovery, and Promise. Journal of Biological Chemistry. 2012 Nov;287(49):40850–7.

24. Chiu T, Davies D. Structure and Function of HIV-1 Integrase. Curr Top Med Chem. 2004 May 1;4(9):965–77.

25. Helseth E, Olshevsky U, Furman C, Sodroski J. Human immunodeficiency virus type 1 gp120 envelope glycoprotein regions important for association with the gp41 transmembrane glycoprotein. J Virol. 1991 Apr;65(4):2119–23.

26. Yoon V, Fridkis-Hareli M, Munisamy S, Lee J, Anastasiades D, Stevceva L. The GP120 Molecule of HIV-1 and its Interaction with T Cells. Curr Med Chem. 2010 Mar 1;17(8):741–9.

27. Wyatt R, Sodroski J. The HIV-1 Envelope Glycoproteins: Fusogens, Antigens, and Immunogens. Science (1979). 1998 Jun 19;280(5371):1884–8.

28. Helseth E, Olshevsky U, Furman C, Sodroski J. Human immunodeficiency virus type 1 gp120 envelope glycoprotein regions important for association with the gp41 transmembrane glycoprotein. J Virol. 1991 Apr;65(4):2119–23.

29. Huang C chin, Tang M, Zhang MY, Majeed S, Montabana E, Stanfield RL, et al. Structure of a V3-Containing HIV-1 gp120 Core. Science (1979). 2005 Nov 11;310(5750):1025–8.

30. Kuppuswamy M, Subramanian T, Srinivasan A, Chinnadurai G. Multiple functional domains of Tat, the trans -activator of HIV-1, defined by mutational analysis. Nucleic Acids Res. 1989;17(9):3551–61.

31. Jeang KT, Xiao H, Rich EA. Multifaceted Activities of the HIV-1 Transactivator of Transcription, Tat. Journal of Biological Chemistry. 1999 Oct;274(41):28837–40.

32. Chang HK, Gallo RC, Ensoli B. Regulation of cellular gene expression and function by the human immunodeficiency virus type 1 tat protein. J Biomed Sci. 1995 Aug;2(3):189–202.

33. Chang HC, Samaniego F, Nair BC, Buonaguro L, Ensoli B. HIV-1 Tat protein exits from cells via a leaderless secretory pathway and binds to extracellular matrix-associated heparan sulfate proteoglycans through its basic region. AIDS. 1997 Oct;11(12):1421–31.

34. Pollard VW, Malim MH. THE HIV-1 REV PROTEIN. Annu Rev Microbiol. 1998 Oct;52(1):491–532.

35. Rausch J, Grice S. HIV Rev Assembly on the Rev Response Element (RRE): A Structural Perspective. Viruses. 2015 Jun 12;7(6):3053–75.

36. Rose KM, Marin M, Kozak SL, Kabat D. The viral infectivity factor (Vif) of HIV-1 unveiled. Trends Mol Med. 2004 Jun;10(6):291–7.

37. Goila-Gaur R, Strebel K. HIV-1 Vif, APOBEC, and Intrinsic Immunity. Retrovirology. 2008;5(1):51.

38. Vodicka MA, Koepp DM, Silver PA, Emerman M. HIV-1 Vpr interacts with the nuclear transport pathway to promote macrophage infection. Genes Dev. 1998 Jan 15;12(2):175–85.

39. Andersen JL, Le Rouzic E, Planelles V. HIV-1 Vpr: Mechanisms of G2 arrest and apoptosis. Exp Mol Pathol. 2008 Aug;85(1):2–10.

40. DeHart JL, Planelles V. Human Immunodeficiency Virus Type 1 Vpr Links Proteasomal Degradation and Checkpoint Activation. J Virol. 2008 Feb;82(3):1066–72.

41. Ruiz A, Guatelli JC, Stephens EB. The Vpu Protein: New Concepts in Virus Release and CD4 Down-Modulation. Curr HIV Res. 2010 Apr 1;8(3):240–52.

42. Basmaciogullari S, Pizzato M. The activity of Nef on HIV-1 infectivity. Front Microbiol. 2014 May 20;5.

43. Kestier HW, Ringler DJ, Mori K, Panicali DL, Sehgal PK, Daniel MD, et al. Importance of the nef gene for maintenance of high virus loads and for development of AIDS. Cell. 1991 May;65(4):651–62.

44. Kirchhoff F. HIV Life Cycle: Overview. In: Encyclopedia of AIDS. New York, NY: Springer New York; 2013. p. 1–9.

45. Chen B. Molecular Mechanism of HIV-1 Entry. Trends Microbiol. 2019 Oct;27(10):878–91.

46. Wu L, Gerard NP, Wyatt R, Choe H, Parolin C, Ruffing N, et al. CD4-induced interaction of primary HIV-1 gp120 glycoproteins with the chemokine receptor CCR-5. Nature. 1996 Nov;384(6605):179–83.

47. Wilen CB, Tilton JC, Doms RW. HIV: Cell Binding and Entry. Cold Spring Harb Perspect Med. 2012 Aug 1;2(8):a006866–a006866.

48. Lawless MK, Barney S, Guthrie KI, Bucy TB, Petteway , Stephen R., Merutka G. HIV-1 Membrane Fusion Mechanism: Structural Studies of the Interactions between Biologically-Active Peptides from gp41. Biochemistry. 1996 Jan 1;35(42):13697–708.

49. Bracq L, Xie M, Benichou S, Bouchet J. Mechanisms for Cell-to-Cell Transmission of HIV-1. Front Immunol. 2018 Feb 19;9.

50. Forshey BM, von Schwedler U, Sundquist WI, Aiken C. Formation of a Human Immunodeficiency Virus Type 1 Core of Optimal Stability Is Crucial for Viral Replication. J Virol. 2002 Jun;76(11):5667–77.

51. Mamede JI, Cianci GC, Anderson MR, Hope TJ. Early cytoplasmic uncoating is associated with infectivity of HIV-1. Proceedings of the National Academy of Sciences. 2017 Aug 22;114(34).

52. Hu WS, Hughes SH. HIV-1 Reverse Transcription. Cold Spring Harb Perspect Med. 2012 Oct 1;2(10):a006882–a006882.

53. Liu R diao, Wu J, Shao R, Xue Y hua. Mechanism and factors that control HIV-1 transcription and latency activation. J Zhejiang Univ Sci B. 2014 May 1;15(5):455–65.

54. Craigie R, Bushman FD. HIV DNA Integration. Cold Spring Harb Perspect Med. 2012 Jul 1;2(7):a006890–a006890.

55. Holman AG, Coffin JM. Symmetrical base preferences surrounding HIV-1, avian sarcoma/leukosis virus, and murine leukemia virus integration sites. Proceedings of the National Academy of Sciences. 2005 Apr 26;102(17):6103–7.

56. Grandgenett DP. Symmetrical recognition of cellular DNA target sequences during retroviral integration. Proceedings of the National Academy of Sciences. 2005 Apr 26;102(17):5903–4.

57. Lusic M, Siliciano RF. Nuclear landscape of HIV-1 infection and integration. Nat Rev Microbiol. 2017 Feb 12;15(2):69–82.

58. Levy JA. HIV pathogenesis: 25 years of progress and persistent challenges. AIDS. 2009 Jan 14;23(2):147–60.

59. Lassen K, Han Y, Zhou Y, Siliciano J, Siliciano RF. The multifactorial nature of HIV-1 latency. Trends Mol Med. 2004 Nov;10(11):525–31.

60. Agosto LM, Henderson AJ. CD4 + T Cell Subsets and Pathways to HIV Latency. AIDS Res Hum Retroviruses. 2018 Sep;34(9):780–9.

61. Martinez-Picado J, Zurakowski R, Buzón MJ, Stevenson M. Episomal HIV-1 DNA and its relationship to other markers of HIV-1 persistence. Retrovirology. 2018 Dec 30;15(1):15.

62. Hamid F Bin, Kim J, Shin CG. Distribution and fate of HIV-1 unintegrated DNA species: a comprehensive update. AIDS Res Ther. 2017 Dec 16;14(1):9.

63. Engelman A, Cherepanov P. The structural biology of HIV-1: mechanistic and therapeutic insights. Nat Rev Microbiol. 2012 Apr 16;10(4):279–90.

64. Karn J, Stoltzfus CM. Transcriptional and Posttranscriptional Regulation of HIV-1 Gene Expression. Cold Spring Harb Perspect Med. 2012 Feb 1;2(2):a006916–a006916.

65. Truman CTS, Järvelin A, Davis I, Castello A. HIV Rev-isited. Open Biol. 2020 Dec 23;10(12):200320.

66. Suhasini M, Reddy T. Cellular Proteins and HIV-1 Rev Function. Curr HIV Res. 2009 Jan 1;7(1):91–100.

67. Freed EO. HIV-1 assembly, release and maturation. Nat Rev Microbiol. 2015 Aug 29;13(8):484–96.

68. Sherer NM, Swanson CM, Papaioannou S, Malim MH. Matrix Mediates the Functional Link between Human Immunodeficiency Virus Type 1 RNA Nuclear Export Elements and the Assembly Competency of Gag in Murine Cells. J Virol. 2009 Sep;83(17):8525–35.

69. Summers MF, Henderson LE, Chance MR, South TL, Blake PR, Perez-Alvarado G, et al. Nucleocapsid zinc fingers detected in retroviruses: EXAFS studies of intact viruses and the solution-state structure of the nucleocapsid protein from HIV-1. Protein Science. 1992 May 31;1(5):563–74.

70. Karacostas V, Wolffe EJ, Nagashima K, Gonda MA, Moss B. Overexpression of the HIV-1 Gag-Pol Polyprotein Results in Intracellular Activation of HIV-1 Protease and Inhibition of Assembly and Budding of Virus-like Particles. Virology. 1993 Apr;193(2):661–71.

71. Centers for Disease Control and Prevention. HIV Basics [Internet]. Available from: https://www.cdc.gov/

72. Deeks SG, Overbaugh J, Phillips A, Buchbinder S. HIV infection. Nat Rev Dis Primers. 2015 Oct 1;1(1):15035.

73. Perreau M, Levy Y, Pantaleo G. Immune response to HIV. Curr Opin HIV AIDS. 2013 Jun;1.

74. Stevenson M. HIV-1 pathogenesis. Nat Med. 2003 Jul;9(7):853–60.

75. Coffin J, Swanstrom R. HIV Pathogenesis: Dynamics and Genetics of Viral Populations and Infected Cells. Cold Spring Harb Perspect Med. 2013 Jan 1;3(1):a012526–a012526.

76. Lackner AA, Lederman MM, Rodriguez B. HIV Pathogenesis: The Host. Cold Spring Harb Perspect Med. 2012 Sep 1;2(9):a007005–a007005.

77. Carter CA, Ehrlich LS. Cell Biology of HIV-1 Infection of Macrophages. Annu Rev Microbiol. 2008 Oct 1;62(1):425–43.

78. Shasha D, Karel D, Angiuli O, Greenblatt A, Ghebremichael M, Yu X, et al. Elite controller CD8+ T cells exhibit comparable viral inhibition capacity, but better sustained effector properties compared to chronic progressors. J Leukoc Biol. 2016 Dec 1;100(6):1425–33.

79. Cockerham LR, Hatano H, Deeks SG. Post-Treatment Controllers: Role in HIV “Cure” Research. Curr HIV/AIDS Rep. 2016 Feb 19;13(1):1–9.

80. Okulicz JF, Lambotte O. Epidemiology and clinical characteristics of elite controllers. Curr Opin HIV AIDS. 2011 May;6(3):163–8.

81. European Centre for Disease Prevention and Control. HIV testing [Internet]. Available from: https://www.ecdc.europa.eu/en/infectious-disease-topics/z-disease-list/hiv-infection-and-aids/prevention-and-control/hiv-testing

82. SIMIT - Società Italiana di Malattie Infettive e Tropicali e Ministero della Salute. Linee Guida Italiane sull’utilizzo della Terapia Antiretrovirale e la gestione diagnostico-clinica delle persone con infezione da HIV-1. Available from: https://www.salute.gov.it/imgs/C_17_pubblicazioni_2696_allegato.pdf

83. Suligoi B, Regine V, Raimondo M, Rodella A, Terlenghi L, Caruso A, et al. HIV avidity index performance using a modified fourth-generation immunoassay to detect recent HIV infections. Clinical Chemistry and Laboratory Medicine (CCLM). 2017 Jan 26;55(12).

84. Mocroft A, Phillips AN, Ledergerber B, Smith C, Bogner JR, Lacombe K, et al. Estimated average annual rate of change of CD4 + T-cell counts in patients on combination antiretroviral therapy. Antivir Ther. 2010 May 1;15(4):563–70.

85. Trotta MP, Cozzi-Lepri A, Ammassari A, Vecchiet J, Cassola G, Caramello P, et al. Rate of CD4 + Cell Count Increase over Periods of Viral Load Suppression: Relationship with the Number of Previous Virological Failures. Clinical Infectious Diseases. 2010 Aug 15;51(4):456–64.

86. Serrano-Villar S, Deeks SG. CD4/CD8 ratio: an emerging biomarker for HIV. Lancet HIV. 2015 Mar;2(3):e76–7.

87. McBride JA, Striker R. Imbalance in the game of T cells: What can the CD4/CD8 T-cell ratio tell us about HIV and health? PLoS Pathog. 2017 Nov 2;13(11):e1006624.

88. Deeks SG, Lewin SR, Havlir D V. The end of AIDS: HIV infection as a chronic disease. The Lancet. 2013 Nov;382(9903):1525–33.

89. Carr A, Cooper DA. Adverse effects of antiretroviral therapy. The Lancet. 2000 Oct;356(9239):1423–30.

90. A Trial of Early Antiretrovirals and Isoniazid Preventive Therapy in Africa. New England Journal of Medicine. 2015 Aug 27;373(9):808–22.

91. Leyre L, Kroon E, Vandergeeten C, Sacdalan C, Colby DJ, Buranapraditkun S, et al. Abundant HIV-infected cells in blood and tissues are rapidly cleared upon ART initiation during acute HIV infection. Sci Transl Med. 2020 Mar 4;12(533).

92. Bertoldi A, De Crignis E, Miserocchi A, Bon I, Musumeci G, Longo S, et al. HIV and kidney: a dangerous liaison. New Microbiol. 2017 Jan;40(1):1–10.

93. Oldfield V, Keating GM, Plosker G. Enfuvirtide: A Review of its Use in the Management of HIV Infection. Drugs. 2005;65(8):1139–60.

94. Gartland M, Cahn P, DeJesus E, Diaz RS, Grossberg R, Kozal M, et al. Week 96 Genotypic and Phenotypic Results of the Fostemsavir Phase 3 BRIGHTE Study in Heavily Treatment-Experienced Adults Living with Multidrug-Resistant HIV-1. Antimicrob Agents Chemother. 2022 Jun 21;66(6).

95. Alessandri-Gradt E, Charpentier C, Leoz M, Mourez T, Descamps D, Plantier JC. Impact of natural polymorphisms of HIV-1 non-group M on genotypic susceptibility to the attachment inhibitor fostemsavir. Journal of Antimicrobial Chemotherapy. 2018 Oct 1;73(10):2716–20.

96. Kirchhoff F, Schindler M, Specht A, Arhel N, Münch J. Role of Nef in primate lentiviral immunopathogenesis. Cellular and Molecular Life Sciences. 2008 Sep 26;65(17):2621–36.

97. Ahmad N, Venkatesan S. Nef Protein of HIV-1 Is a Transcriptional Repressor of HIV-1 LTR. Science (1979). 1988 Sep 16;241(4872):1481–5.

98. Kirchhoff F, Greenough TC, Brettler DB, Sullivan JL, Desrosiers RC. Absence of Intact nef Sequences in a Long-Term Survivor with Nonprogressive HIV-1 Infection. New England Journal of Medicine. 1995 Jan 26;332(4):228–32.

99. Deacon NJ, Tsykin A, Solomon A, Smith K, Ludford-Menting M, Hooker DJ, et al. Genomic Structure of an Attenuated Quasi Species of HIV-1 from a Blood Transfusion Donor and Recipients. Science (1979). 1995 Nov 10;270(5238):988–91.

100. Salvi R, Garbuglia AR, Di Caro A, Pulciani S, Montella F, Benedetto A. Grossly Defective nef Gene Sequences in a Human Immunodeficiency Virus Type 1-Seropositive Long-Term Nonprogressor. J Virol. 1998 May;72(5):3646–57.

101. Gorry PR, Churchill M, Learmont J, Cherry C, Dyer WB, Wesselingh SL, et al. Replication-Dependent Pathogenicity of Attenuated nef-Deleted HIV-1 In Vivo. JAIDS Journal of Acquired Immune Deficiency Syndromes. 2007 Dec 1;46(4):390–4.

102. Greenough TC, Sullivan JL, Desrosiers RC. Declining CD4 T-Cell Counts in a Person Infected with nef -Deleted HIV-1. New England Journal of Medicine. 1999 Jan 21;340(3):236–7.

103. Baba TW, Liska V, Khimani AH, Ray NB, Dailey PJ, Penninck D, et al. Live attenuated, multiply deleted simian immunodeficiency virus causes AIDS in infant and adult macaques. Nat Med. 1999 Feb;5(2):194–203.

104. Hanna Z, Kay DG, Cool M, Jothy S, Rebai N, Jolicoeur P. Transgenic Mice Expressing Human Immunodeficiency Virus Type 1 in Immune Cells Develop a Severe AIDS-Like Disease. J Virol. 1998 Jan;72(1):121–32.

105. Hanna Z, Kay DG, Rebai N, Guimond A, Jothy S, Jolicoeur P. Nef Harbors a Major Determinant of Pathogenicity for an AIDS-like Disease Induced by HIV-1 in Transgenic Mice. Cell. 1998 Oct;95(2):163–75.

106. Bentham M, Mazaleyrat S, Harris M. Role of myristoylation and N-terminal basic residues in membrane association of the human immunodeficiency virus type 1 Nef protein. Journal of General Virology. 2006 Mar 1;87(3):563–71.

107. Breuer S, Gerlach H, Kolaric B, Urbanke C, Opitz N, Geyer M. Biochemical Indication for Myristoylation-Dependent Conformational Changes in HIV-1 Nef. Biochemistry. 2006 Feb 1;45(7):2339–49.

108. Geyer M, Fackler OT, Peterlin BM. Structure–function relationships in HIV-1 Nef. EMBO Rep. 2001 Jul;2(7):580–5.

109. Pandori MW, Fitch NJ, Craig HM, Richman DD, Spina CA, Guatelli JC. Producer-cell modification of human immunodeficiency virus type 1: Nef is a virion protein. J Virol. 1996 Jul;70(7):4283–90.

110. Arold ST, Baur AS. Dynamic Nef and Nef dynamics: how structure could explain the complex activities of this small HIV protein. Trends Biochem Sci. 2001 Jun;26(6):356–63.

111. Basmaciogullari S, Pizzato M. The activity of Nef on HIV-1 infectivity. Front Microbiol. 2014 May 20;5.

112. Das SR, Jameel S. Biology of the HIV Nef protein. Indian J Med Res. 2005 Apr;121(4):315–32.

113. Lama J, Ware CF. Human Immunodeficiency Virus Type 1 Nef Mediates Sustained Membrane Expression of Tumor Necrosis Factor and the Related Cytokine LIGHT on Activated T Cells. J Virol. 2000 Oct 15;74(20):9396–402.

114. Sol-Foulon N, Moris A, Nobile C, Boccaccio C, Engering A, Abastado JP, et al. HIV-1 Nef-Induced Upregulation of DC-SIGN in Dendritic Cells Promotes Lymphocyte Clustering and Viral Spread. Immunity. 2002 Jan;16(1):145–55.

115. Schindler M, Würfl S, Benaroch P, Greenough TC, Daniels R, Easterbrook P, et al. Down-Modulation of Mature Major Histocompatibility Complex Class II and Up-Regulation of Invariant Chain Cell Surface Expression Are Well-Conserved Functions of Human and Simian Immunodeficiency Virus nef Alleles. J Virol. 2003 Oct;77(19):10548–56.

116. Schindler M, Münch J, Kutsch O, Li H, Santiago ML, Bibollet-Ruche F, et al. Nef-Mediated Suppression of T Cell Activation Was Lost in a Lentiviral Lineage that Gave Rise to HIV-1. Cell. 2006 Jun;125(6):1055–67.

117. Willard-Gallo KE, Furtado M, Burny A, Wolinsky SM. Down-modulation of TCR/CD3 surface complexes after HIV-1 infection is associated with differential expression of the viral regulatory genes. Eur J Immunol. 2001 Apr;31(4):969–79.

118. Zhang F, Wilson SJ, Landford WC, Virgen B, Gregory D, Johnson MC, et al. Nef Proteins from Simian Immunodeficiency Viruses Are Tetherin Antagonists. Cell Host Microbe. 2009 Jul;6(1):54–67.

119. Stove V, Van de Walle I, Naessens E, Coene E, Stove C, Plum J, et al. Human Immunodeficiency Virus Nef Induces Rapid Internalization of the T-Cell Coreceptor CD8αβ. J Virol. 2005 Sep;79(17):11422–33.

120. Swigut T. Mechanism for down-regulation of CD28 by Nef. EMBO J. 2001 Apr 2;20(7):1593–604.

121. Hrecka K, Swigut T, Schindler M, Kirchhoff F, Skowronski J. Nef Proteins from Diverse Groups of Primate Lentiviruses Downmodulate CXCR4 To Inhibit Migration to the Chemokine Stromal Derived Factor 1. J Virol. 2005 Aug 15;79(16):10650–9.

122. Michel N, Allespach I, Venzke S, Fackler OT, Keppler OT. The Nef Protein of Human Immunodeficiency Virus Establishes Superinfection Immunity by a Dual Strategy to Downregulate Cell-Surface CCR5 and CD4. Current Biology. 2005 Apr;15(8):714–23.

123. Michel N, Ganter K, Venzke S, Bitzegeio J, Fackler OT, Keppler OT. The Nef Protein of Human Immunodeficiency Virus Is a Broad-Spectrum Modulator of Chemokine Receptor Cell Surface Levels That Acts Independently of Classical Motifs for Receptor Endocytosis and Gαi Signaling. Mol Biol Cell. 2006 Aug;17(8):3578–90.

124. Shinya E, Owaki A, Shimizu M, Takeuchi J, Kawashima T, Hidaka C, et al. Endogenously expressed HIV-1 nef down-regulates antigen-presenting molecules, not only class I MHC but also CD1a, in immature dendritic cells. Virology. 2004 Aug;326(1):79–89.

125. Chaudhry A, Das SR, Hussain A, Mayor S, George A, Bal V, et al. The Nef Protein of HIV-1 Induces Loss of Cell Surface Costimulatory Molecules CD80 and CD86 in APCs. The Journal of Immunology. 2005 Oct 1;175(7):4566–74.

126. El-Far M, Isabelle C, Chomont N, Bourbonnière M, Fonseca S, Ancuta P, et al. Down-Regulation of CTLA-4 by HIV-1 Nef Protein. PLoS One. 2013 Jan 23;8(1):e54295.

127. Staudt RP, Alvarado JJ, Emert-Sedlak LA, Shi H, Shu ST, Wales TE, et al. Structure, function, and inhibitor targeting of HIV-1 Nef-effector kinase complexes. Journal of Biological Chemistry. 2020 Oct;295(44):15158–71.

128. Roeth JF, Williams M, Kasper MR, Filzen TM, Collins KL. HIV-1 Nef disrupts MHC-I trafficking by recruiting AP-1 to the MHC-I cytoplasmic tail. J Cell Biol. 2004 Dec 6;167(5):903–13.

129. Ren X, Park SY, Bonifacino JS, Hurley JH. How HIV-1 Nef hijacks the AP-2 clathrin adaptor to downregulate CD4. Elife. 2014 Jan 28;3.

130. Rosa A, Chande A, Ziglio S, De Sanctis V, Bertorelli R, Goh SL, et al. HIV-1 Nef promotes infection by excluding SERINC5 from virion incorporation. Nature. 2015 Oct 8;526(7572):212–7.

131. Usami Y, Wu Y, Göttlinger HG. SERINC3 and SERINC5 restrict HIV-1 infectivity and are counteracted by Nef. Nature. 2015 Oct 8;526(7572):218–23.

132. Shi J, Xiong R, Zhou T, Su P, Zhang X, Qiu X, et al. HIV-1 Nef Antagonizes SERINC5 Restriction by Downregulation of SERINC5 via the Endosome/Lysosome System. J Virol. 2018 Jun;92(11).

133. Buffalo CZ, Iwamoto Y, Hurley JH, Ren X. How HIV Nef Proteins Hijack Membrane Traffic To Promote Infection. J Virol. 2019 Dec;93(24).

134. Pereira EA, daSilva LLP. HIV-1 Nef: Taking Control of Protein Trafficking. Traffic. 2016 Sep 3;17(9):976–96.

135. Blander JM. The comings and goings of MHC class I molecules herald a new dawn in cross-presentation. Immunol Rev. 2016 Jul 20;272(1):65–79.

136. Blander JM. Regulation of the Cell Biology of Antigen Cross-Presentation. Annu Rev Immunol. 2018 Apr 26;36(1):717–53.

137. Jia X, Singh R, Homann S, Yang H, Guatelli J, Xiong Y. Structural basis of evasion of cellular adaptive immunity by HIV-1 Nef. Nat Struct Mol Biol. 2012 Jul 17;19(7):701–6.

138. Greenberg ME. The SH3 domain-binding surface and an acidic motif in HIV-1 Nef regulate trafficking of class I MHC complexes. EMBO J. 1998 May 15;17(10):2777–89.

139. Mangasarian A, Piguet V, Wang JK, Chen YL, Trono D. Nef-Induced CD4 and Major Histocompatibility Complex Class I (MHC-I) Down-Regulation Are

Governed by Distinct Determinants: N-Terminal Alpha Helix and Proline Repeat of Nef Selectively Regulate MHC-I Trafficking. J Virol. 1999 Mar;73(3):1964–73.

140. Wonderlich ER, Leonard JA, Kulpa DA, Leopold KE, Norman JM, Collins KL. ADP Ribosylation Factor 1 Activity Is Required To Recruit AP-1 to the Major Histocompatibility Complex Class I (MHC-I) Cytoplasmic Tail and Disrupt MHC-I Trafficking in HIV-1-Infected Primary T Cells. J Virol. 2011 Dec;85(23):12216–26.

141. Mann JK, Byakwaga H, Kuang XT, Le AQ, Brumme CJ, Mwimanzi P, et al. Ability of HIV-1 Nef to downregulate CD4 and HLA class I differs among viral subtypes. Retrovirology. 2013 Dec 16;10(1):100.

142. Turk G, Gundlach S, Carobene M, Schindler M, Salomon H, Benaroch P. Single Nef Proteins from HIV Type 1 Subtypes C and F Fail to Upregulate Invariant Chain Cell Surface Expression But Are Active for Other Functions. AIDS Res Hum Retroviruses. 2009 Mar;25(3):285–96.

143. Yoon K, Gyun Jeong J, Yoon H, Lee JS, Kim S. Differential Effects of Primary Human Immunodeficiency Virus Type 1 nef Sequences on Downregulation of CD4 and MHC Class I. Biochem Biophys Res Commun. 2001 Jun;284(3):638–42.

144. Brady RL, Barclay AN. The Structure of CD4. In 1996. p. 1–18.

145. Pitcher C, Höning S, Fingerhut A, Bowers K, Marsh M. Cluster of Differentiation Antigen 4 (CD4) Endocytosis and Adaptor Complex Binding Require Activation of the CD4 Endocytosis Signal by Serine Phosphorylation. Mol Biol Cell. 1999 Mar;10(3):677–91.

146. Pelchen-Matthews A, Boulet I, Littman D, Fagard R, Marsh M. The protein tyrosine kinase p56lck inhibits CD4 endocytosis by preventing entry of CD4 into coated pits. J Cell Biol. 1992 Apr 15;117(2):279–90.

147. Craig HM, Pandori MW, Guatelli JC. Interaction of HIV-1 Nef with the cellular dileucine-based sorting pathway is required for CD4 down-regulation and optimal viral infectivity. Proceedings of the National Academy of Sciences. 1998 Sep 15;95(19):11229–34.

148. Benson RE, Sanfridson A, Ottinger JS, Doyle C, Cullen BR. Downregulation of cell-surface CD4 expression by simian immunodeficiency virus Nef prevents viral super infection. J Exp Med. 1993 Jun 1;177(6):1561–6.

149. Lama J, Mangasarian A, Trono D. Cell-surface expression of CD4 reduces HIV-1 infectivity by blocking Env incorporation in a Nef- and Vpu-inhibitable manner. Current Biology. 1999 Jun;9(12):622–31.

150. Ross TM, Oran AE, Cullen BR. Inhibition of HIV-1 progeny virion release by cell-surface CD4 is relieved by expression of the viral Nef protein. Current Biology. 1999 Jun;9(12):613–21.

151. Argañaraz ER, Schindler M, Kirchhoff F, Cortes MJ, Lama J. Enhanced CD4 Down-modulation by Late Stage HIV-1 nef Alleles Is Associated with Increased Env Incorporation and Viral Replication. Journal of Biological Chemistry. 2003 Sep;278(36):33912–9.

152. Garcia JV, Miller AD. Serine phosphorylation-independent downregulation of cell-surface CD4 by nef. Nature. 1991 Apr 11;350(6318):508–11.

153. Burtey A, Rappoport JZ, Bouchet J, Basmaciogullari S, Guatelli J, Simon SM, et al. Dynamic Interaction of HIV-1 Nef with the Clathrin-Mediated Endocytic Pathway at the Plasma Membrane. Traffic. 2007 Jan 26;8(1):61–76.

154. Greenberg ME. Co-localization of HIV-1 Nef with the AP-2 adaptor protein complex correlates with Nef-induced CD4 down-regulation. EMBO J. 1997 Dec 1;16(23):6964–76.

155. Doray B, Lee I, Knisely J, Bu G, Kornfeld S. The γ/σ1 and α/σ2 Hemicomplexes of Clathrin Adaptors AP-1 and AP-2 Harbor the Dileucine Recognition Site. Mol Biol Cell. 2007 May;18(5):1887–96.

156. Chaudhuri R, Lindwasser OW, Smith WJ, Hurley JH, Bonifacino JS. Downregulation of CD4 by Human Immunodeficiency Virus Type 1 Nef Is Dependent on Clathrin and Involves Direct Interaction of Nef with the AP2 Clathrin Adaptor. J Virol. 2007 Apr 15;81(8):3877–90.

157. Chaudhuri R, Mattera R, Lindwasser OW, Robinson MS, Bonifacino JS. A Basic Patch on α-Adaptin Is Required for Binding of Human Immunodeficiency Virus Type 1 Nef and Cooperative Assembly of a CD4-Nef-AP-2 Complex. J Virol. 2009 Mar 15;83(6):2518–30.

158. Jin YJ, Cai CY, Mezei M, Ohlmeyer M, Sanchez R, Burakoff SJ. Identification of a Novel Binding Site Between HIV Type 1 Nef C-Terminal Flexible Loop and AP2 Required for Nef-Mediated CD4 Downregulation. AIDS Res Hum Retroviruses. 2013 Apr;29(4):725–31.

159. Kwon Y, Kaake RM, Echeverria I, Suarez M, Karimian Shamsabadi M, Stoneham C, et al. Structural basis of CD4 downregulation by HIV-1 Nef. Nat Struct Mol Biol. 2020 Sep 27;27(9):822–8.

160. ROSSI F, GALLINA A, MILANESI G. NEF-CD4 Physical Interaction Sensed with the Yeast Two-Hybrid System. Virology. 1996 Mar;217(1):397–403.

161. Preusser A, Briese L, Baur AS, Willbold D. Direct In Vitro Binding of Full-Length Human Immunodeficiency Virus Type 1 Nef Protein to CD4 Cytoplasmic Domain. J Virol. 2001 Apr 15;75(8):3960–4.

162. Salghetti S, Mariani R, Skowronski J. Human immunodeficiency virus type 1 Nef and p56lck protein-tyrosine kinase interact with a common element in CD4 cytoplasmic tail. Proceedings of the National Academy of Sciences. 1995 Jan 17;92(2):349–53.

163. Mann JK, Chopera D, Omarjee S, Kuang XT, Le AQ, Anmole G, et al. Nef-mediated down-regulation of CD4 and HLA class I in HIV-1 subtype C infection: Association with disease progression and influence of immune pressure. Virology. 2014 Nov;468–470:214–25.

164. Chowers MY, Spina CA, Kwoh TJ, Fitch NJ, Richman DD, Guatelli JC. Optimal infectivity in vitro of human immunodeficiency virus type 1 requires an intact nef gene. J Virol. 1994 May;68(5):2906–14.

165. Inuzuka M, Hayakawa M, Ingi T. Serinc, an Activity-regulated Protein Family, Incorporates Serine into Membrane Lipid Synthesis. Journal of Biological Chemistry. 2005 Oct;280(42):35776–83.

166. Firrito C, Bertelli C, Vanzo T, Chande A, Pizzato M. SERINC5 as a New Restriction Factor for Human Immunodeficiency Virus and Murine Leukemia Virus. Annu Rev Virol. 2018 Sep 29;5(1):323–40.

167. Zhang X, Zhou T, Yang J, Lin Y, Shi J, Zhang X, et al. Identification of SERINC5-001 as the Predominant Spliced Isoform for HIV-1 Restriction. J Virol. 2017 May 15;91(10).

168. Brügger B, Glass B, Haberkant P, Leibrecht I, Wieland FT, Kräusslich HG. The HIV lipidome: A raft with an unusual composition. Proceedings of the National Academy of Sciences. 2006 Feb 21;103(8):2641–6.

169. Trautz B, Pierini V, Wombacher R, Stolp B, Chase AJ, Pizzato M, et al. The Antagonism of HIV-1 Nef to SERINC5 Particle Infectivity Restriction Involves the Counteraction of Virion-Associated Pools of the Restriction Factor. J Virol. 2016 Dec;90(23):10915–27.

170. Sood C, Marin M, Chande A, Pizzato M, Melikyan GB. SERINC5 protein inhibits HIV-1 fusion pore formation by promoting functional inactivation of envelope glycoproteins. Journal of Biological Chemistry. 2017 Apr;292(14):6014–26.

171. Dai W, Usami Y, Wu Y, Göttlinger H. A Long Cytoplasmic Loop Governs the Sensitivity of the Anti-viral Host Protein SERINC5 to HIV-1 Nef. Cell Rep. 2018 Jan;22(4):869–75.

172. Pizzato M, Helander A, Popova E, Calistri A, Zamborlini A, Palù G, et al. Dynamin 2 is required for the enhancement of HIV-1 infectivity by Nef. Proceedings of the National Academy of Sciences. 2007 Apr 17;104(16):6812–7.

173. Jin SW, Mwimanzi FM, Mann JK, Bwana MB, Lee GQ, Brumme CJ, et al. Variation in HIV-1 Nef function within and among viral subtypes reveals genetically

separable antagonism of SERINC3 and SERINC5. PLoS Pathog. 2020 Sep 14;16(9):e1008813.

174. Jin SW, Alsahafi N, Kuang XT, Swann SA, Toyoda M, Göttlinger H, et al. Natural HIV-1 Nef Polymorphisms Impair SERINC5 Downregulation Activity. Cell Rep. 2019 Nov;29(6):1449-1457.e5.

175. Kruize Z, van Nuenen AC, van Wijk SW, Girigorie AF, van Dort KA, Booiman T, et al. Nef Obtained from Individuals with HIV-1 Vary in Their Ability to Antagonize SERINC3- and SERINC5-Mediated HIV-1 Restriction. Viruses. 2021 Mar 6;13(3):423.

176. Firrito C, Bertelli C, Rosa A, Chande A, Ananth S, van Dijk H, et al. A Conserved Acidic Residue in the C-Terminal Flexible Loop of HIV-1 Nef Contributes to the Activity of SERINC5 and CD4 Downregulation. Viruses. 2023 Feb 28;15(3):652.

177. Bentham M, Mazaleyrat S, Harris M. Role of myristoylation and N-terminal basic residues in membrane association of the human immunodeficiency virus type 1 Nef protein. Journal of General Virology. 2006 Mar 1;87(3):563–71.

178. Dennis CA, Baron A, Grossmann JG, Mazaleyrat S, Harris M, Jaeger J. Co-translational myristoylation alters the quaternary structure of HIV-1 Nef in solution. Proteins: Structure, Function, and Bioinformatics. 2005 Sep 14;60(4):658–69.

179. Breuer S, Gerlach H, Kolaric B, Urbanke C, Opitz N, Geyer M. Biochemical Indication for Myristoylation-Dependent Conformational Changes in HIV-1 Nef. Biochemistry. 2006 Feb 1;45(7):2339–49.

180. Liu LX, Margottin F, Le Gall S, Schwartz O, Selig L, Benarous R, et al. Binding of HIV-1 Nef to a Novel Thioesterase Enzyme Correlates with Nef-mediated CD4 Down-regulation. Journal of Biological Chemistry. 1997 May;272(21):13779–85.

181. Watanabe H, Shiratori T, Shoji H, Miyatake S, Okazaki Y, Ikuta K, et al. A Novel acyl-CoA Thioesterase Enhances Its Enzymatic Activity by Direct Binding with HIV Nef. Biochem Biophys Res Commun. 1997 Sep;238(1):234–9.

182. Jones JM, Nau K, Geraghty MT, Erdmann R, Gould SJ. Identification of Peroxisomal Acyl-CoA Thioesterases in Yeast and Humans. Journal of Biological Chemistry. 1999 Apr;274(14):9216–23.

183. Colquhoun DR, Lyashkov AE, Mohien CU, Aquino VN, Bullock BT, Dinglasan RR, et al. Bioorthogonal mimetics of palmitoyl-CoA and myristoyl-CoA and their subsequent isolation by click chemistry and characterization by mass spectrometry reveal novel acylated host-proteins modified by HIV-1 infection. Proteomics. 2015 Jun 26;15(12):2066–77.

184. Bizzozero OA, Bixler HA, Pastuszyn A. Structural determinants influencing the reaction of cysteine-containing peptides with palmitoyl-coenzyme A and other thioesters. Biochimica et Biophysica Acta (BBA) - Protein Structure and Molecular Enzymology. 2001 Feb;1545(1–2):278–88.

185. Duncan JA, Gilman AG. A Cytoplasmic Acyl-Protein Thioesterase That Removes Palmitate from G Protein α Subunits and p21RAS. Journal of Biological Chemistry. 1998 Jun;273(25):15830–7.

186. Berthiaume LG. Insider Information: How Palmitoylation of Ras Makes It a Signaling Double Agent. Science's STKE. 2002 Oct;2002(152).

187. Resh MD. Fatty acylation of proteins: new insights into membrane targeting of myristoylated and palmitoylated proteins. Biochimica et Biophysica Acta (BBA) - Molecular Cell Research. 1999 Aug;1451(1):1–16.

188. Smotrys JE, Linder ME. Palmitoylation of Intracellular Signaling Proteins: Regulation and Function. Annu Rev Biochem. 2004 Jun;73(1):559–87.

189. Vérollet C, Zhang YM, Le Cabec V, Mazzolini J, Charrière G, Labrousse A, et al. HIV-1 Nef Triggers Macrophage Fusion in a p61Hck- and Protease-Dependent Manner. The Journal of Immunology. 2010 Jun 15;184(12):7030–9.

190. Benichou S, Bomsel M, Bodéus M, Durand H, Douté M, Letourneur F, et al. Physical interaction of the HIV-1 Nef protein with beta-COP, a component of non-

clathrin-coated vesicles essential for membrane traffic. J Biol Chem. 1994 Dec 2;269(48):30073–6.

191. Cohen GB, Rangan VS, Chen BK, Smith S, Baltimore D. The Human Thioesterase II Protein Binds to a Site on HIV-1 Nef Critical for CD4 Down-regulation. Journal of Biological Chemistry. 2000 Jul;275(30):23097–105.

192. Liu LX, Heveker N, Fackler OT, Arold S, Le Gall S, Janvier K, et al. Mutation of a Conserved Residue (D123) Required for Oligomerization of Human Immunodeficiency Virus Type 1 Nef Protein Abolishes Interaction with Human Thioesterase and Results in Impairment of Nef Biological Functions. J Virol. 2000 Jun;74(11):5310–9.

193. Serena M, Giorgetti A, Busato M, Gasparini F, Diani E, Romanelli MG, et al. Molecular characterization of HIV-1 Nef and ACOT8 interaction: insights from in silico structural predictions and in vitro functional assays. Sci Rep. 2016 Mar 1;6(1):22319.

194. Palmeira J da F, Argañaraz GA, de Oliveira GXLM, Argañaraz ER. Physiological relevance of ACOT8-Nef interaction in HIV infection. Rev Med Virol. 2019 Sep 9;29(5).

195. Zhang Y, Werling U, Edelmann W. Seamless Ligation Cloning Extract (SLiCE) Cloning Method. In 2014. p. 235–44.

196. Motohashi K. Seamless Ligation Cloning Extract (SLiCE) Method Using Cell Lysates from Laboratory Escherichia coli Strains and its Application to SLiP Site-Directed Mutagenesis. In 2017. p. 349–57.

197. Casartelli N, Di Matteo G, Potestà M, Rossi P, Doria M. CD4 and Major Histocompatibility Complex Class I Downregulation by the Human Immunodeficiency Virus Type 1 Nef Protein in Pediatric AIDS Progression. J Virol. 2003 Nov;77(21):11536–45.

198. Ananth S, Morath K, Trautz B, Tibroni N, Shytaj IL, Obermaier B, et al. Multifunctional Roles of the N-Terminal Region of HIV-1 SF2 Nef Are Mediated by Three Independent Protein Interaction Sites. J Virol. 2019 Dec 12;94(1).

199. Piguet V, Wan L, Borel C, Mangasarian A, Demaurex N, Thomas G, et al. HIV-1 Nef protein binds to the cellular protein PACS-1 to downregulate class I major histocompatibility complexes. Nat Cell Biol. 2000 Mar 9;2(3):163–7.

200. Mwimanzi P, Markle TJ, Martin E, Ogata Y, Kuang XT, Tokunaga M, et al. Attenuation of multiple Nef functions in HIV-1 elite controllers. Retrovirology. 2013 Dec 7;10(1):1.

201. Kuang XT, Li X, Anmole G, Mwimanzi P, Shahid A, Le AQ, et al. Impaired Nef Function Is Associated with Early Control of HIV-1 Viremia. J Virol. 2014 Sep;88(17):10200–13.

202. Omondi FH, Chandrarathna S, Mujib S, Brumme CJ, Jin SW, Sudderuddin H, et al. HIV Subtype and Nef-Mediated Immune Evasion Function Correlate with Viral Reservoir Size in Early-Treated Individuals. J Virol. 2019 Mar 15;93(6).

203. Lundquist CA, Tobiume M, Zhou J, Unutmaz D, Aiken C. Nef-Mediated Downregulation of CD4 Enhances Human Immunodeficiency Virus Type 1 Replication in Primary T Lymphocytes. J Virol. 2002 May;76(9):4625–33.

204. Naicker D, Sonela N, Jin SW, Mulaudzi T, Ojwach D, Reddy T, et al. HIV-1 subtype C Nef-mediated SERINC5 down-regulation significantly contributes to overall Nef activity. Retrovirology. 2023 Mar 31;20(1):3.

205. Swigut T, Alexander L, Morgan J, Lifson J, Mansfield KG, Lang S, et al. Impact of Nef-Mediated Downregulation of Major Histocompatibility Complex Class I on Immune Response to Simian Immunodeficiency Virus. J Virol. 2004 Dec;78(23):13335–44.

206. Passos V, Zillinger T, Casartelli N, Wachs AS, Xu S, Malassa A, et al. Characterization of Endogenous SERINC5 Protein as Anti-HIV-1 Factor. J Virol. 2019 Dec;93(24).

207. Fackler OT, Moris A, Tibroni N, Giese SI, Glass B, Schwartz O, et al. Functional characterization of HIV-1 Nef mutants in the context of viral infection. Virology. 2006 Aug;351(2):322–39.